Supporting Information for

Protected Amino Acids as a Nonbonding Source of Chirality in Induction of Single-Handed Screw-Sense to Helical Macromolecular Catalysts

Shoma Ikeda, Ryohei Takeda, Takuya Fujie, Naoto Ariki, Yuuya Nagata,* and Michinori Suginome*

Department of Synthetic Chemistry and Biological Chemistry, Graduate School of Engineering, Kyoto University, Kyoto 606-8501, Japan
615-8510, Japan

*To whom correspondence should be addressed.
E-mail: suginome@sbchem.kyoto-u.ac.jp
nagata@icredd.hokudai.ac.jp

Contents

1 General

All reactions were carried out under an atmosphere of nitrogen with magnetic stirring. ^{1}H, ^{13}C, and ^{31}P NMR spectra were recorded on a Varian 400-MR or JEOL JNM-ECA600P spectrometer at ambient temperature unless otherwise noted. ^{1}H NMR data are reported as follows: chemical shift in ppm downfield from tetramethylsilane (δ scale), multiplicity (s = singlet, d = doublet, t = triplet, q = quartet, quint = quintet, sex = sextet, m = multiplet and br = broad), coupling constant (Hz), and integration. All ^{13}C NMR spectra were obtained with complete proton decoupling. IR spectra were obtained using a Shimadzu FTIR-8400 Fourier transform infrared (FT-IR) spectrometer equipped with PIKE MIRacle attenuated total reflection (MIR-ATR) attachment. The GPC analysis was carried out with TSKgel GMH_{XL} (THF, polystyrene standards). Preparative GPC was performed on JAI LC-908 equipped with JAIGEL-1H and - 2H columns in a series ($CHCl_3$). UV spectra were recorded on a JASCO V-750 spectrometer equipped with a JASCO ETC-505T temperature/stirring controller at 20 °C. CD spectra were recorded on a JASCO J-1500 spectrometer equipped with a JASCO PTC-510 temperature/stirring controller at 20 °C. The chiral SFC analysis was carried out on TOSOH 8020 series (*n*-hexane and 2-propanol), JASCO SF-2000 analytical SFC system and JASCO EXTREMA analytical SFC system (CO_2 and 2-propanol) equipped with Daicel CHIRALCEL® OZ-H or AD-H.

Monomer **Q**,[1] acetic formic anhydride (AFA), [2] *o*-TolNiCl$(PMe_3)_2$,[3] were prepared according to the reported procedures. Tetrahydrofurane (THF) and toluene were dried and deoxygenized using an alumina/catalyst column system (Glass Contour Co.). Acetonitrile were distilled over CaH_2 and degassed prior to use for reactions. Et_3N was distilled over KOH and degassed prior to use. $POCl_3$ was distilled prior to use. Boc-*L*-Pip-OMe, Boc-*L*-*t*-Leu-OMe, Boc-*L*-Glu(OMe)-OMe, Boc-*L*-Gln-OMe, Boc-*L*-Asp(OMe)-OMe, Boc-*L*-Pro-OEt, Boc-*L*-Pro-O-*n*-C_6H_{13} were obtained by esterification of the corresponding Boc-*L*-AA-OH.[4] Piv-*L*-Pro-OMe, TFAc-*L*-Pro-OMe, Piv-*L*-Leu-OMe, TFAc-*L*-Leu-OMe were obtained by amidation of *L*-AA-OMe.[5,6] The rest of the amino acid derivatives were purchased from the commercial sources and were used without further purification.

2 Experimental Procedures and Spectral Data for Synthesized Compounds

General procedure for the synthesis of homopolymers PQX

*PQX homopolymers with different polymerization degrees were synthesized by living polymerization of monomer **Q** in the presence of o-TolNiCl(PMe$_3$)$_2$ as an initiator according to the procedure reported in reference 14 as shown below.*

To a THF solution of *o*-TolNiCl(PMe$_3$)$_2$ in THF (1 mL) was added a THF solution of **Q** in THF (1 mL). After stirring for 24 h, $NaBH_4$ (2.50 mg, 66.7 μmol) was added to the reaction mixture at room temperature. After stirring for 1 h at room temperature, distilled water (10 mL) was added and extracted with $CHCl_3$ (10 mL). The organic layer was washed with brine (10 mL) and dried over Na_2SO_4 followed by preparative GPC gave **PQX** as a beige solid.

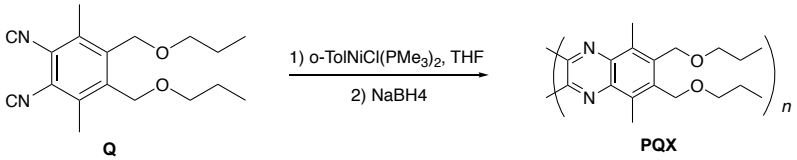

Scheme S1. Synthesis of Homopolymer PQX

PQX 30mer: *o*-TolNiCl(PMe$_3$)$_2$ (50 mM solution in THF, 44 μL, 2.22 μmol) and **Q** (20 mg, 66.7 μmol) were used for the synthesis of PQX 30mer (19.8 mg, 99%). ^{1}H NMR ($CDCl_3$) δ 4.65 (4×30, br s), 3.45 (4×30, br s), 2.35 (6×30, br s), 1.61 (4×30, br m), 0.91 (6×30, br m) GPC ($CHCl_3$, g/mol): $M_n = 8.8\times10^3$ $M_w/M_n = 1.14$

PQX 60mer: *o*-TolNiCl(PMe$_3$)$_2$ (50 mM solution in THF, 22 μL, 1.11 μmol) and **Q** (20 mg, 66.7 μmol) were used for the synthesis of PQX 60mer (19.0 mg, 95%). ^{1}H NMR ($CDCl_3$) δ 4.65 (4×60, br s), 3.45 (4×60, br s), 2.35 (6×60, br s), 1.61 (4×60, br m), 0.91 (6×60, br m) GPC ($CHCl_3$, g/mol): $M_n = 2.0\times10^4$ $M_w/M_n = 1.10$

PQX 100mer: *o*-TolNiCl(PMe$_3$)$_2$ (50 mM solution in THF, 13 μL, 0.67 μmol) and **Q** (20 mg, 66.7 μmol) were used for the synthesis of PQX 100mer (19.6 mg, 98%). ^{1}H NMR ($CDCl_3$) δ 4.65 (4×100, br s), 3.45 (4×100, br s), 2.35 (6×100, br s), 1.61 (4×100, br m), 0.91 (6×100, br m) GPC ($CHCl_3$, g/mol): $M_n = 3.0\times10^4$ $M_w/M_n = 1.11$

PQX 150mer: *o*-TolNiCl(PMe_3)$_2$ (50 mM solution in THF, 8.9 μL, 0.44 μmol) and **Q** (20 mg, 66.7 μmol) were used for the synthesis of PQX 150mer (19.4 mg, 97%). ^{1}H NMR ($CDCl_3$) δ 4.65 (4×150, br s), 3.45 (4×150, br s), 2.35 (6×150, br s), 1.61 (4×150, br m), 0.91 (6×150, br m) GPC ($CHCl_3$, g/mol): $M_n = 3.4\times10^4$ $M_w/M_n = 1.14$

PQX 200mer: *o*-TolNiCl(PMe_3)$_2$ (50 mM solution in THF, 6.8 μL, 0.34 μmol) and **Q** (20 mg, 66.7 μmol) were used for the synthesis of PQX 200mer (19.6 mg, 98%). ^{1}H NMR ($CDCl_3$) δ 4.65 (4×200, br s), 3.45 (4×200, br s), 2.35 (6×200, br s), 1.61 (4×200, br m), 0.91 (6×200, br m) GPC ($CHCl_3$, g/mol): $M_n = 4.6\times10^4$ $M_w/M_n = 1.10$

PQX 250mer: *o*-TolNiCl(PMe_3)$_2$ (50 mM solution in THF, 5.3 μL, 0.27 μmol) and **Q** (20 mg, 66.7 μmol) were used for the synthesis of PQX 250mer (19.2 mg, 96%). ^{1}H NMR ($CDCl_3$) δ 4.65 (4×250, br s), 3.45 (4×250, br s), 2.35 (6×250, br s), 1.61 (4×250, br m), 0.91 (6×250, br m) GPC ($CHCl_3$, g/mol): $M_n = 5.8\times10^4$ $M_w/M_n = 1.13$

PQX 300mer: *o*-TolNiCl(PMe_3)$_2$ (50 mM solution in THF, 4.4 μL, 0.22 μmol) and **Q** (20 mg, 66.7 μmol) were used for the synthesis of PQX 300mer (19.4 mg, 97%). ^{1}H NMR ($CDCl_3$) δ 4.65 (4×300, br s), 3.45 (4×300, br s), 2.35 (6×300, br s), 1.61 (4×300, br m), 0.91 (6×300, br m) GPC ($CHCl_3$, g/mol): $M_n = 1.0\times10^5$ $M_w/M_n = 1.13$

PQX 400mer: *o*-TolNiCl(PMe_3)$_2$ (50 mM solution in THF, 3.3 μL, 0.17 μmol) and **Q** (20 mg, 66.7 μmol) were used for the synthesis of PQX 400mer (19.0 mg, 95%). ^{1}H NMR ($CDCl_3$) δ 4.65 (4×400, br s), 3.45 (4×400, br s), 2.35 (6×400, br s), 1.61 (4×400, br m), 0.91 (6×400, br m) GPC ($CHCl_3$, g/mol): $M_n = 1.3\times10^5$ $M_w/M_n = 1.12$

Procedures for the synthesis of macromolecular ligand PQXphos

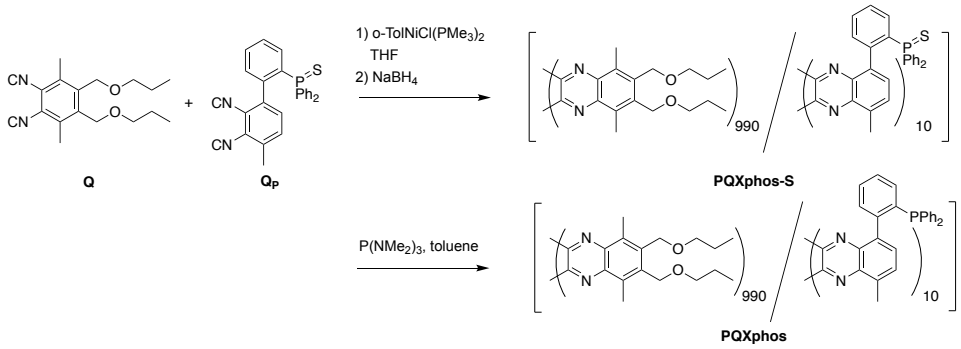

Scheme S2. Synthesis of PQXphos

Synthesis of PQXphos-S

Step 1: A THF solution of *o*-TolNiCl(PMe_3)$_2$ (50 mM, 33.6 μL, 1.68 μmol) was quickly added to a solution containing monomer **Q** (500 mg, 1668 μmol) and **Q$_P$** (3.09 mg, 16.8 μmol) in THF (30 mL). The mixture was stirred for 24 h at room temperature. To the reaction mixture was added $NaBH_4$ (62.5 mg, 1.7 mmol), and the mixture was stirred for 1 h. The mixture was poured into vigorously stirred methanol (600 mL), and precipitated polymer was collected by filtration. After drying in vacuo, **PQXphos-S** was obtained as fibriform solid (503 mg). **PQXphos-S** was used without further purification in the next step.

Step 2: A mixture of **PQXphos-S** (16.8 μmol P) and $P(NMe_2)_3$ (123 μL, 0.67 mmol) in toluene (8 mL) was stirred at 110 °C for 19 h. The mixture was poured into vigorously stirred MeOH (600 mL). Precipitated material was collected by filtration to give **PQXphos** as fibriform solid (475 mg, 95%). ^{1}H NMR ($CDCl_3$) δ 4.65 (4 × 990 H, br s), 3.45 (4 H × 990, br s), 2.35 (6 H × 990, br s), 1.61 (4 H × 990, br s), 0.91 (6 H × 990, br s); ^{31}P NMR ($CDCl_3$) δ –15.3 (br s); GPC ($CHCl_3$, g/mol): $M_n = 2.6 \times 10^5$, $M_w/M_n = 2.69$

Typical procedure for the measurements of UV and CD spectra (Table 1, entry 1).

PQX 100mer (2.1 mg, 7.0 μmol) was dissolved in THF (10 mL) in a volumetric flask. A 1 mL portion of the solution is transferred to a vial and te solvent was removed in vacuo. In a second vial, Boc-*L*-Pro-OMe (628 mg, 2.74 mmol) was dissolved in THF (2.00 mL, 24.7 mmol, measured with volumetric pipet). This solution of Boc-*L*-Pro-OMe in THF (1.00 mL, measured with volumetric pipet) was transferred to the first vial containing PQX (0.21 mg, 0.70 7.0 μmol). This solution containing PQX and Boc-*L*-Pro-OMe was subjected to UV/Vis and CD meaasurements. The remaining THF solution in the second vial containing Boc-*L*-Pro-OMe was used as a reference. Other UV/Vis and CD measurements were carried out according to this typical procedure by varying PQX, aminoacid derivatives, and solvents along with their concentrations.

Detemination of Helix stabilization energies ΔG_h (Figure 3 and Table 3)

According to the typical procedure, UV/Vis and CD spectra of **PQX** 30, 60, 100, 150, 200, 300, and 400mer were collected in the presence of Ac-*L*-Pro-OMe and TFAc-*L*-Pro-OMe (10 mol% in the solution mixture) in THF and MTBE.

ΔG_h, i.e., the energy difference between *P* and *M*-helices per a chiral unit, was determined according to our previous report,[7] which is based on the report by Lifson and Green.[8] The following equation (1) is subjected to nonlinear least-square fitting of g_{abs} versus N using the Solver Function in Microsoft Office Excel 2011, where g_{abs}, N, R, and T are the observed dissymmetry factor (Figure 3), the polymerization degree, the gas constant (8.314 J K^{-1} mol^{-1}), and operating temperature (293 K), respectively. Sums of the squares of the deviation were minimized by varying two parameters g_{max} and ΔG_h.

$$g_{abs} = \tanh(-\Delta G_h N / 2RT) \times g_{max} \quad (1)$$

The parameters g_{max} and ΔG_h are successfully converged in each case and the final values are summarized in Table 3. The screw sense excesses (se) were determined by g_{abs}/g_{max}.

NMR measurements of Ac-L-Pro-OMe in the presence of PQX(100) in various solvents (Figure 2 (A))

^{1}H NMR spectra of Ac-L-Pro-OMe (13 mM) were recorded in the absence and presence of **PQX(100)** (50 mM based on a monomer unit) on a JEOL JNM-ECZ500R spectrometer at ambient temperature in $CDCl_3$, toluene-d_8, THF-d_8, 1,4-dioxane-d_8, and a mixture of MTBE and C_6D_{12} (4/1) (0.6 mL each). The shift ($\Delta\delta$) of chemical shift (δ) for Ac and OMe group are listed in Fig. 2(A).

NMR measurements of Ac-L-Pro-OMe in the presence of PQX(100) in C_6D_{12} (Figure 2 (B))

^{1}H NMR spectra of Ac-L-Pro-OMe (57 mM) were recorded in the absence and presence of **PQX(100)** (157 mM based on a monomer unit) on a JEOL JNM-ECZ500R spectrometer at 8.5, 19.4, and 38.3 °C in C_6D_{12} (0.6 mL). For the assignment of proton signals, homonuclear broadband decoupled ^{1}H NMR spectra were taken using PSYCHE pulse sequence in addition to the native ^{1}H NMR spectra. The temperature of the solution was calibrated using ethylene glycol in DMSO-d_8. The shifts ($\Delta\delta$) of chemical shift (δ) for all the proton signals at 8.5 °C are shown in Fig. 2(B).

(A)

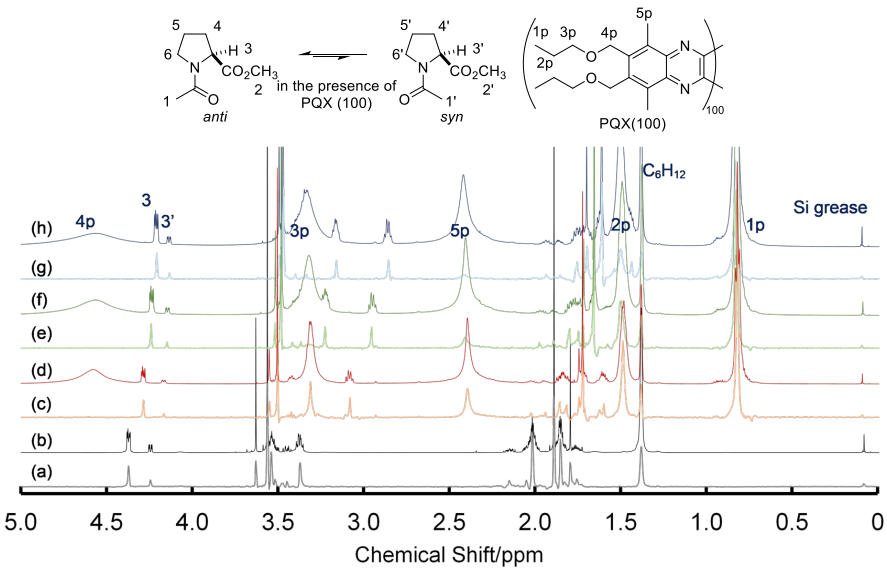

(B)

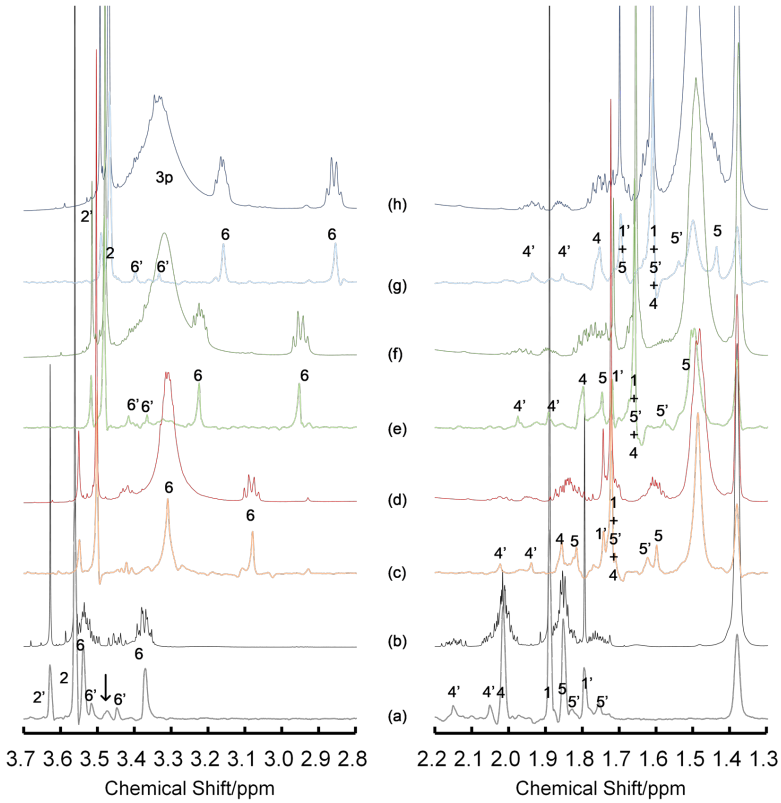

Figure S0. (A) ^{1}H NMR spectrum of Ac-L-Pro-OMe in cyclohexane-d_{12} in the absence (a,b) and presence (c-h) of PQX(100). (B) Enlarged spectra.

(a) Homonuclear broadband decoupled ^{1}H NMR spectrum at 8.5 °C in the absence of **PQX(100)**; (b) The corresponding native ^{1}H NMR spectrum. (c) Homonuclear broadband decoupled ^{1}H NMR spectrum at 38.3 °C in the presence of **PQX(100)**; (d) The corresponding native ^{1}H NMR spectrum. (e) Homonuclear broadband decoupled ^{1}H NMR spectrum at 19.4 °C in the presence of **PQX(100)**; (f) The corresponding native ^{1}H NMR spectrum. (g) Homonuclear broadband decoupled ^{1}H NMR spectrum at 8.5 °C in the presence of **PQX(100)**; (h) The corresponding native ^{1}H NMR spectrum. Note: a signal indicated by the downward arrow in spectrum (a) is attributed to an artifact with the PSYCHE pulse sequence.

Typical procedure for asymmetric Suzuki-Miyaura coupling in the presence of PQXphos and aminoacid derivatives (Table 4, entry 14).

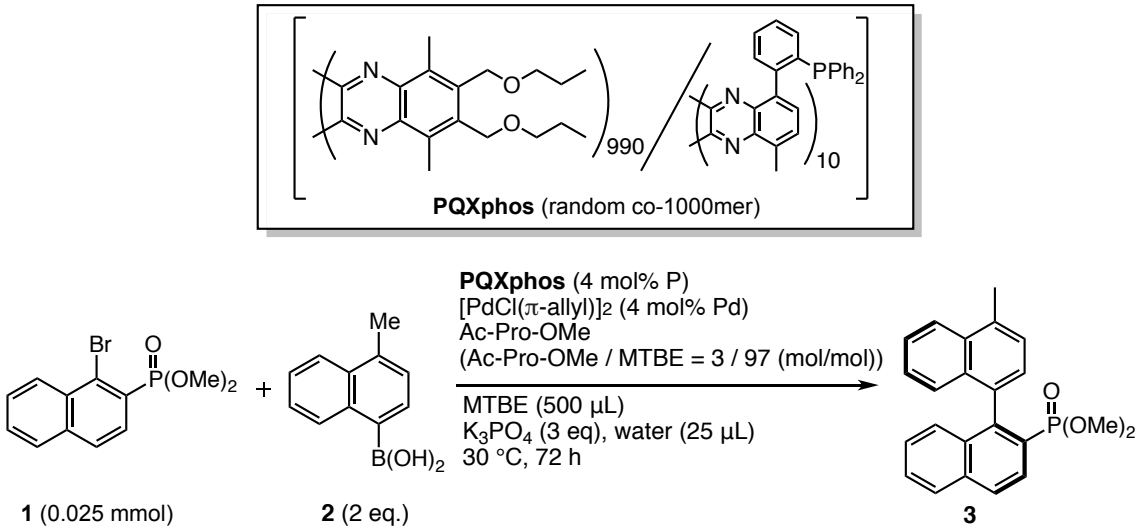

Scheme S3. Suzuki-Miyaura cross-coupling reaction using Ac-Pro-OMe in MTBE (3/97, mol/mol)

A solution of **PQXphos** (30 mg, 1.0 μmol of phosphorus atom) in MTBE (0.5 mL) was prepared in a vial, to which a THF solution of $[PdCl(\pi\text{-allyl})]_2$ (0.055 M, 9.1 μL, 0.48 μmol) was added at 30 °C. The solution was stirred at 30 °C for 1 h. To this solution, Ac-*L*-Pro-OMe (22 mg, 0.13 mmol) was added, and the resultant solution was stirred at 30 °C for 24 h. Dimethyl(1-bromonaphtahlen-2- yl)phophonate **1** (7.9 mg, 0.025 mmol), (4-methy-1-naphthalene)boronic acid **2** (9.3 mg, 0.05 mmol), K_3PO_4 (15.9 mg, 0.075 mmol) and H_2O (25 μL) were added to the solution in this order. The mixture was stirred at 30 °C for 72 h. MeCN (10 mL) was added to the reaction mixture, resulting in precipitation of the **PQXphos**. The suspension was filtrated using MeCN as an eluent. The crude product was obtained from the filtrate and subjected to PTLC (AcOEt). The product was further purified by preparative GPC to give coupling product **3** (6.0 mg, 64%). The enantiomeric excess of the product was determined by SFC with CHIRALCEL® AD-H (Eluent: CO_2/i-PrOH = 100/25, v/v, Flow rate: 3.75 mL/min, Retention time: t_R of (+)-isomer = 5.1 min, t_R of (−)-isomer = 7.8 min).

Procedure for asymmetric Suzuki-Miyaura coupling in the presence of PQXphos and aminoacid derivatives (Scheme 3).

A solution of **PQXphos** (300 mg, 10 μmol of phosphorus atom, ca. 1.0 mmol of monomer units) in MTBE (0.5 mL) was prepared in a vial, to which a THF solution of $[PdCl(\pi\text{-allyl})]_2$ (0.055 M, 91 μL, 5.0 μmol) was added at 30 °C. The mixture was stirred at 30 °C for 1 h (the photo of the

mixture is shown in Figure S1(a)). To this solution, Ac-*L*-Pro-OMe (22 mg, 0.13 mmol) was added, and the resultant viscos mixture was stirred at 30 °C for 24 h (Figure S1(b)). MTBE was removed from the solution in vacuo (Figure S1(c)). To the resultant pumice-like solid residue, were added dimethyl(1-bromonaphtahlen-2- yl)phophonate **1** (79 mg, 0.25 mmol), (4-methy-1-naphthalene)boronic acid **2** (93 mg, 0.5 mmol), K_3PO_4 (159 mg, 0.75 mmol), and 1-propanol (5.0 mL) (Figure S1(d)). The heterogeneous mixture was stirred at 30 °C for 72 h (Figure S1(e)) After removal of 1-propanol in vacuo, MeCN (20 mL) was added to the reaction mixture, and the resulting suspension was filtrated using MeCN as an eluent. The crude product was obtained by evaporation of the solvent from the filtrate and subjected to PTLC (AcOEt). The product was further purified by preparative GPC to give coupling product **3** (63 mg, 67%). The enantiomeric excess of the product was determined by SFC with CHIRALCEL® AD-H (Eluent: CO_2/i-PrOH = 100/25, v/v, Flow rate: 3.75 mL/min, Retention time: t_R of (+)-isomer = 5.1 min, t_R of (−)-isomer = 7.8 min).

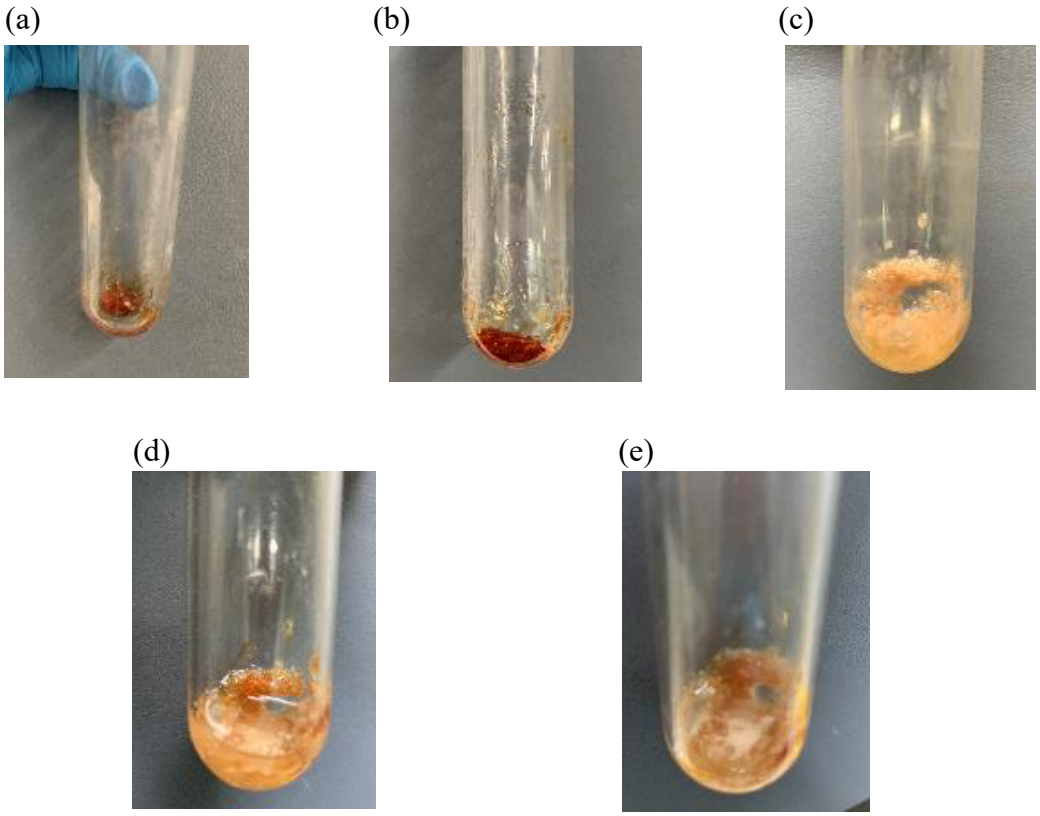

Figure S1. The photos of the reaction mixture

3 References for SI

1 Fields, D. L.; Reynolds, D. D.; Miller, J. B. Preparation of Acetoxybenzyl Bromides. *J. Org. Chem.* **1964***, 29*, 2640-2647.

2 Krimen, L. I. Acetic Formic Anhydride. *Org. Synth.* **1970**, ***50***, 1-3.

3 Ito, Y.; Ihara, E.; Uesaka, T.; Murakami, M. Synthesis of Novel Thermotropic Liquid-Crystalline Poly(2,3-Quinoxaline)s. *Macromolecules* **1992**, *25*, 6711-6713.

4 Sferrazza, A.; Triolo, A.; Migneco, L.; Caminiti, R. Synthesis and Small and Wide Angle X-Ray Scattering Characterization of L-Proline Based Chiral Ionic Liquids. *Curr. Org. Chem* **2015**, ***18***, 99-104.

5 Damodara, R.; Ravula, T.; Shama, T.; Erode, P. A method for stabilizing the cis prolyl peptide bond: influence of an unusual $n \rightarrow \pi^*$ interaction in 1,3-oxazine and 1,3-thiazine containing peptidomimetics. *Tetrahedron Lett.* **2012***, 53*, 4413-4417.

6 Nieves, P.; Dionisio, R.; Haydee, V.; Ricardo, M.; Daniel, M. M.; Belen, C.; Concepcion C. G.; Antonio J. H. Chemoselective Intramolecular Functionalization of Methyl Groups in Nonconstrained Molecules Promoted by N-Iodosulfonamides. *Org. Lett.* **17**, 2370-2373 (2015).

7 Nagata, Y.; Yamada, T.; Adachi, T.; Akai, Y.; Yamamoto, T.; Suginome, M. Solvent-Dependent Switch of Helical Main-Chain Chirality in Sergeants-and-Soldiers-Type Poly(quinoxaline-2,3-diyl)s: Effect of the Position and Structures of the “Sergeant” Chiral Units on the Screw-Sense Induction, *J. Am. Chem. Soc.* **2013**, *135*, 10104-10113.

8 Lifson, S.; Andreola, C.; Peterson, N. C.; Green, M. M. Macromolecular Stereochemistry: Helical Sense Preference in Optically Active Polyisocyanates. Amplification of a Conformational Equilibrium Deuterium Isotope Effect, *J. Am. Chem. Soc.* **1989**, *111*, 8850−8858

4 UV-vis and CD Spectra

-for Table 1, entry 1

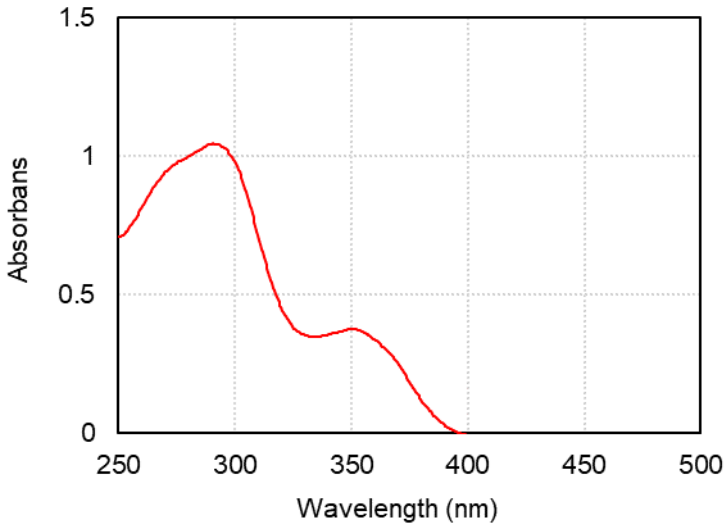

Figure S2. UV-vis absorption spectrum of PQX 100mer in THF containing Boc-*L*-Pro-OMe (2.10×10^{-1} g/L, path length = 1.0 mm).

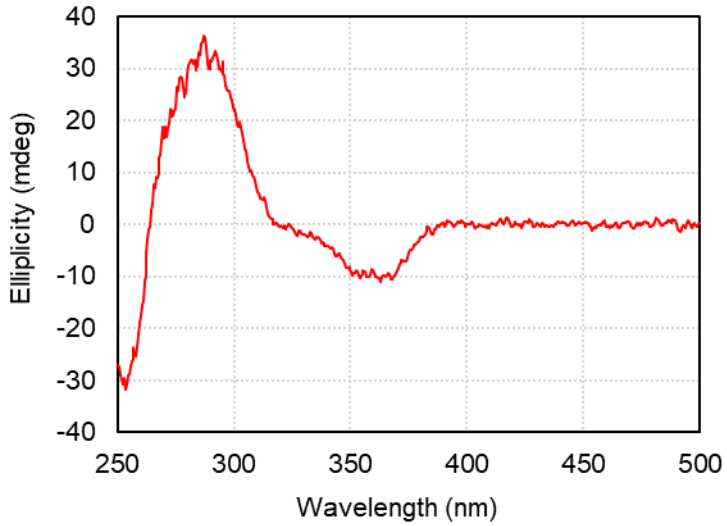

Figure S3. CD spectrum of PQX 100mer in THF containing Boc-*L*-Pro-OMe (2.10×10^{-1} g/L, path length = 1.0 mm).

-for Table 1, entry 2

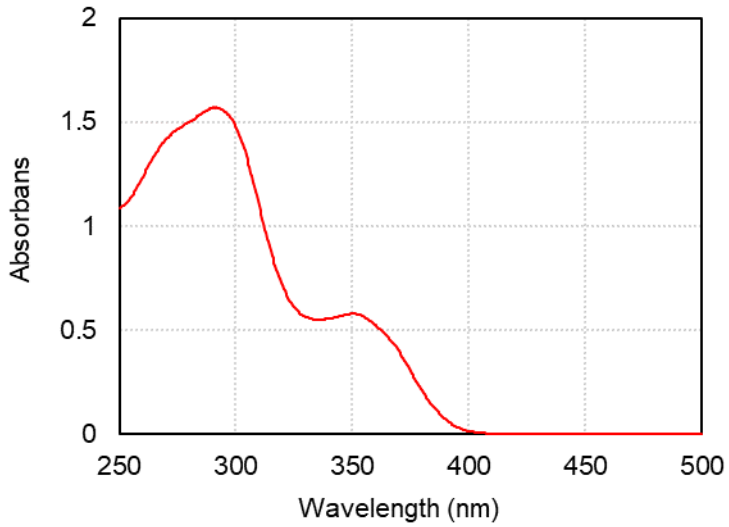

Figure S4. UV-vis absorption spectrum of PQX 100mer in THF containing Boc-*D*-Pip-OMe (2.10×10^{-1} g/L, path length = 1.0 mm).

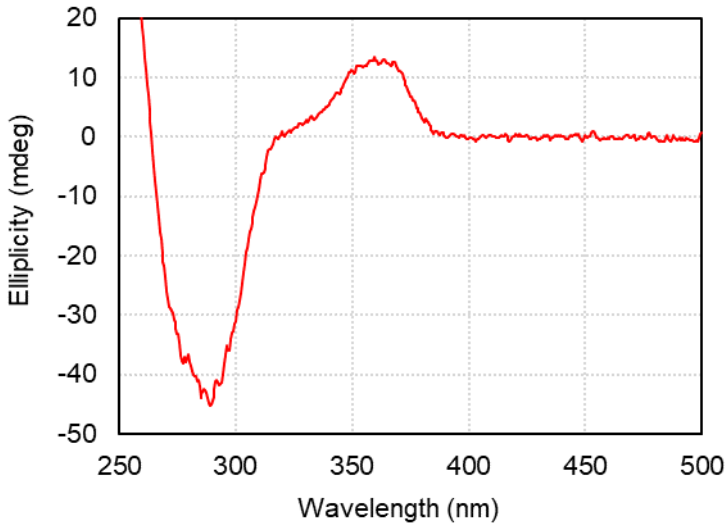

Figure S5. CD spectrum of PQX 100mer in THF containing Boc-*D*-Pip-OMe (2.10×10^{-1} g/L, path length = 1.0 mm).

-for Table 1, entry 3

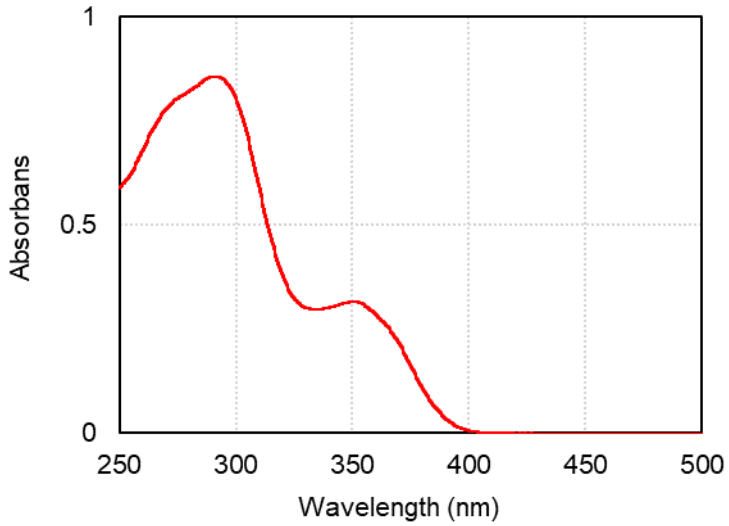

Figure S6. UV-vis absorption spectrum of PQX 100mer in THF containing Boc-*L*-Ala-OMe (2.10×10^{-1} g/L, path length = 1.0 mm).

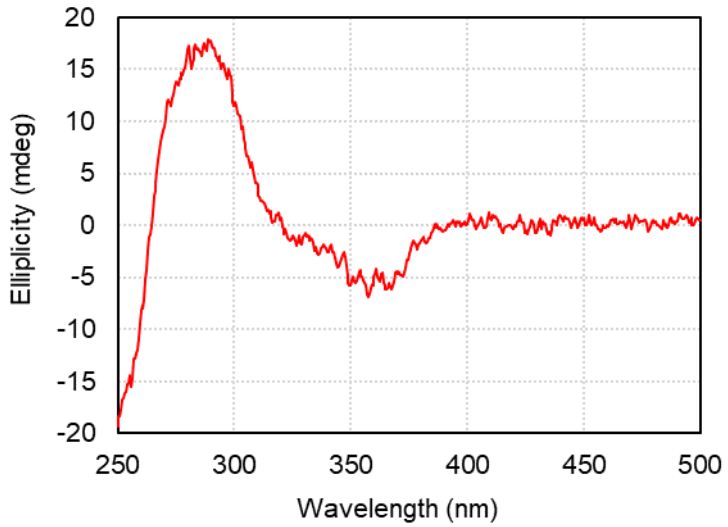

Figure S7. CD spectrum of PQX 100mer in THF containing Boc-*L*-Ala-OMe (2.10×10^{-1} g/L, path length = 1.0 mm).

-for Table 1, entry 4

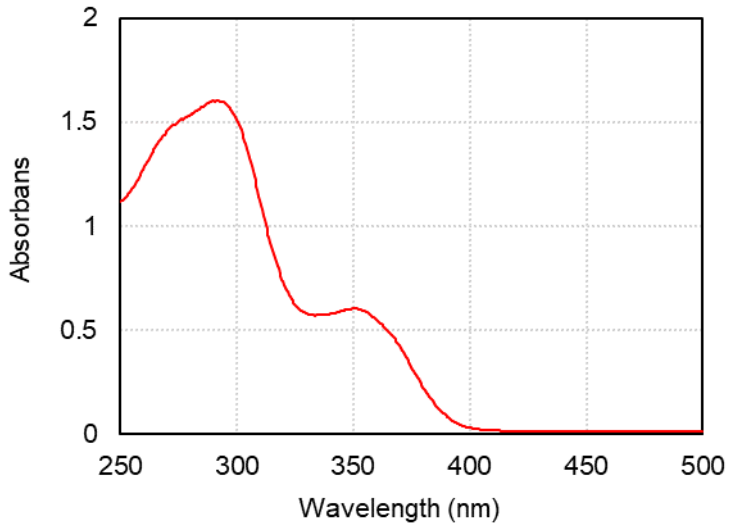

Figure S8. UV-vis absorption spectrum of PQX 100mer in THF containing Boc-*L*-Thr-OMe (2.10×10^{-1} g/L, path length = 1.0 mm).

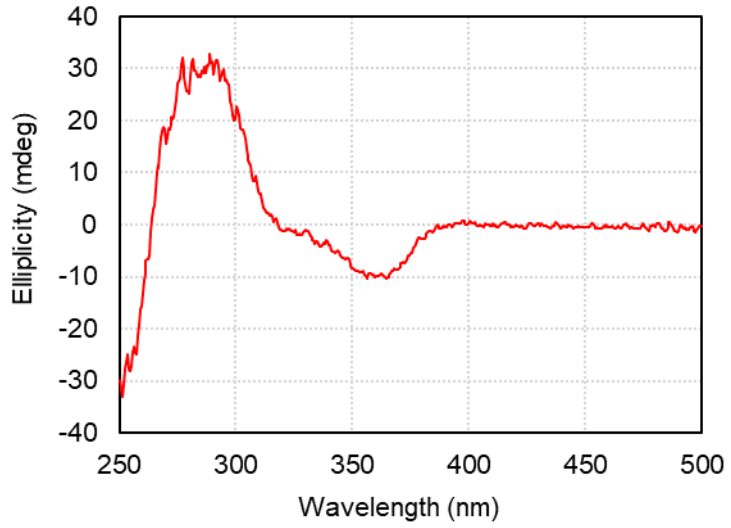

Figure S9. CD spectrum of PQX 100mer in THF containing Boc-*L*-Thr-OMe (2.10×10^{-1} g/L, path length = 1.0 mm).

-for Table 1, entry 5

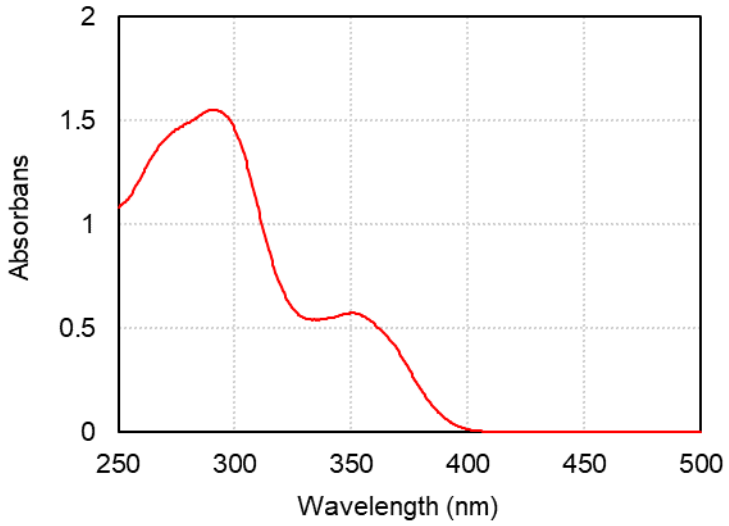

Figure S10. UV-vis absorption spectrum of PQX 100mer in THF containing Boc-*L*-*t*-Leu-OMe (2.10×10^{-1} g/L, path length = 1.0 mm).

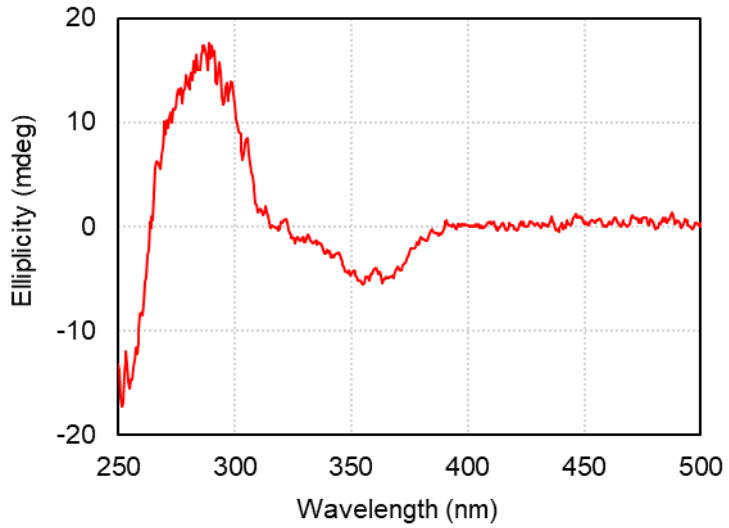

Figure S11. CD spectrum of PQX 100mer in THF containing Boc-*L*-*t*-Leu-OMe (2.10×10^{-1} g/L, path length = 1.0 mm).

-for Table 1, entry 6

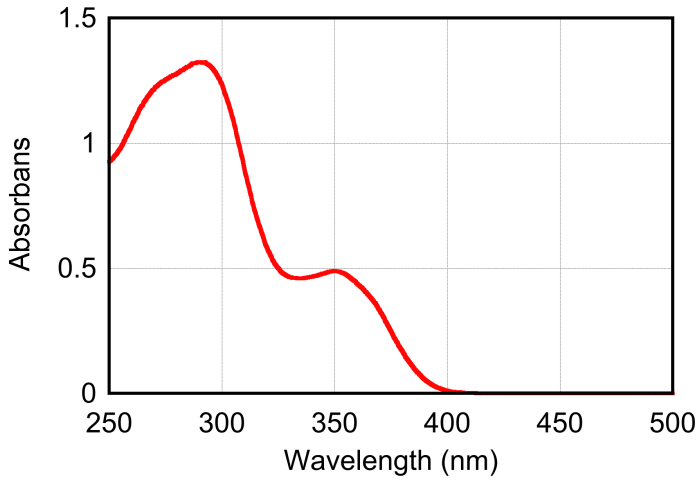

Figure S12. UV-vis absorption spectrum of PQX 100mer in THF containing Boc-*L*-Glu(OMe)-OMe (2.10×10^{-1} g/L, path length = 1.0 mm).

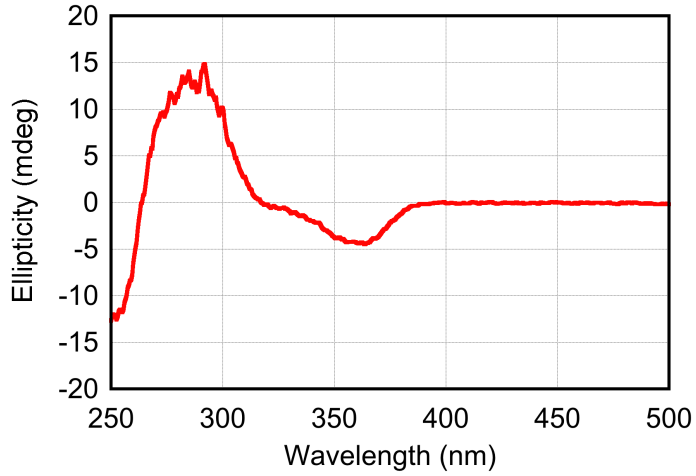

Figure S13. CD spectrum of PQX 100mer in THF containing Boc-*L*-Glu(OMe)-OMe (2.10×10^{-1} g/L, path length = 1.0 mm).

-for Table 1, entry 7

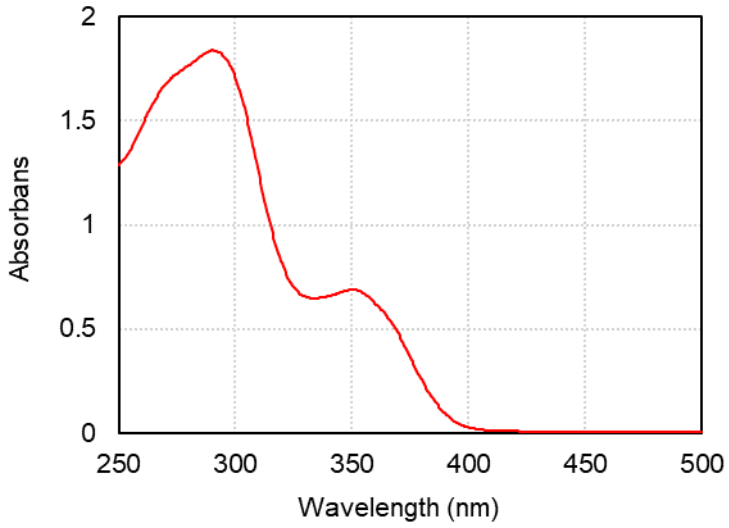

Figure S14. UV-vis absorption spectrum of PQX 100mer in THF containing Boc-*L*-Ile-OMe (2.10×10^{-1} g/L, path length = 1.0 mm).

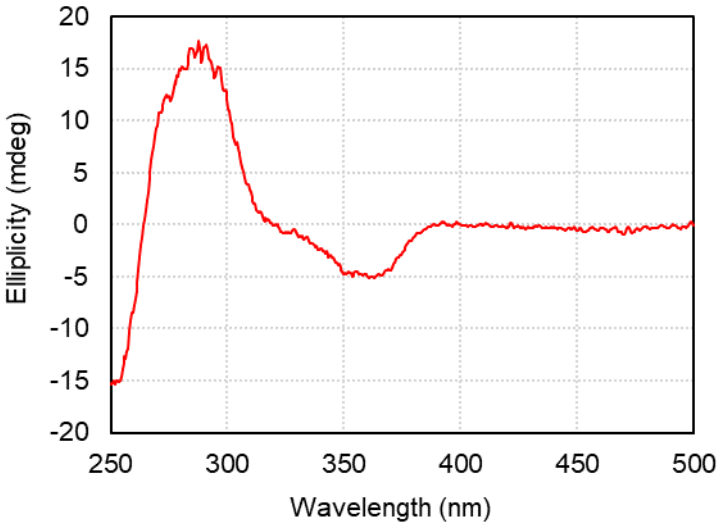

Figure S15. CD spectrum of PQX 100mer in THF containing Boc-*L*-Ile-OMe (2.10×10^{-1} g/L, path length = 1.0 mm).

-for Table 1, entry 8

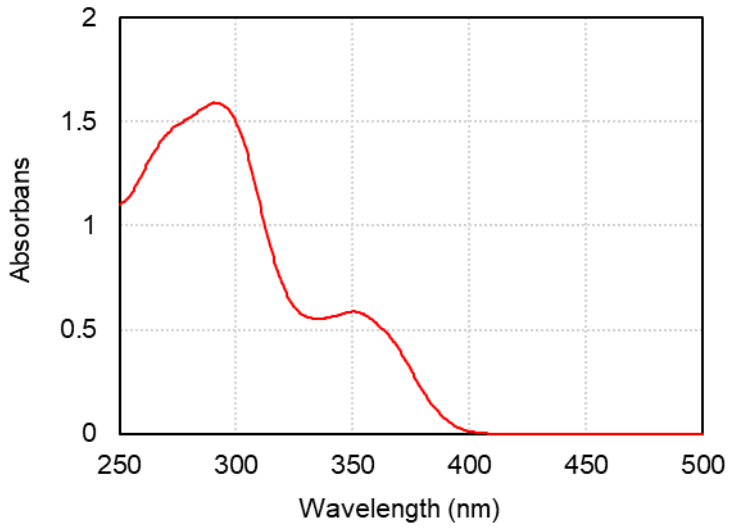

Figure S16. UV-vis absorption spectrum of PQX 100mer in THF containing Boc-*L*-Asn-OMe (2.10×10^{-1} g/L, path length = 1.0 mm).

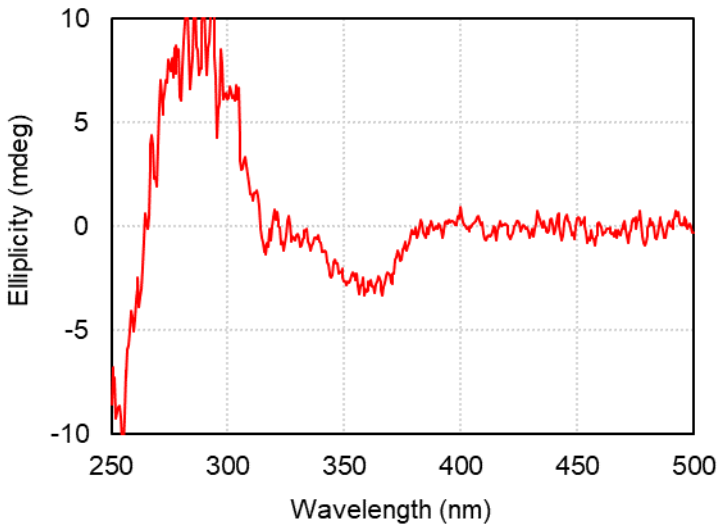

Figure S17. CD spectrum of PQX 100mer in THF containing Boc-*L*-Asn-OMe (2.10×10^{-1} g/L, path length = 1.0 mm).

-for Table 1, entry 9

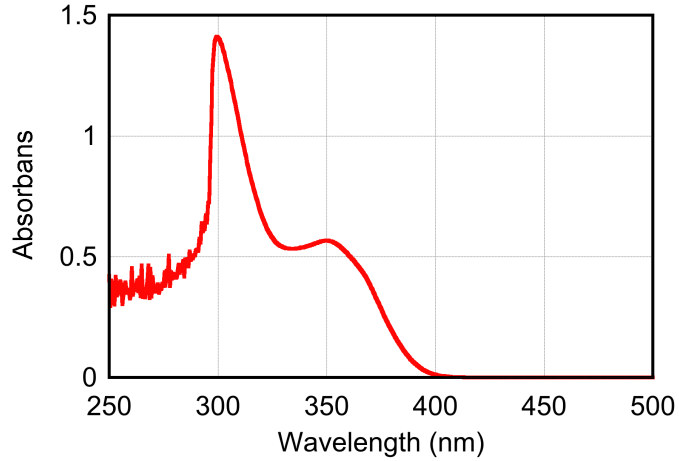

Figure S18. UV-vis absorption spectrum of PQX 100mer in THF containing Boc-*L*-Tyr-OMe (2.10×10^{-1} g/L, path length = 1.0 mm).

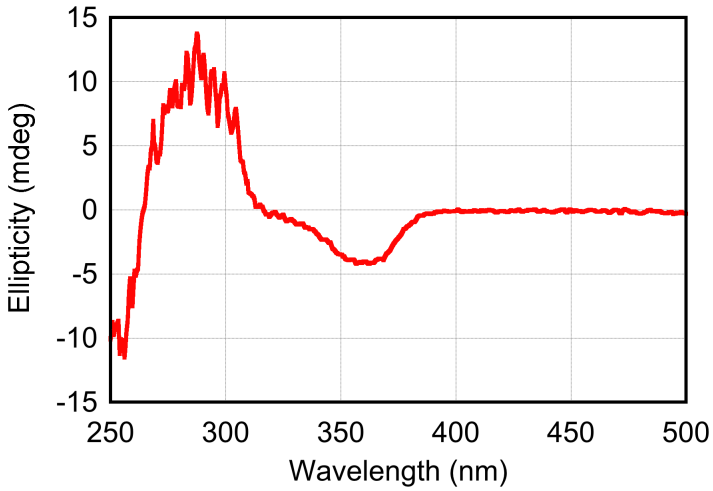

Figure S19. CD spectrum of PQX 100mer in THF containing Boc-*L*-Tyr-OMe (2.10×10^{-1} g/L, path length = 1.0 mm).

-for Table 1, entry 10

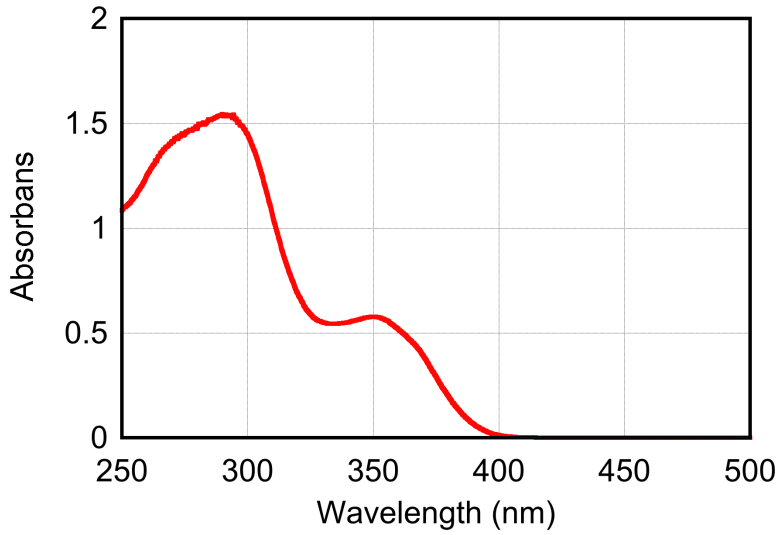

Figure S20. UV-vis absorption spectrum of PQX 100mer in THF containing Boc-*L*-Ser-OMe (2.10×10^{-1} g/L, path length = 1.0 mm).

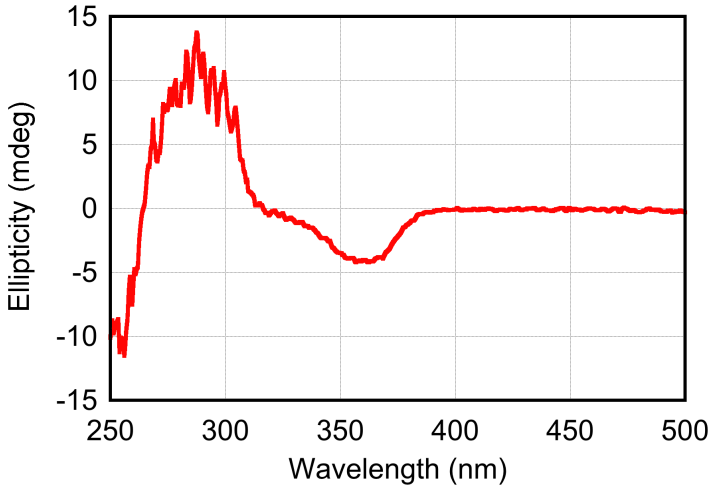

Figure S21. CD spectrum of PQX 100mer in THF containing Boc-*L*-Ser-OMe (2.10×10^{-1} g/L, path length = 1.0 mm).

-for Table 1, entry 11

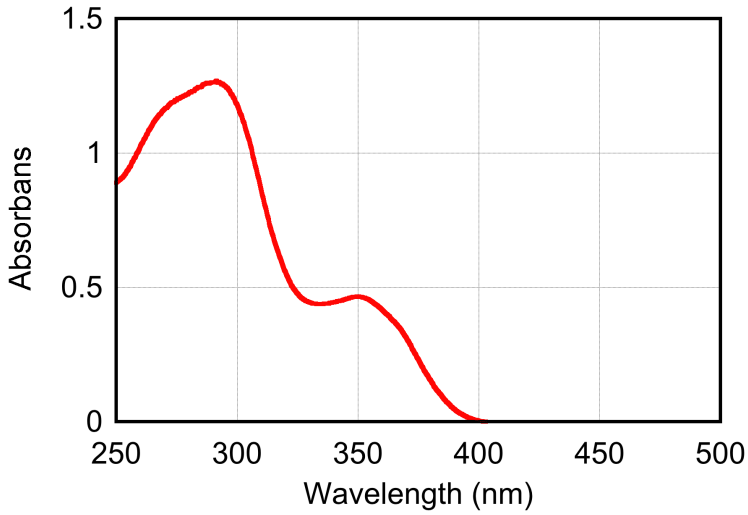

Figure S22. UV-vis absorption spectrum of PQX 100mer in THF containing Boc-*L*-Gln-OMe (2.10×10^{-1} g/L, path length = 1.0 mm).

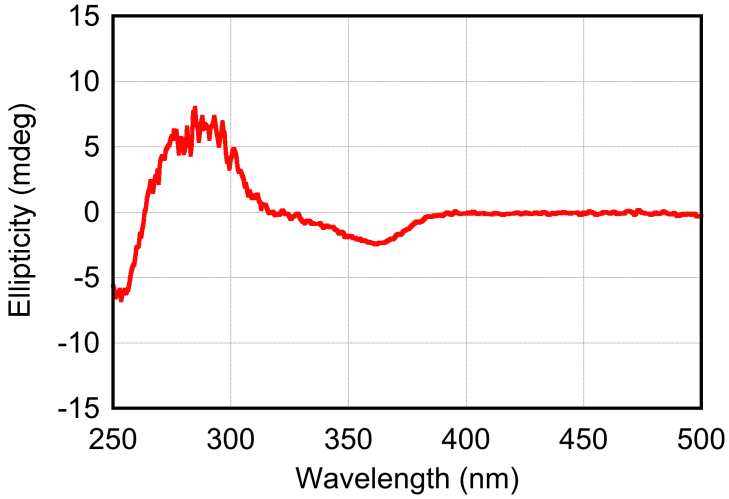

Figure S23. CD spectrum of PQX 100mer in THF containing Boc-*L*-Gln-OMe (2.10×10^{-1} g/L, path length = 1.0 mm).

-for Table 1, entry 12

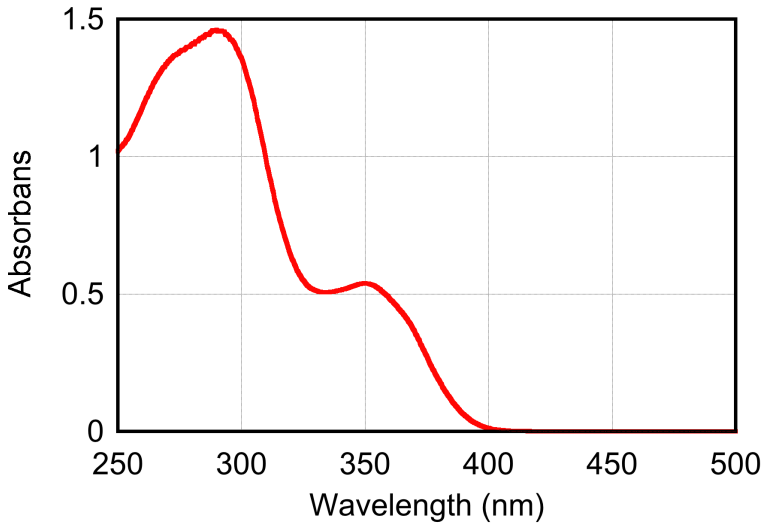

Figure S24. UV-vis absorption spectrum of PQX 100mer in THF containing Boc-*L*-Val-OMe (2.10×10^{-1} g/L, path length = 1.0 mm).

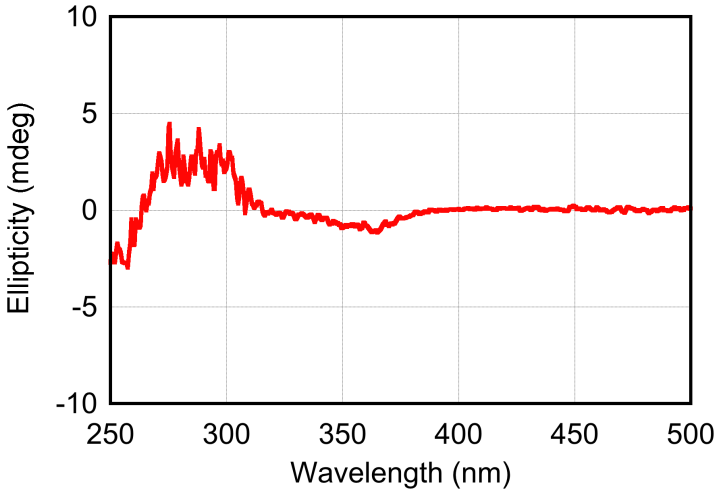

Figure S25. CD spectrum of PQX 100mer in THF containing Boc-*L*-Val-OMe (2.10×10^{-1} g/L, path length = 1.0 mm).

-for Table 1, entry 13

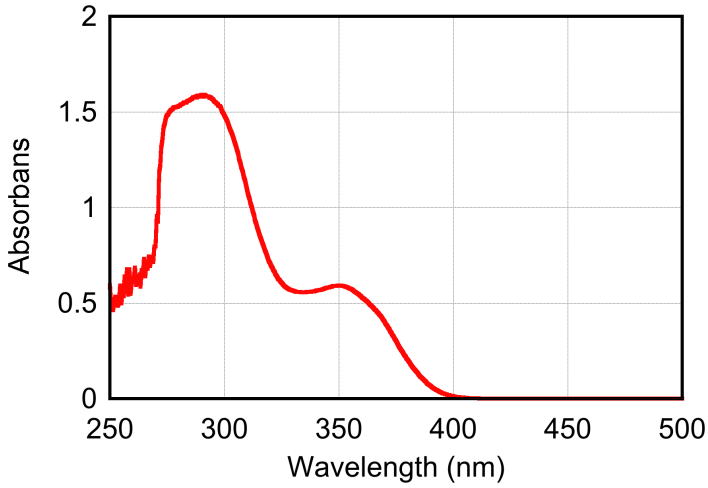

Figure S26. UV-vis absorption spectrum of PQX 100mer in THF containing Boc-*L*-Phe-OMe (2.10×10^{-1} g/L, path length = 1.0 mm).

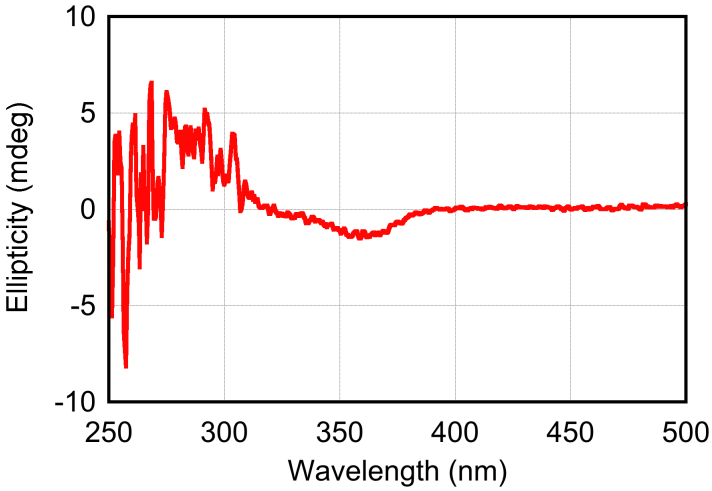

Figure S27. CD spectrum of PQX 100mer in THF containing Boc-*L*-Phe-OMe (2.10×10^{-1} g/L, path length = 1.0 mm).

-for Table 1, entry 14

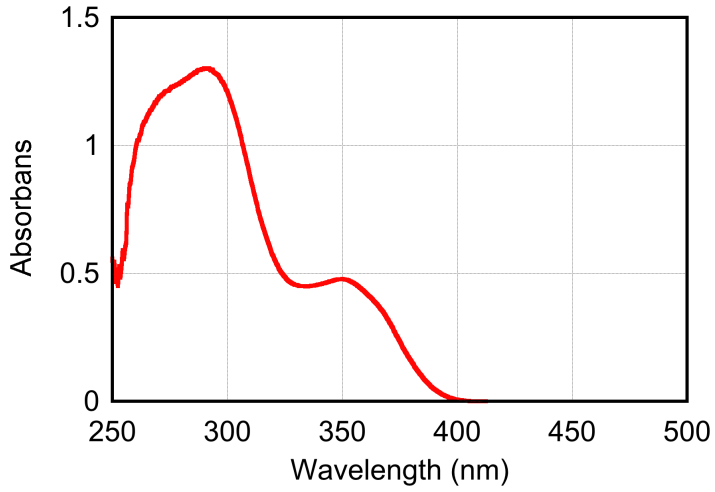

Figure S28. UV-vis absorption spectrum of PQX 100mer in THF containing Boc-*L*-Cys-OMe (2.10×10^{-1} g/L, path length = 1.0 mm).

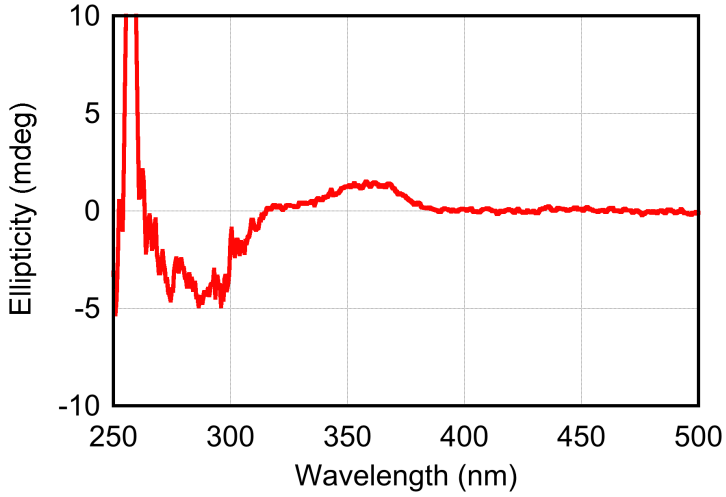

Figure S29. CD spectrum of PQX 100mer in THF containing Boc-*L*-Cys-OMe (2.10×10^{-1} g/L, path length = 1.0 mm).

-for Table 1, entry 15

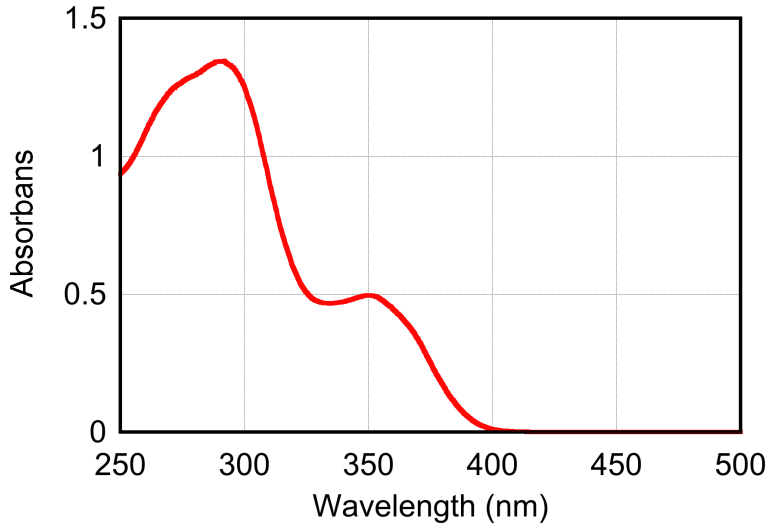

Figure S30. UV-vis absorption spectrum of PQX 100mer in THF containing Boc-*L*-Asp(OMe)-OMe (2.10×10^{-1} g/L, path length = 1.0 mm).

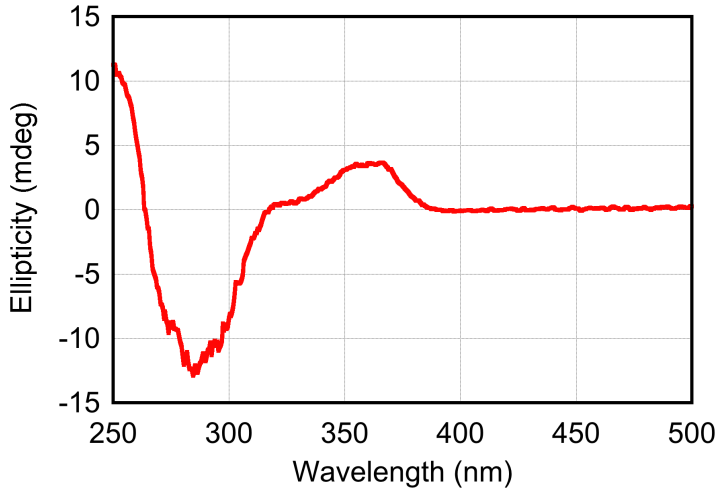

Figure S31. CD spectrum of PQX 100mer in THF containing Boc-*L*-Asp(OMe)-OMe (2.10×10^{-1} g/L, path length = 1.0 mm).

-for Table 1, entry 16

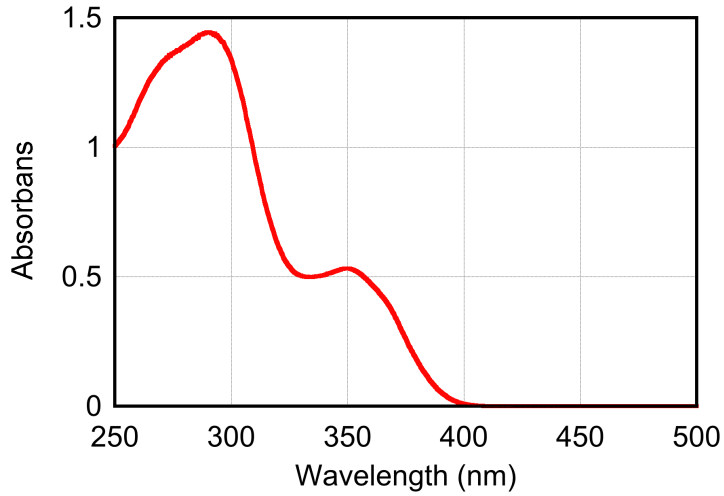

Figure S32. UV-vis absorption spectrum of PQX 100mer in THF containing Boc-*L*-Leu-OMe (2.10×10^{-1} g/L, path length = 1.0 mm).

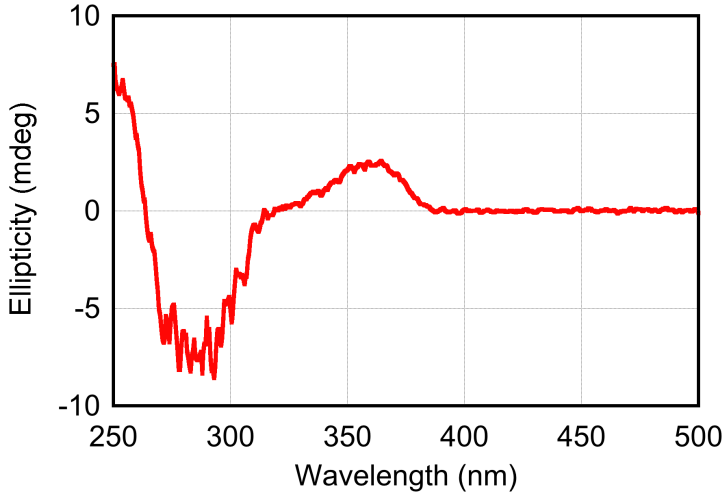

Figure S33. CD spectrum of PQX 100mer in THF containing Boc-*L*-Leu-OMe (2.10×10^{-1} g/L, path length = 1.0 mm).

-for Table 2, entry 2

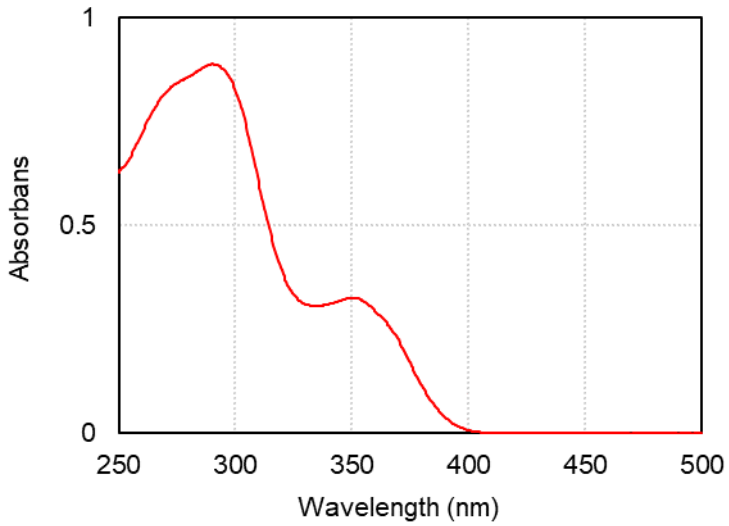

Figure S34. UV-vis absorption spectrum of PQX 100mer in THF containing Boc-*L*-Pro-NH_2 (2.10×10^{-1} g/L, path length = 1.0 mm).

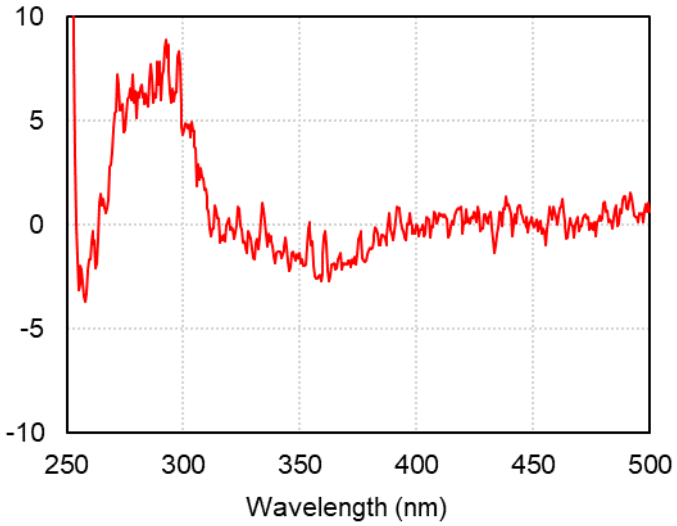

Figure S35. CD spectrum of PQX 100mer in THF containing Boc-*L*-Ala-OMe (2.10×10^{-1} g/L, path length = 1.0 mm).

-for Table 2, entry 3

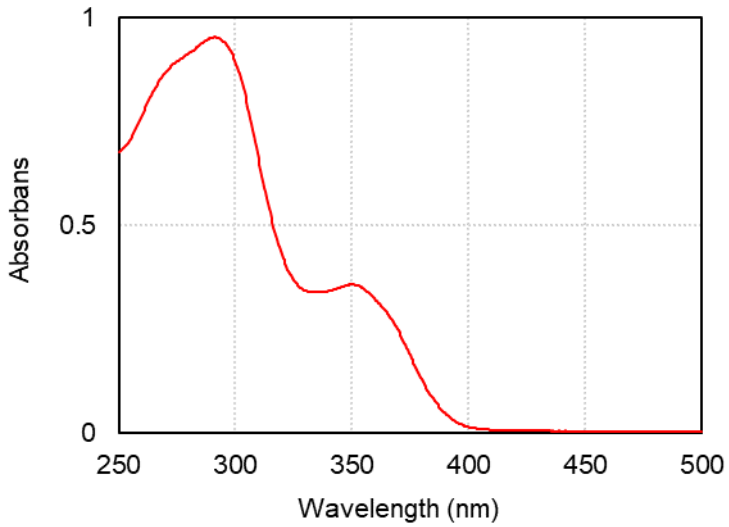

Figure S36. UV-vis absorption spectrum of PQX 100mer in THF containing Boc-*L*-Pro-OH (2.10×10^{-1} g/L, path length = 1.0 mm).

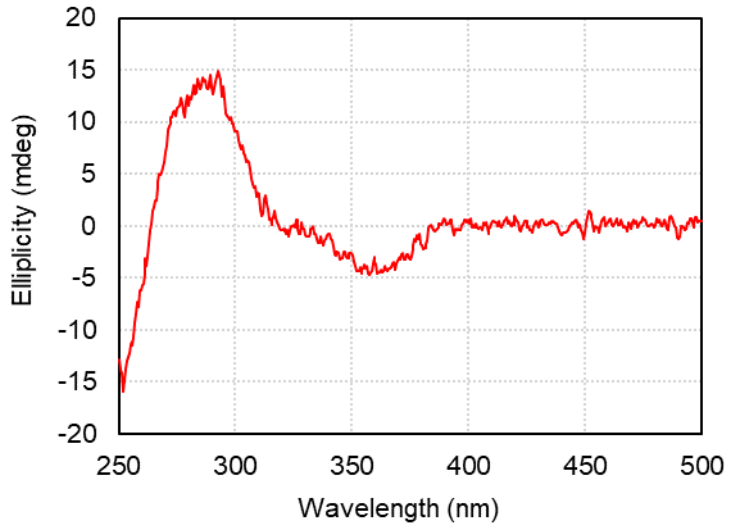

Figure S37. CD spectrum of PQX 100mer in THF containing Boc-*L*-Pro-OH (2.10×10^{-1} g/L, path length = 1.0 mm).

-for Table 2, entry 4

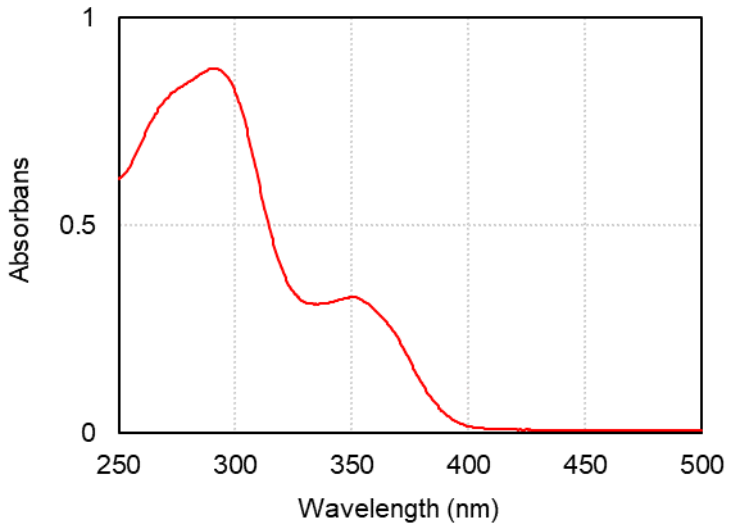

Figure S38. UV-vis absorption spectrum of PQX 100mer in THF containing Boc-*L*-Pro-OEt (2.10×10^{-1} g/L, path length = 1.0 mm).

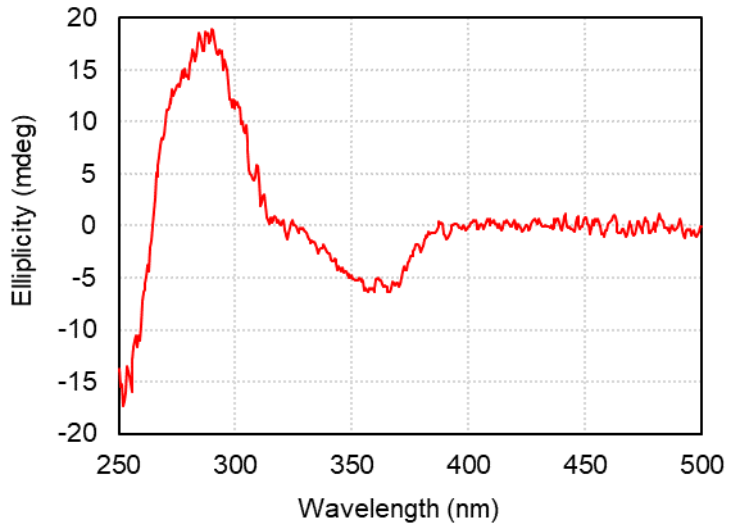

Figure S39. CD spectrum of PQX 100mer in THF containing Boc-*L*-Pro-OEt (2.10×10^{-1} g/L, path length = 1.0 mm).

-for Table 2, entry 5

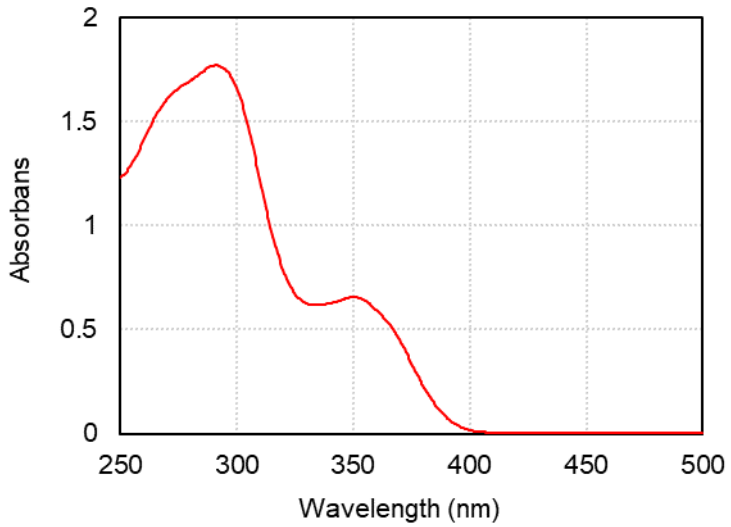

Figure S40. UV-vis absorption spectrum of PQX 100mer in THF containing Boc-*L*-Pro-O-*n*-C_6H_{13} (2.10×10^{-1} g/L, path length = 1.0 mm).

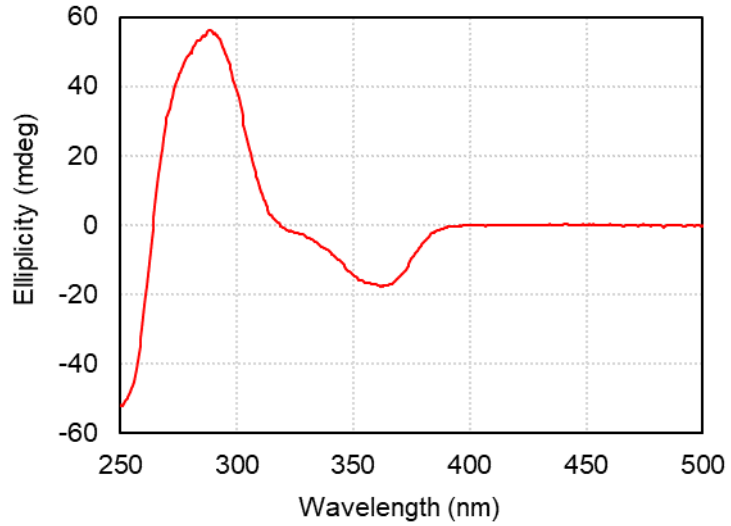

Figure S41. CD spectrum of PQX 100mer in THF containing Boc-*L*-Pro-O-*n*-C_6H_{13} (2.10×10^{-1} g/L, path length = 1.0 mm).

-for Table 2, entry 6

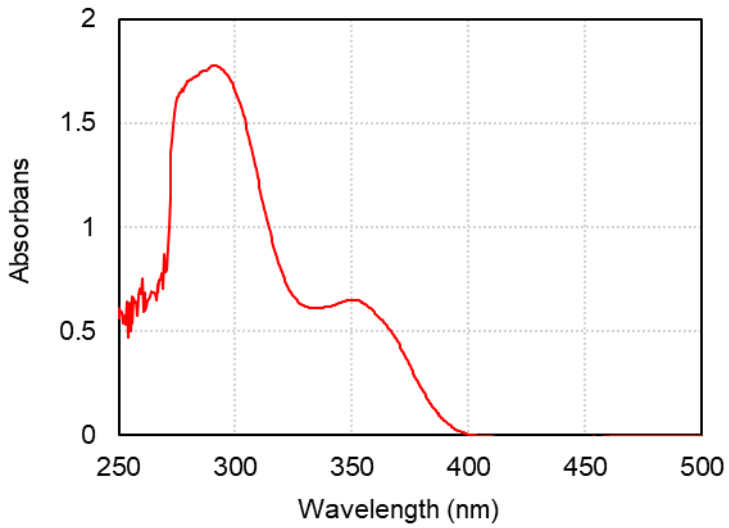

Figure S42. UV-vis absorption spectrum of PQX 100mer in THF containing Cbz-*L*-Pro-OMe (2.10×10^{-1} g/L, path length = 1.0 mm).

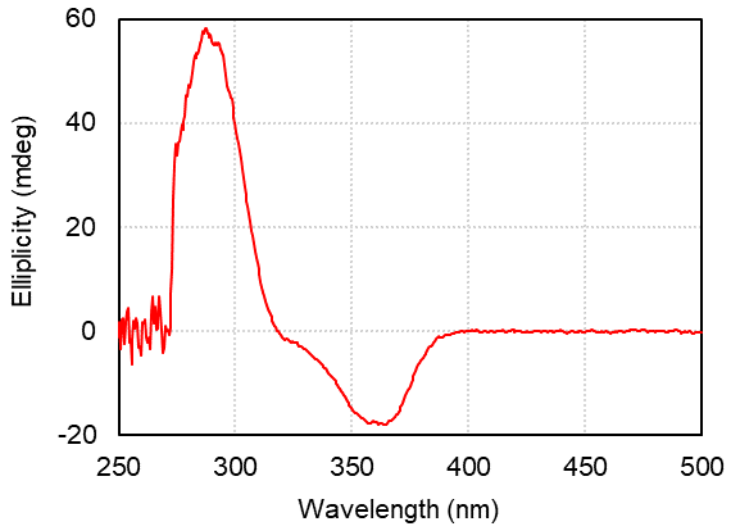

Figure S43. CD spectrum of PQX 100mer in THF containing Cbz-*L*-Pro-OMe (2.10×10^{-1} g/L, path length = 1.0 mm).

-for Table 2, entry 7

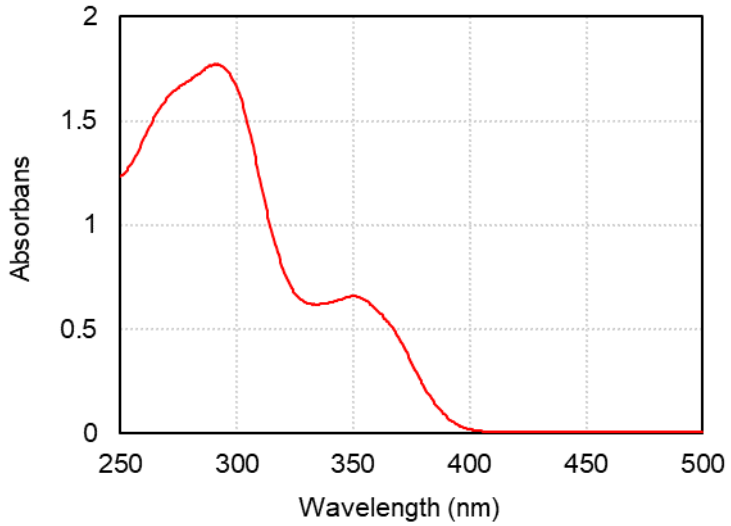

Figure S44. UV-vis absorption spectrum of PQX 100mer in THF containing Piv-*L*-Pro-OMe (2.10×10^{-1} g/L, path length = 1.0 mm).

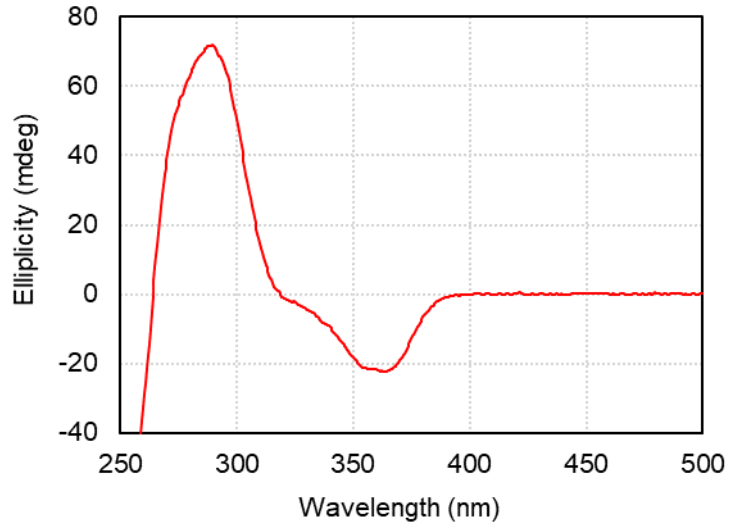

Figure S45. CD spectrum of PQX 100mer in THF containing Piv-*L*-Pro-OMe (2.10×10^{-1} g/L, path length = 1.0 mm).

-for Table 2, entry 8

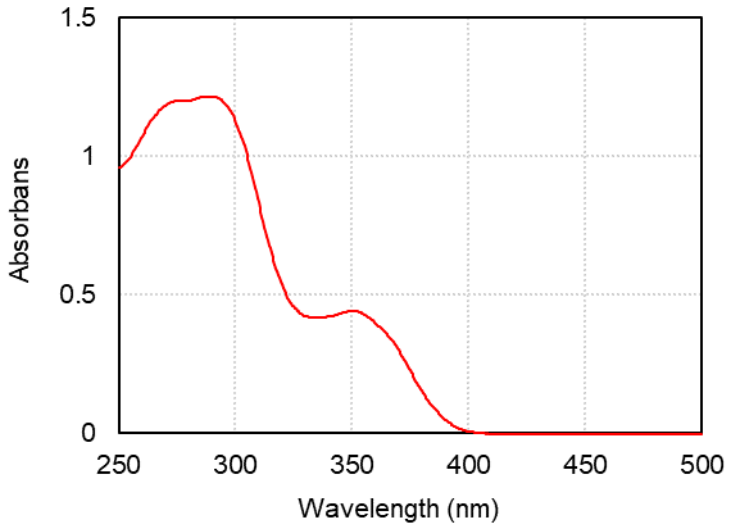

Figure S46. UV-vis absorption spectrum of PQX 100mer in THF containing Ac-*L*-Pro-OMe (2.10×10^{-1} g/L, path length = 1.0 mm).

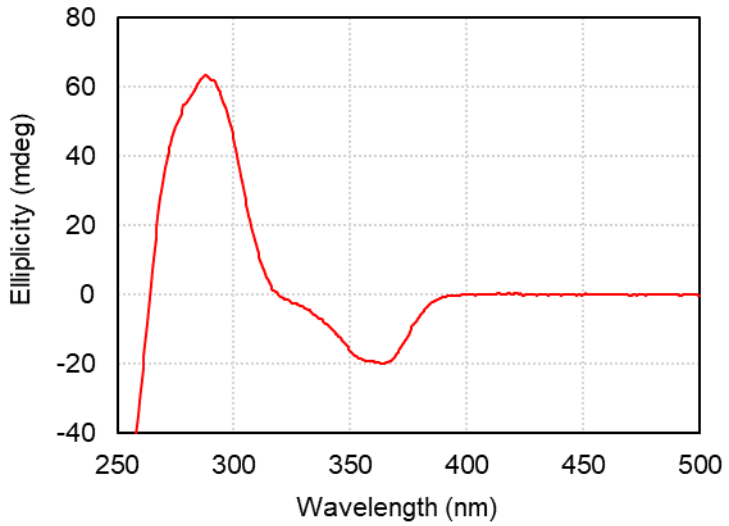

Figure S47. CD spectrum of PQX 100mer in THF containing Ac-*L*-Pro-OMe (2.10×10^{-1} g/L, path length = 1.0 mm).

-for Table 2, entry 9

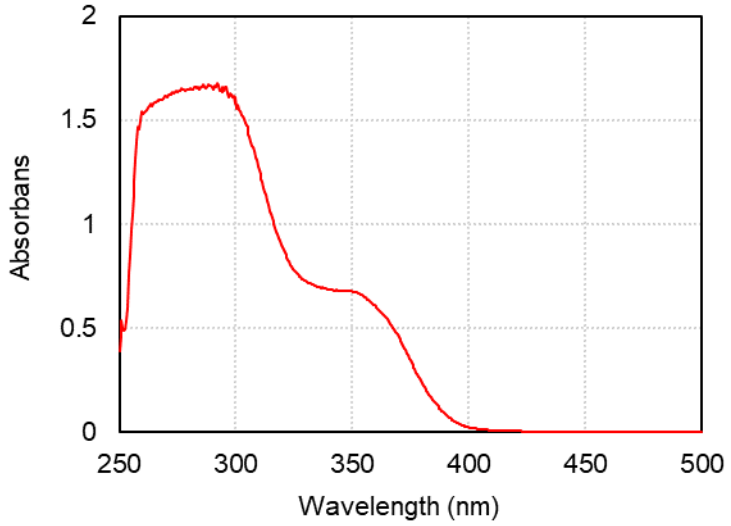

Figure S48. UV-vis absorption spectrum of PQX 100mer in THF containing TFAc-*L*-Pro-OMe (2.10×10^{-1} g/L, path length = 1.0 mm).

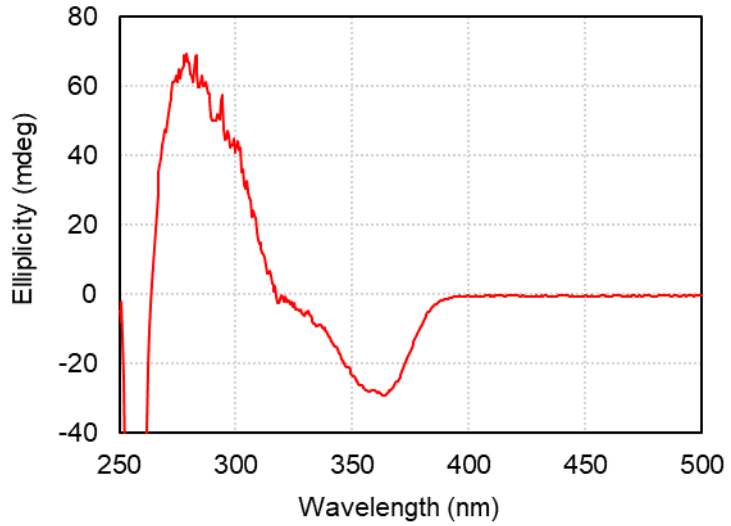

Figure S49. CD spectrum of PQX 100mer in THF containing TFAc-*L*-Pro-OMe (2.10×10^{-1} g/L, path length = 1.0 mm).

-for Figure 1, TFAc-*L*-Pro-OMe in $CHCl_3$

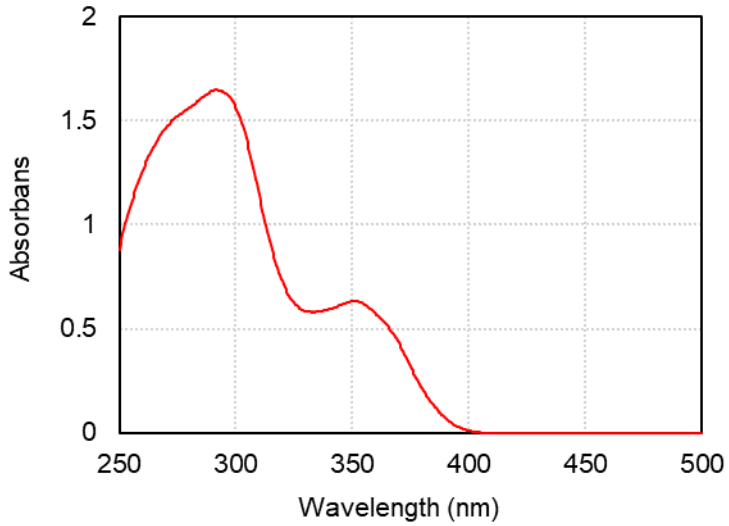

Figure S50. UV-vis absorption spectrum of PQX 30mer in $CHCl_3$ containing TFAc-*L*-Pro-OMe (2.35×10^{-1} g/L, path length = 1.0 mm).

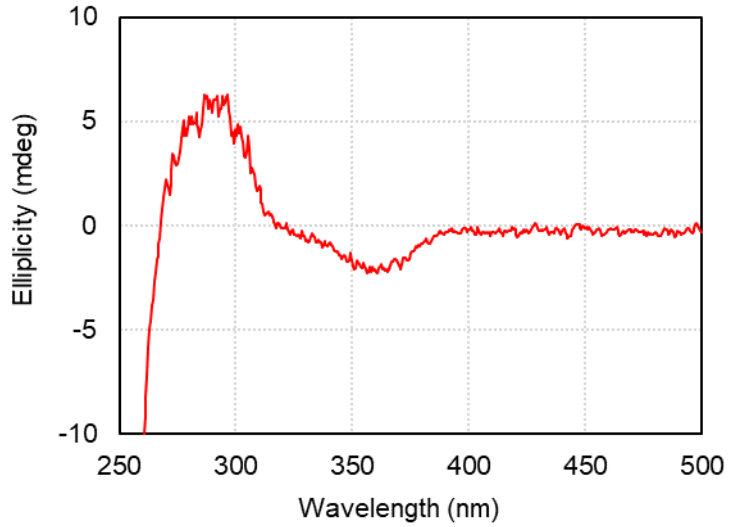

Figure S51. CD spectrum of PQX 30mer in $CHCl_3$ containing TFAc-*L*-Pro-OMe (2.35×10^{-1} g/L, path length = 1.0 mm).

-for Figure 1, TFAc-*L*-Pro-OMe in CH_2Cl_2

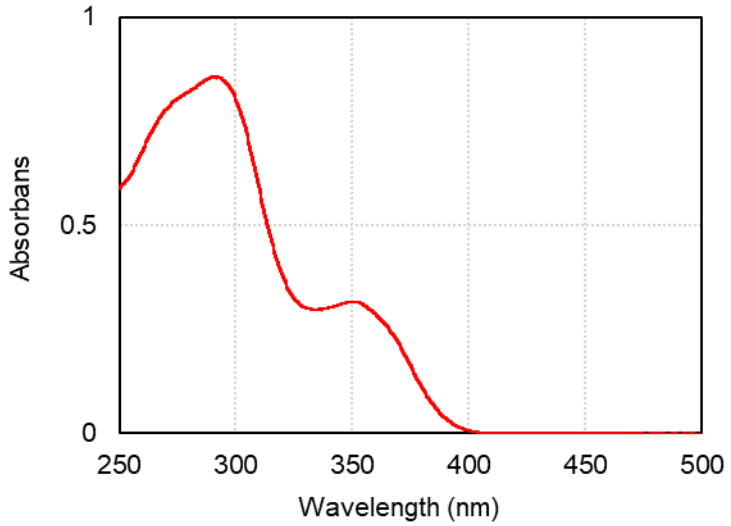

Figure S52. UV-vis absorption spectrum of PQX 30mer in CH_2Cl_2 containing TFAc-*L*-Pro-OMe (2.35×10^{-1} g/L, path length = 1.0 mm).

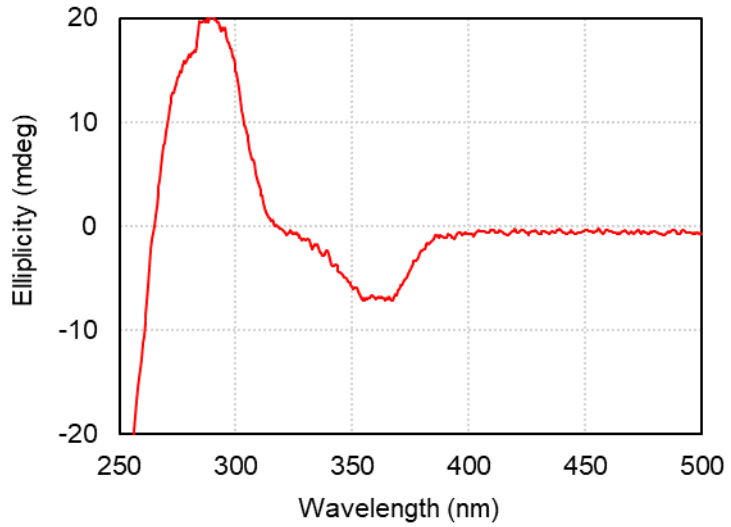

Figure S53. CD spectrum of PQX 30mer in CH_2Cl_2 containing TFAc-*L*-Pro-OMe (2.35×10^{-1} g/L, path length = 1.0 mm).

-for Figure 1, TFAc-*L*-Pro-OMe in 1,2-DCE

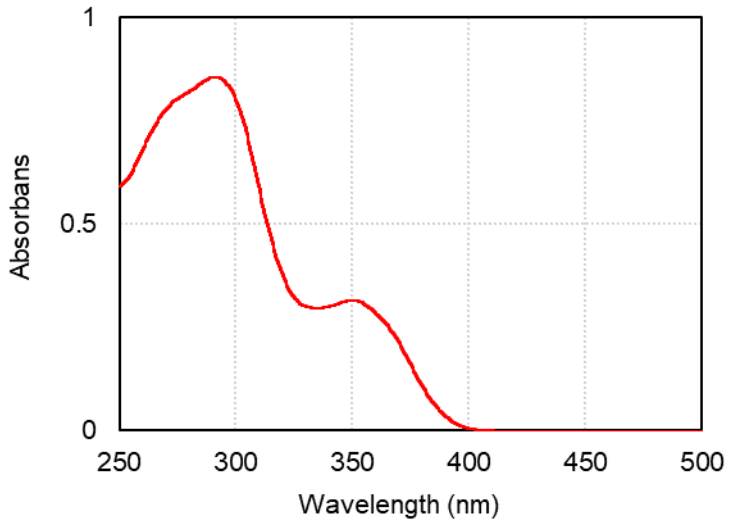

Figure S54. UV-vis absorption spectrum of PQX 30mer in 1,2-DCE containing TFAc-*L*-Pro-OMe (2.35×10^{-1} g/L, path length = 1.0 mm).

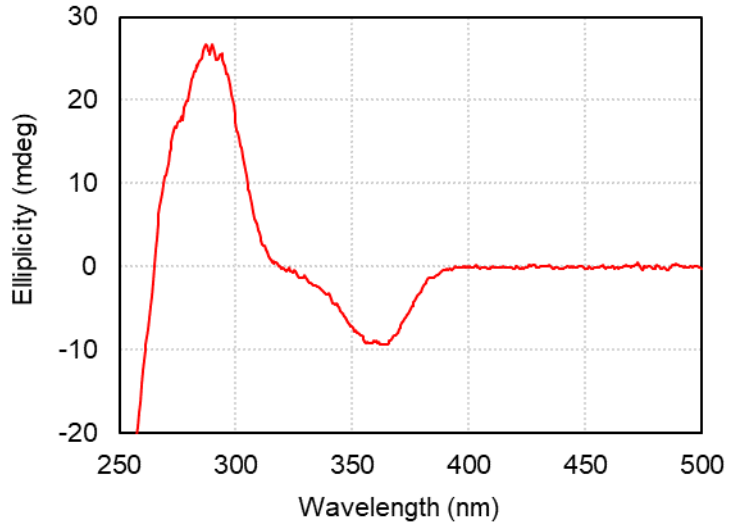

Figure S55. CD spectrum of PQX 30mer in 1,2-DCE containing TFAc-*L*-Pro-OMe (2.35×10^{-1} g/L, path length = 1.0 mm).

-for Figure 1, TFAc-*L*-Pro-OMe in toluene

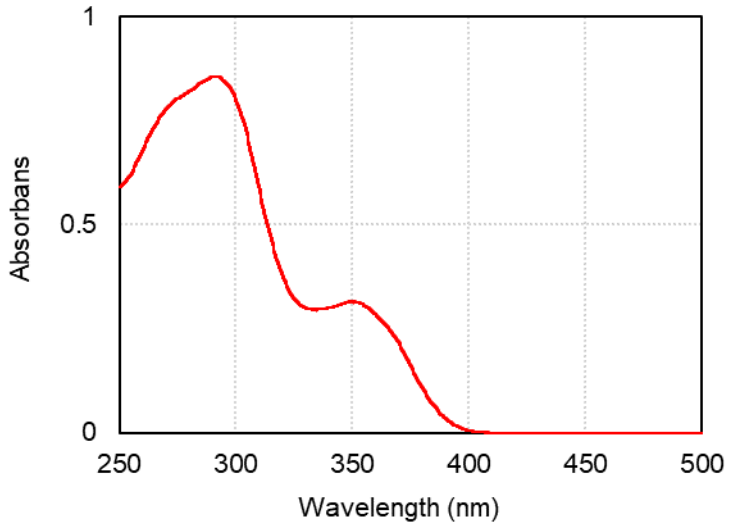

Figure S56. UV-vis absorption spectrum of PQX 30mer in toluene containing TFAc-*L*-Pro-OMe (2.35×10^{-1} g/L, path length = 1.0 mm).

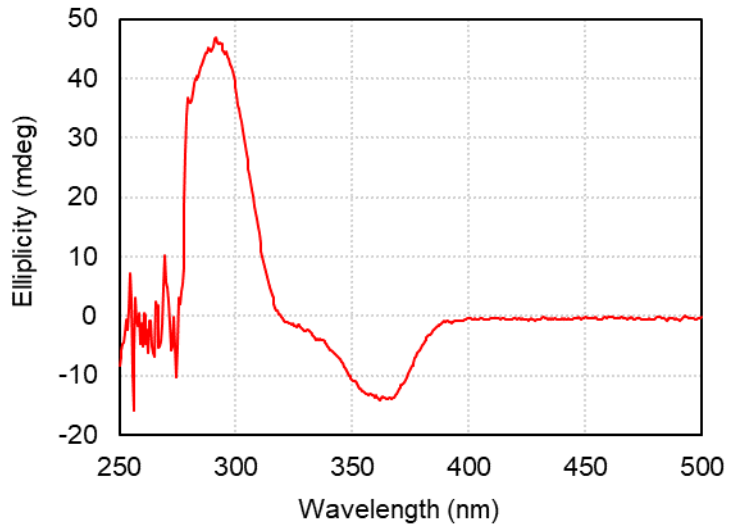

Figure S57. CD spectrum of PQX 30mer in toluene containing TFAc-*L*-Pro-OMe (2.35×10^{-1} g/L, path length = 1.0 mm).

-for Figure 1, TFAc-*L*-Pro-OMe in THF

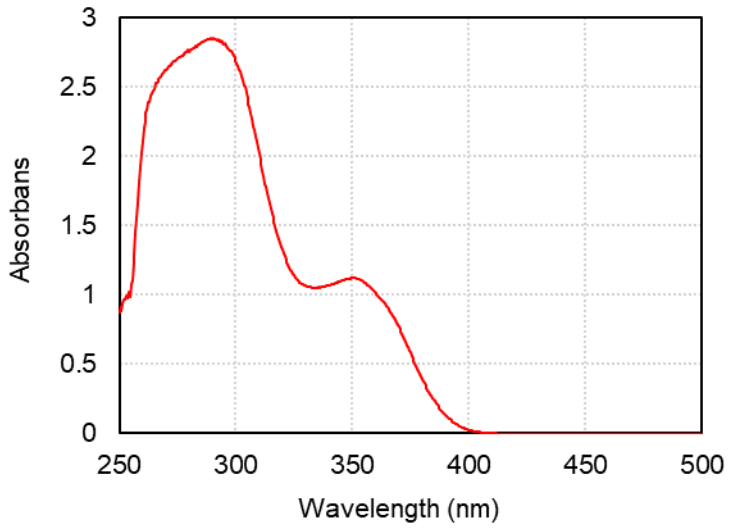

Figure S58. UV-vis absorption spectrum of PQX 30mer in THF containing TFAc-*L*-Pro-OMe (2.35×10^{-1} g/L, path length = 1.0 mm).

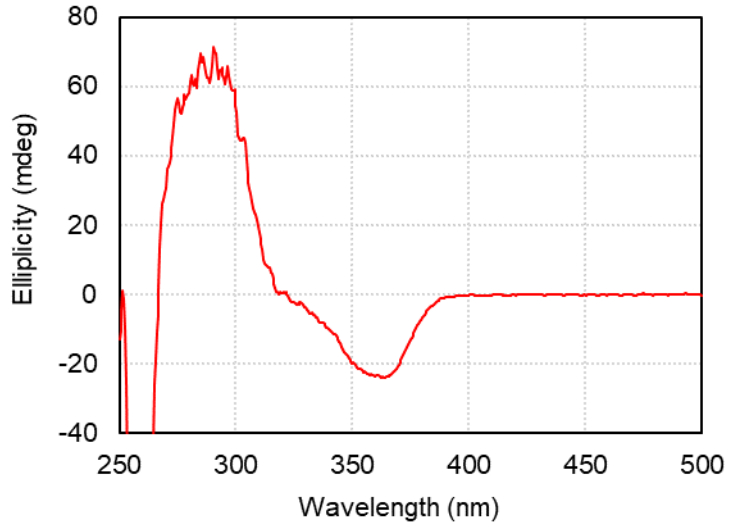

Figure S59. CD spectrum of PQX 30mer in THF containing TFAc-*L*-Pro-OMe (2.35×10^{-1} g/L, path length = 1.0 mm).

-for Figure 1, TFAc-*L*-Pro-OMe in 1,4-dioxane

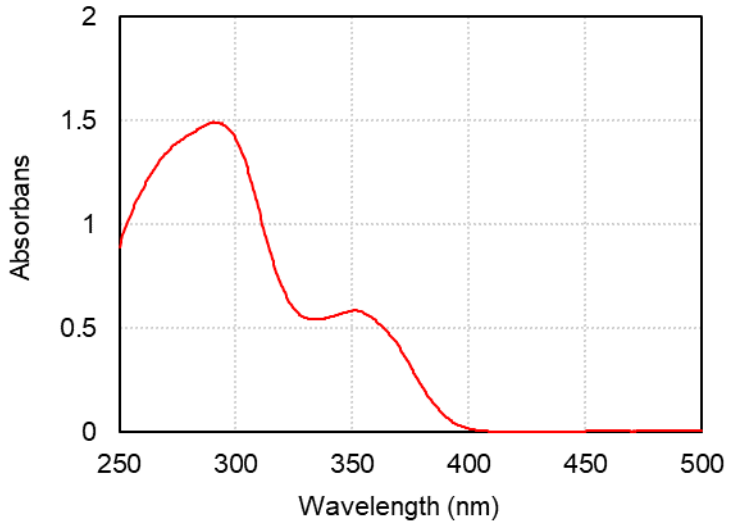

Figure S60. UV-vis absorption spectrum of PQX 30mer in 1,4-dioxane containing TFAc-*L*-Pro-OMe (2.35×10^{-1} g/L, path length = 1.0 mm).

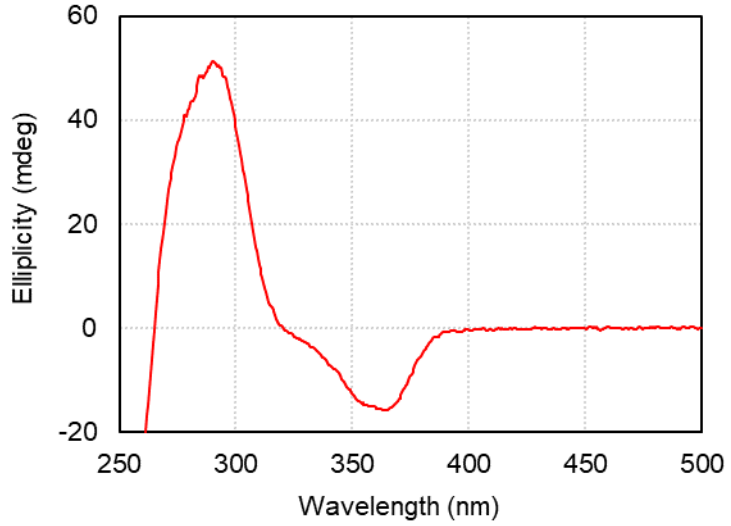

Figure S61. CD spectrum of PQX 30mer in 1,4-dioxane containing TFAc-*L*-Pro-OMe (2.35×10^{-1} g/L, path length = 1.0 mm).

-for Figure 1, TFAc-*L*-Pro-OMe in Et_2O

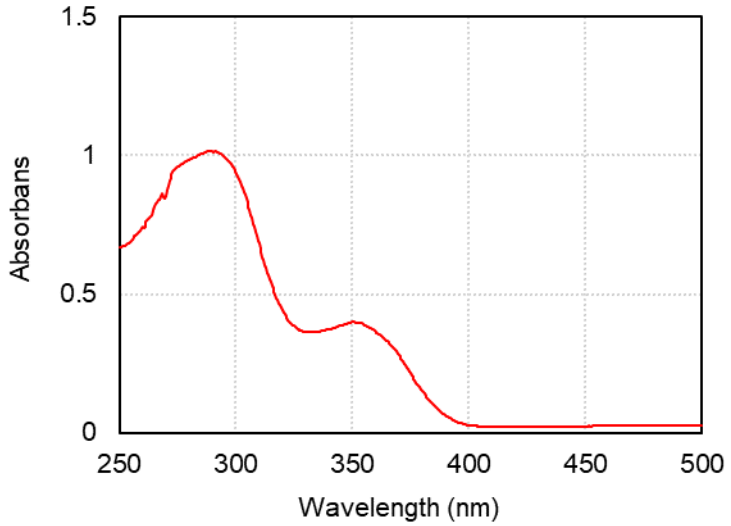

Figure S62. UV-vis absorption spectrum of PQX 30mer in Et_2O containing TFAc-*L*-Pro-OMe (2.35×10^{-1} g/L, path length = 1.0 mm).

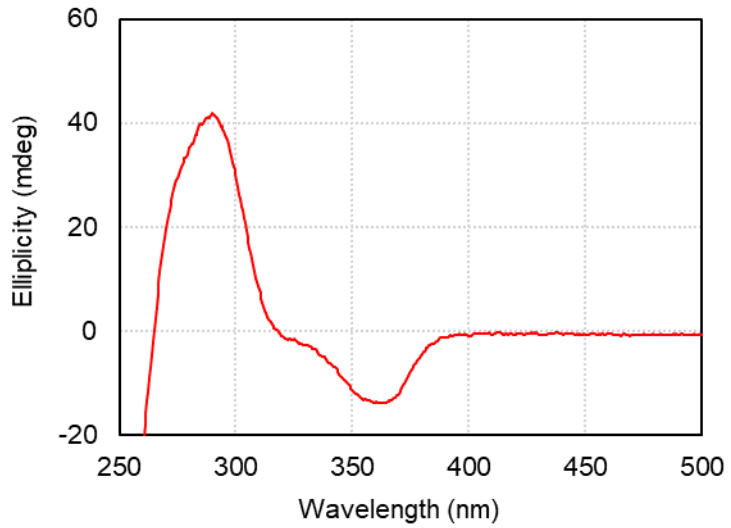

Figure S63. CD spectrum of PQX 30mer in Et_2O containing TFAc-*L*-Pro-OMe (2.35×10^{-1} g/L, path length = 1.0 mm).

-for Figure 1, TFAc-*L*-Pro-OMe in MTBE

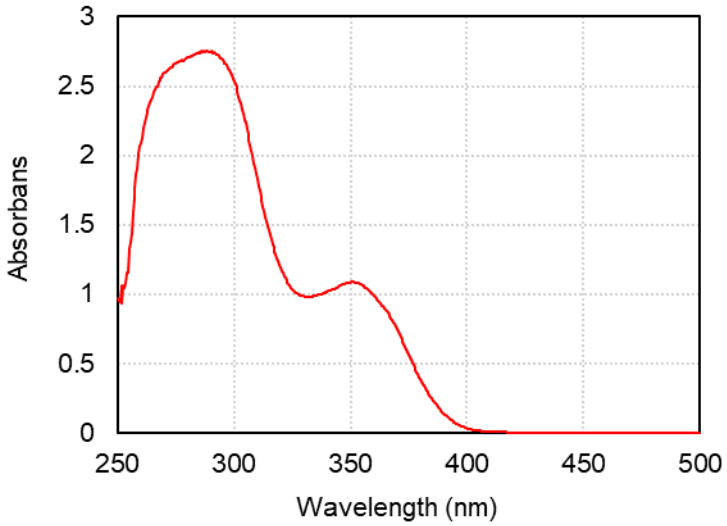

Figure S64. UV-vis absorption spectrum of PQX 30mer in MTBE containing TFAc-*L*-Pro-OMe (2.35×10^{-1} g/L, path length = 1.0 mm).

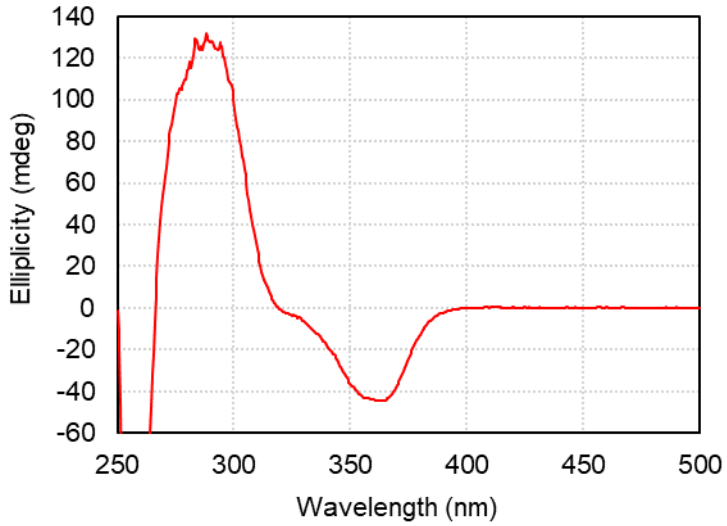

Figure S65. CD spectrum of PQX 30mer in MTBE containing TFAc-*L*-Pro-OMe (2.35×10^{-1} g/L, path length = 1.0 mm).

-for Figure 1, Ac-*L*-Pro-OMe in $CHCl_3$

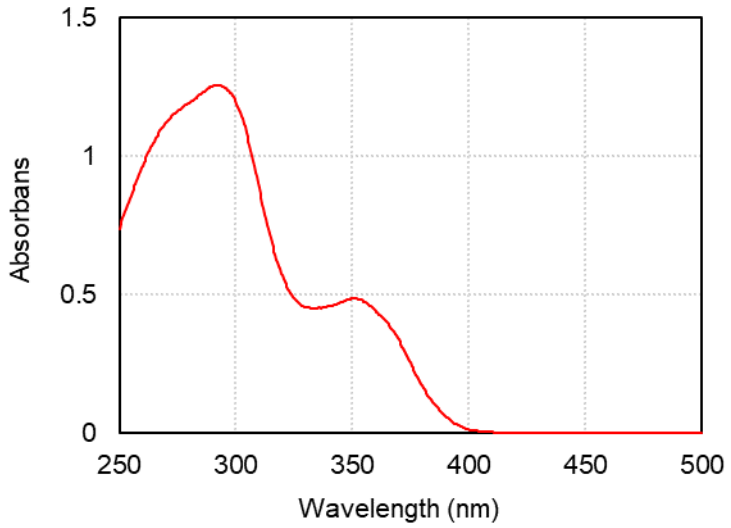

Figure S66. UV-vis absorption spectrum of PQX 30mer in $CHCl_3$ containing Ac-*L*-Pro-OMe (2.35×10^{-1} g/L, path length = 1.0 mm).

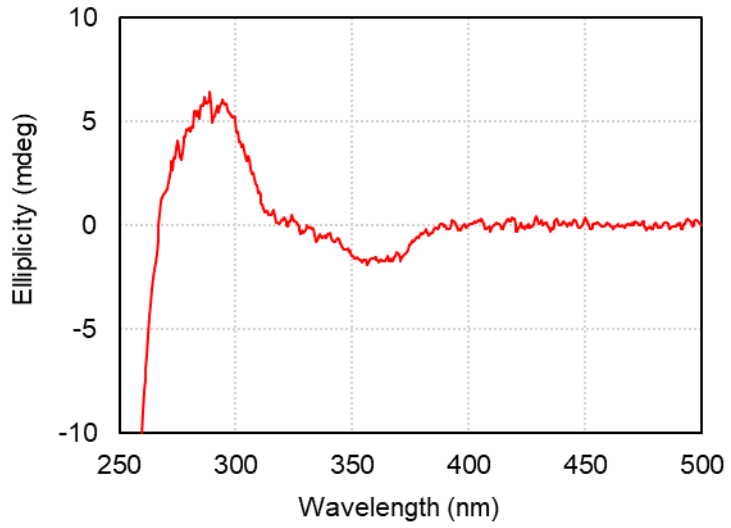

Figure S67. CD spectrum of PQX 30mer in $CHCl_3$ containing Ac-*L*-Pro-OMe (2.35×10^{-1} g/L, path length = 1.0 mm).

-for Figure 1, Ac-*L*-Pro-OMe in $CH_2Cl_{3¥2}$

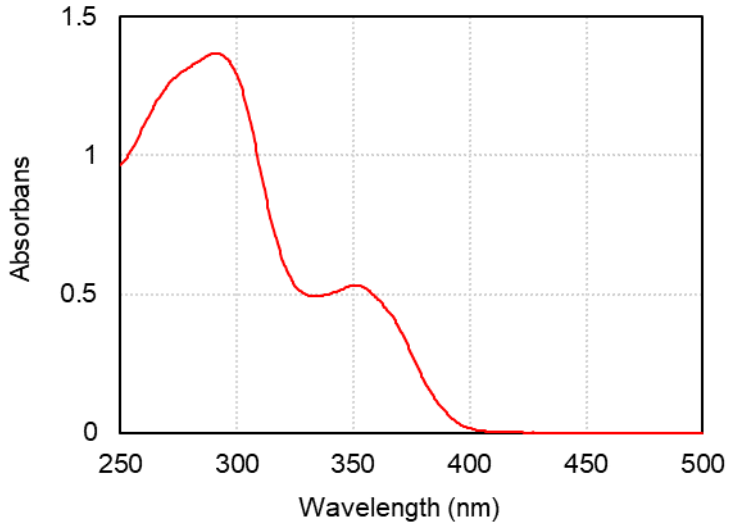

Figure S68. UV-vis absorption spectrum of PQX 30mer in CH_2Cl_2 containing Ac-*L*-Pro-OMe (2.35×10^{-1} g/L, path length = 1.0 mm).

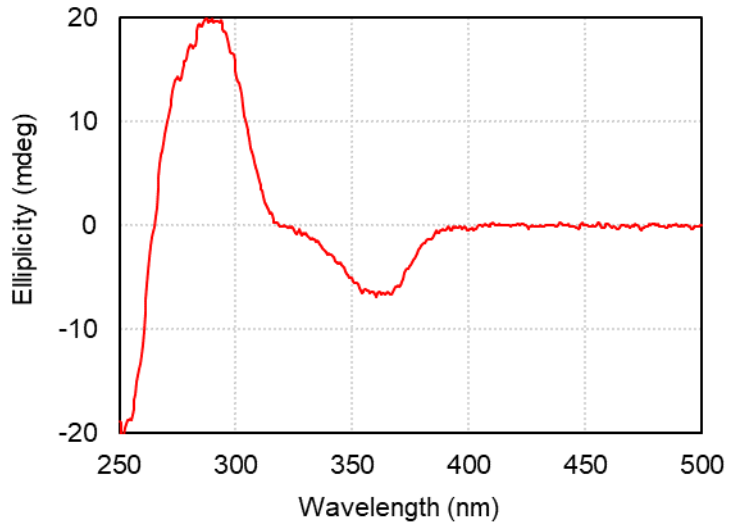

Figure S69. CD spectrum of PQX 30mer in CH_2Cl_2 containing Ac-*L*-Pro-OMe (2.35×10^{-1} g/L, path length = 1.0 mm).

-for Figure 1, Ac-*L*-Pro-OMe in 1,2-DCE

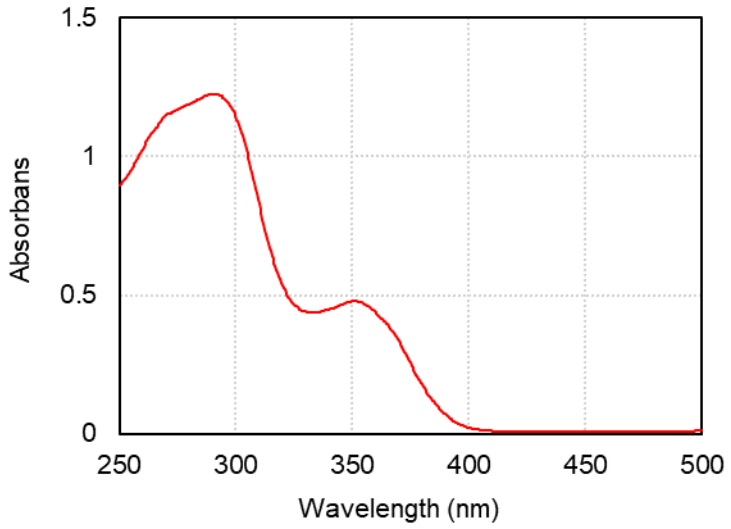

Figure S70. UV-vis absorption spectrum of PQX 30mer in 1,2-DCE containing Ac-*L*-Pro-OMe (2.35×10^{-1} g/L, path length = 1.0 mm).

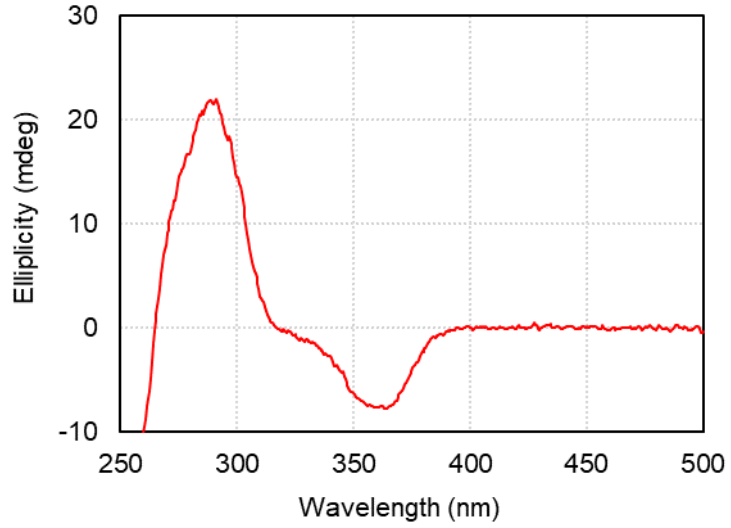

Figure S71. CD spectrum of PQX 30mer in 1,2-DCE containing Ac-*L*-Pro-OMe (2.35×10^{-1} g/L, path length = 1.0 mm).

-for Figure 1, Ac-*L*-Pro-OMe in toluene

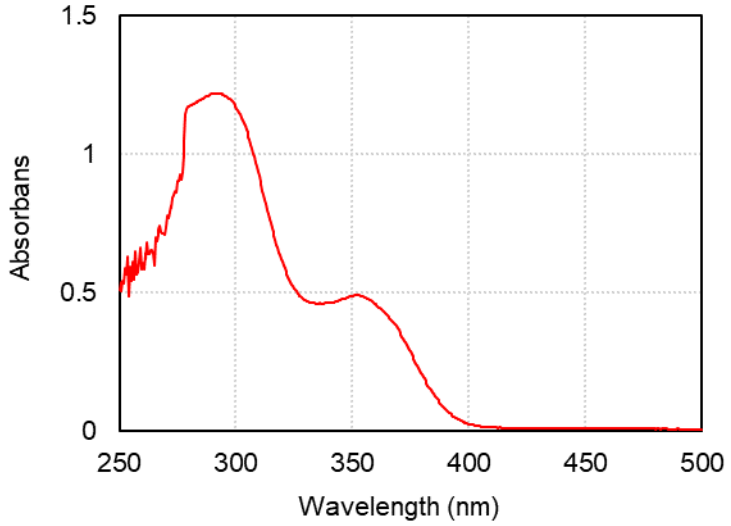

Figure S72. UV-vis absorption spectrum of PQX 30mer in toluene containing Ac-*L*-Pro-OMe (2.35×10^{-1} g/L, path length = 1.0 mm).

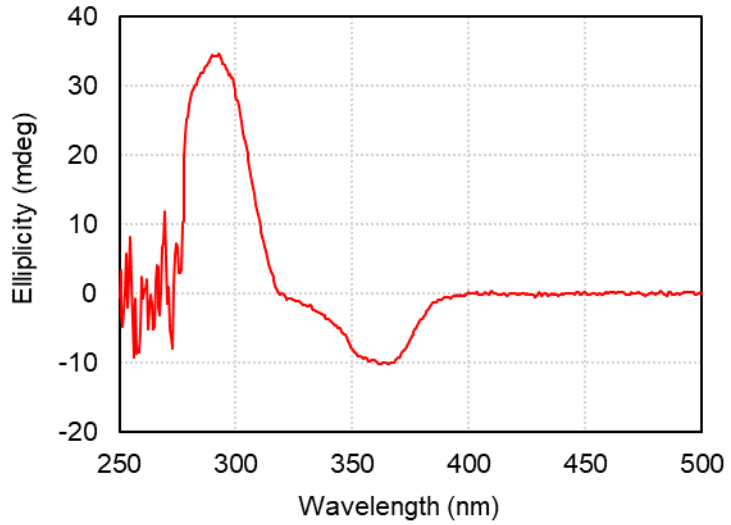

Figure S73. CD spectrum of PQX 30mer in toluene containing Ac-*L*-Pro-OMe (2.35×10^{-1} g/L, path length = 1.0 mm).

-for Figure 1, Ac-*L*-Pro-OMe in THF

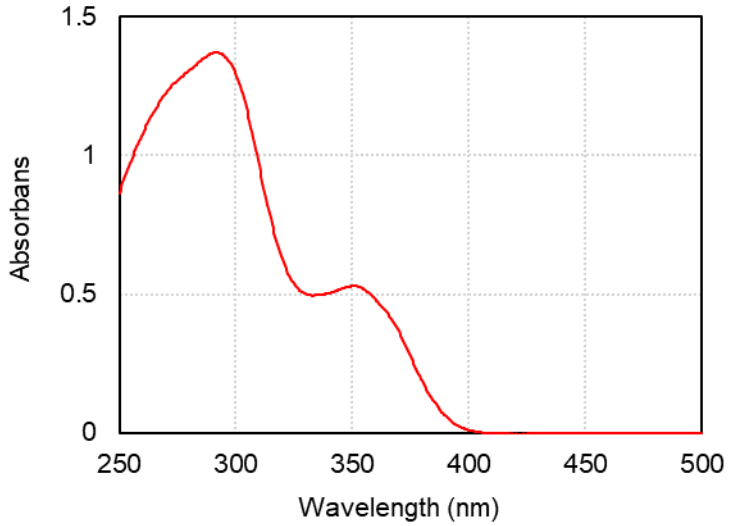

Figure S74. UV-vis absorption spectrum of PQX 30mer in THF containing Ac-*L*-Pro-OMe (2.35×10^{-1} g/L, path length = 1.0 mm).

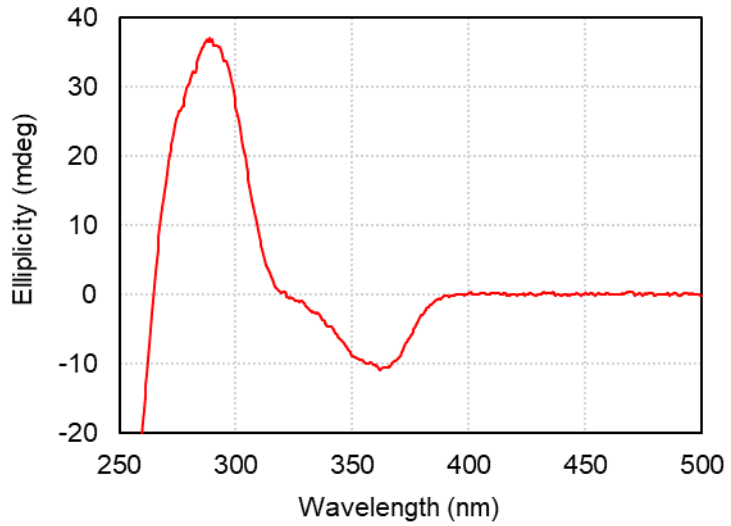

Figure S75. CD spectrum of PQX 30mer in THF containing Ac-*L*-Pro-OMe (2.35×10^{-1} g/L, path length = 1.0 mm).

-for Figure 1, Ac-*L*-Pro-OMe in 1,4-dioxane

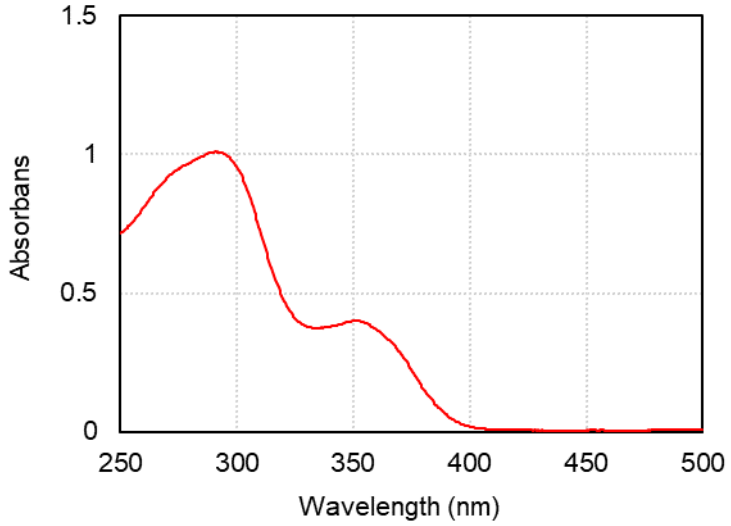

Figure S76. UV-vis absorption spectrum of PQX 30mer in 1,4-dioxane containing Ac-*L*-Pro-OMe (2.35×10^{-1} g/L, path length = 1.0 mm).

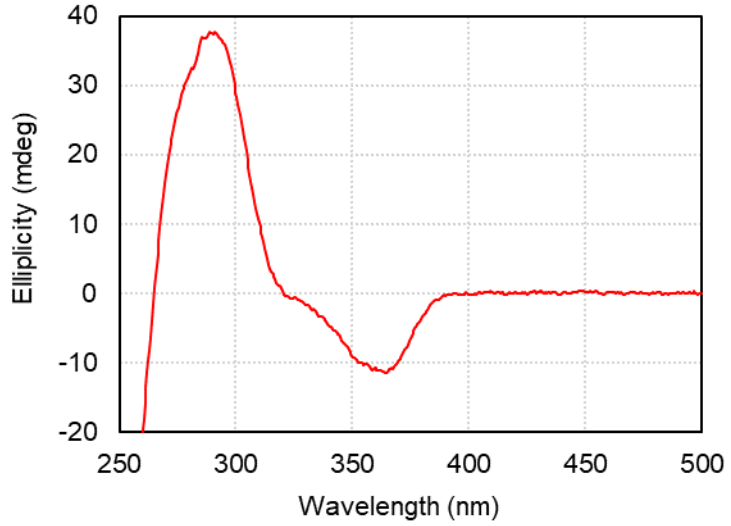

Figure S77. CD spectrum of PQX 30mer in 1,4-dioxane containing Ac-*L*-Pro-OMe (2.35×10^{-1} g/L, path length = 1.0 mm).

-for Figure 1, Ac-*L*-Pro-OMe in Et_2O

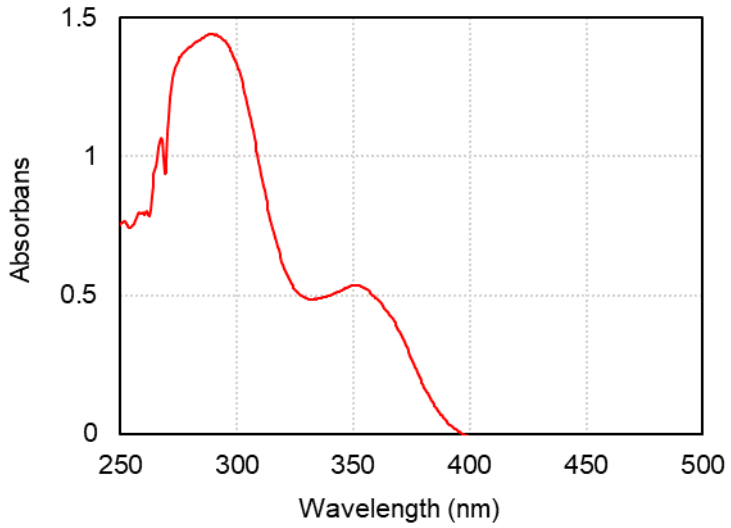

Figure S78. UV-vis absorption spectrum of PQX 30mer in Et_2O containing Ac-*L*-Pro-OMe (2.35×10^{-1} g/L, path length = 1.0 mm).

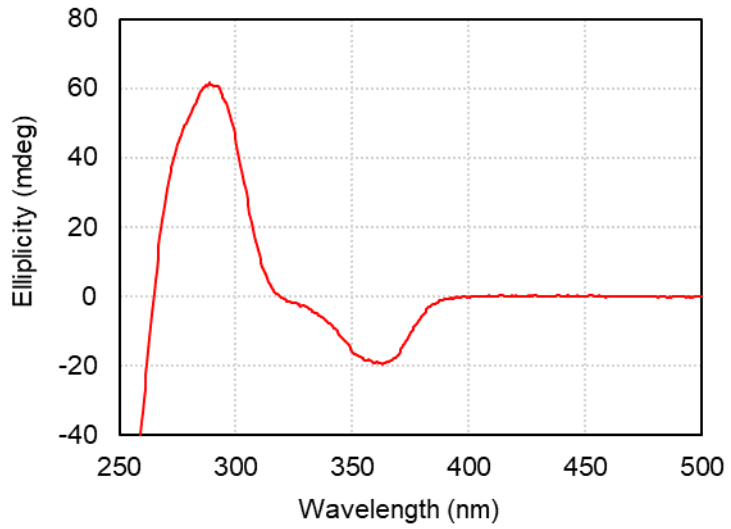

Figure S79. CD spectrum of PQX 30mer in Et_2O containing Ac-*L*-Pro-OMe (2.35×10^{-1} g/L, path length = 1.0 mm).

-for Figure 1, Ac-*L*-Pro-OMe in MTBE

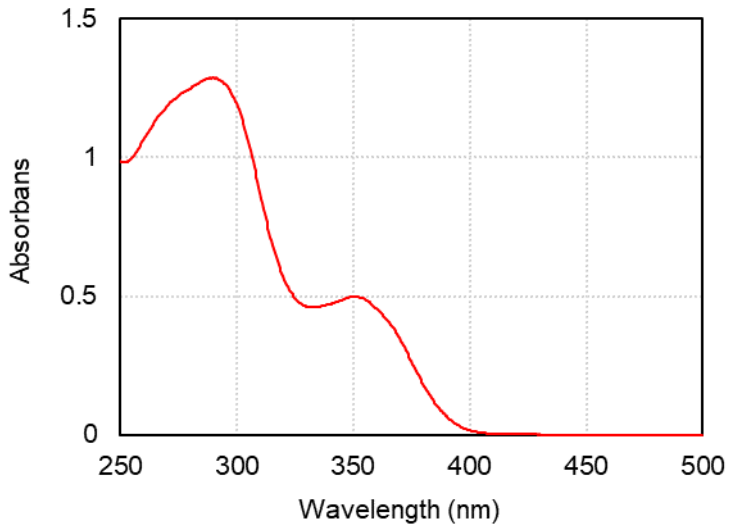

Figure S80. UV-vis absorption spectrum of PQX 30mer in MTBE containing Ac-*L*-Pro-OMe (2.35×10^{-1} g/L, path length = 1.0 mm).

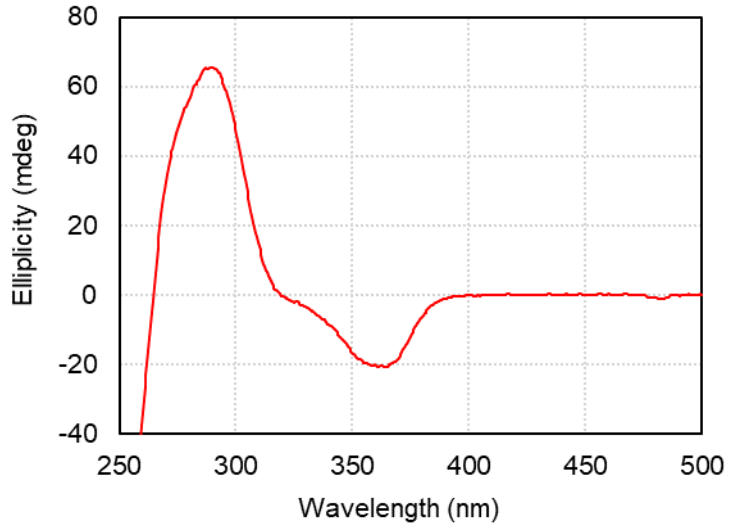

Figure S81. CD spectrum of PQX 30mer in MTBE containing Ac-*L*-Pro-OMe (2.35×10^{-1} g/L, path length = 1.0 mm).

-for Figure 3, TFAc-*L*-Pro-OMe in THF (PQX 60mer)

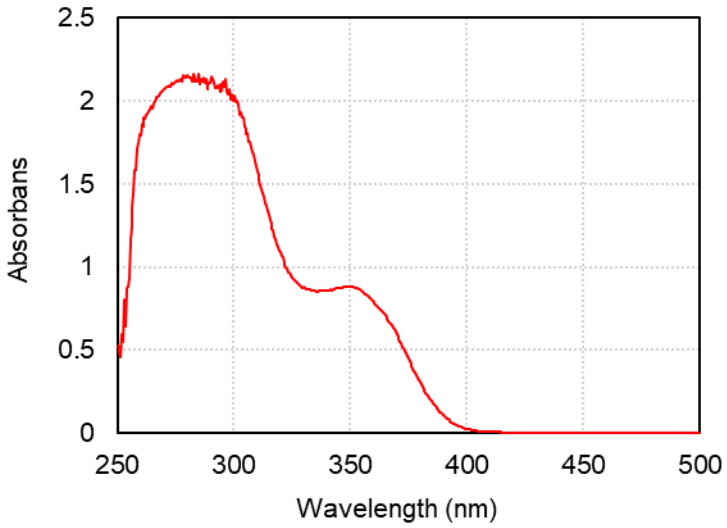

Figure S82. UV-vis absorption spectrum of PQX 60mer in THF containing TFAc-*L*-Pro-OMe (2.68×10^{-1} g/L, path length = 1.0 mm).

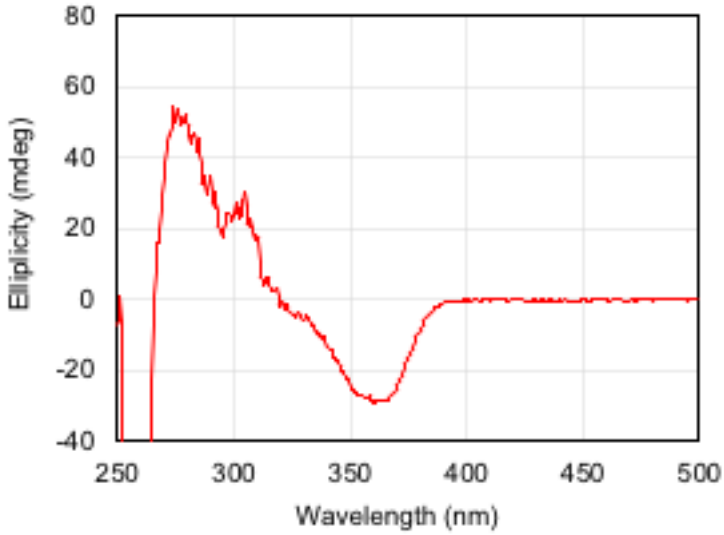

Figure S83. CD spectrum of PQX 60mer in THF containing TFAc-*L*-Pro-OMe (2.68×10^{-1} g/L, path length = 1.0 mm).

-for Figure 3, TFAc-*L*-Pro-OMe in THF (PQX 150mer)

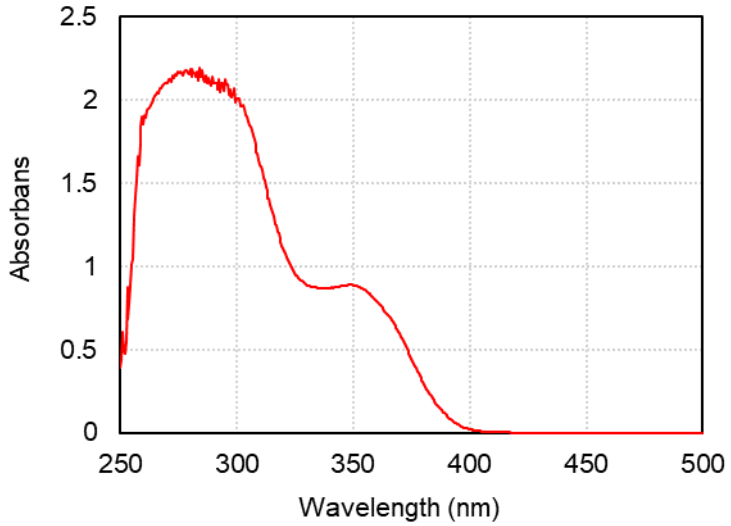

Figure S84. UV-vis absorption spectrum of PQX 150mer in THF containing TFAc-*L*-Pro-OMe (2.65×10^{-1} g/L, path length = 1.0 mm).

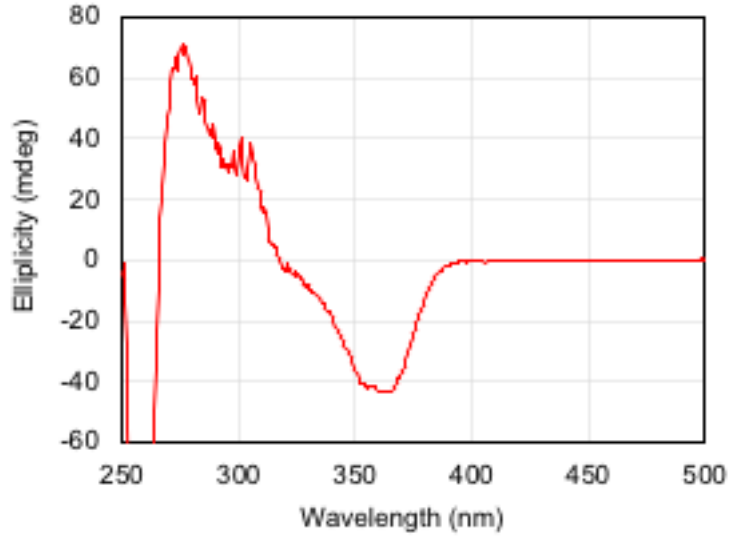

Figure S85. CD spectrum of PQX 150mer in THF containing TFAc-*L*-Pro-OMe (2.65×10^{-1} g/L, path length = 1.0 mm).

-for Figure 3, TFAc-*L*-Pro-OMe in THF (PQX 200mer)

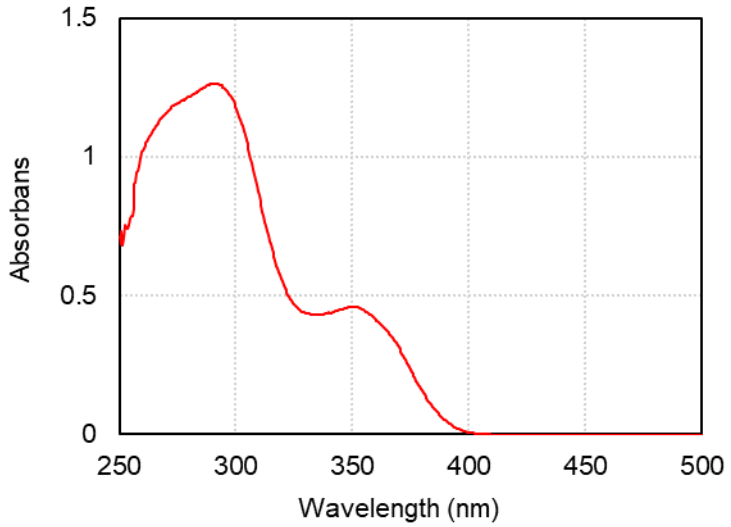

Figure S86. UV-vis absorption spectrum of PQX 200mer in THF containing TFAc-*L*-Pro-OMe (2.23×10^{-1} g/L, path length = 1.0 mm).

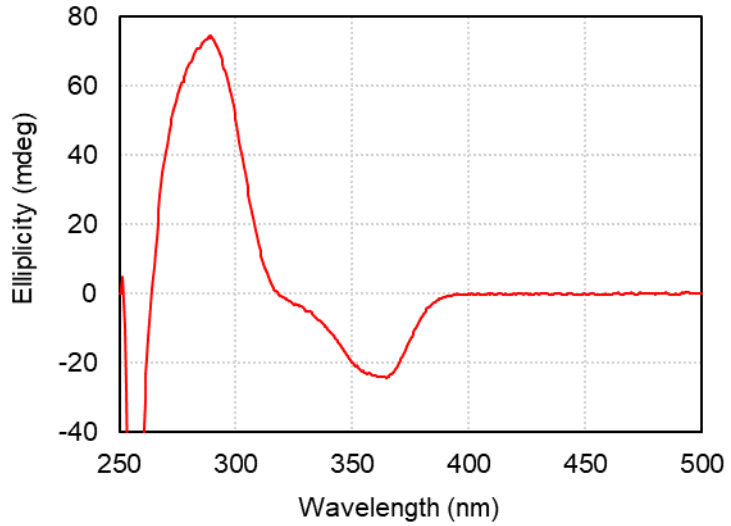

Figure S87. CD spectrum of PQX 200mer in THF containing TFAc-*L*-Pro-OMe (2.23×10^{-1} g/L, path length = 1.0 mm).

-for Figure 3, TFAc-*L*-Pro-OMe in THF (PQX 250mer)

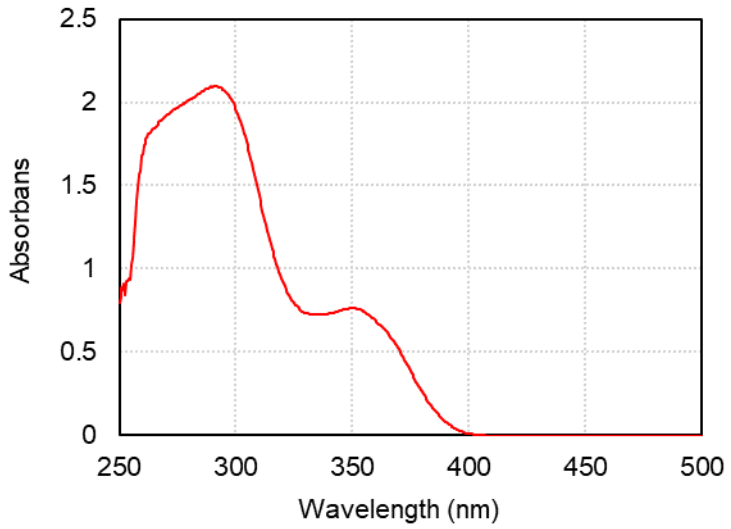

Figure S88. UV-vis absorption spectrum of PQX 250mer in THF containing TFAc-*L*-Pro-OMe (2.26×10^{-1} g/L, path length = 1.0 mm).

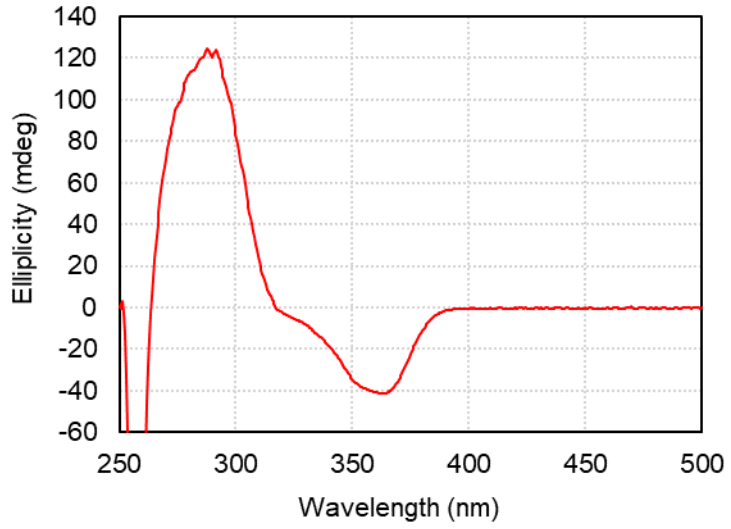

Figure S89. CD spectrum of PQX 250mer in THF containing TFAc-*L*-Pro-OMe (2.26×10^{-1} g/L, path length = 1.0 mm).

-for Figure 3, TFAc-*L*-Pro-OMe in THF (PQX 300mer)

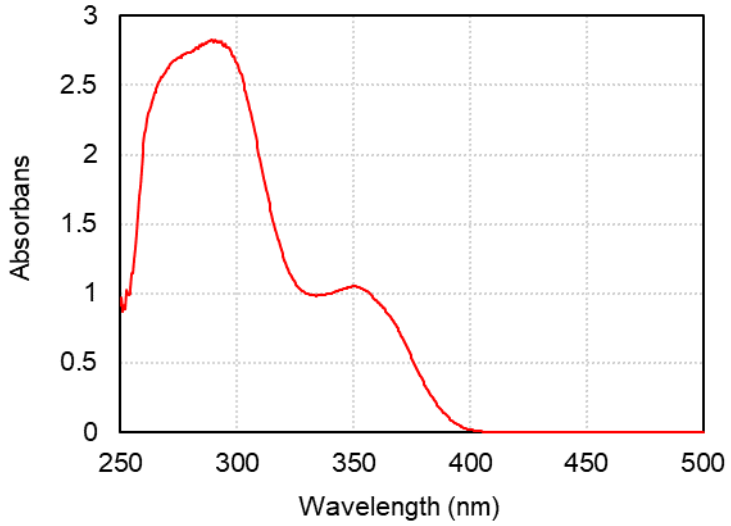

Figure S90. UV-vis absorption spectrum of PQX 300mer in THF containing TFAc-*L*-Pro-OMe (3.18×10^{-1} g/L, path length = 1.0 mm).

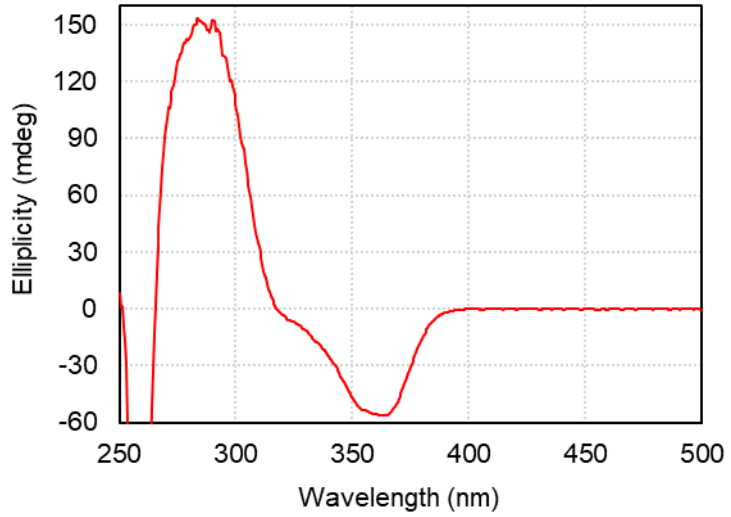

Figure S91. CD spectrum of PQX 300mer in THF containing TFAc-*L*-Pro-OMe (3.18×10^{-1} g/L, path length = 1.0 mm).

-for Figure 3, TFAc-*L*-Pro-OMe in THF (PQX 400mer)

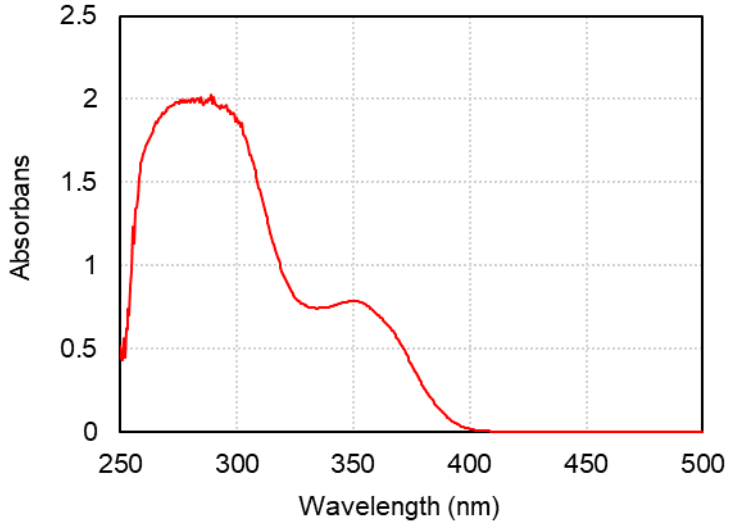

Figure S92. UV-vis absorption spectrum of PQX 400mer in THF containing TFAc-*L*-Pro-OMe (2.54×10^{-1} g/L, path length = 1.0 mm).

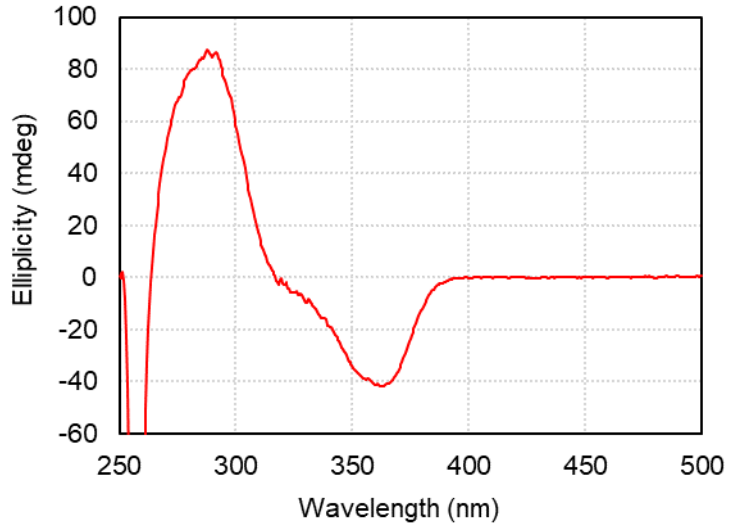

Figure S931. CD spectrum of PQX 400mer in THF containing TFAc-*L*-Pro-OMe (2.54×10^{-1} g/L, path length = 1.0 mm).

-for Figure 3, TFAc-*L*-Pro-OMe in MTBE (PQX 60mer)

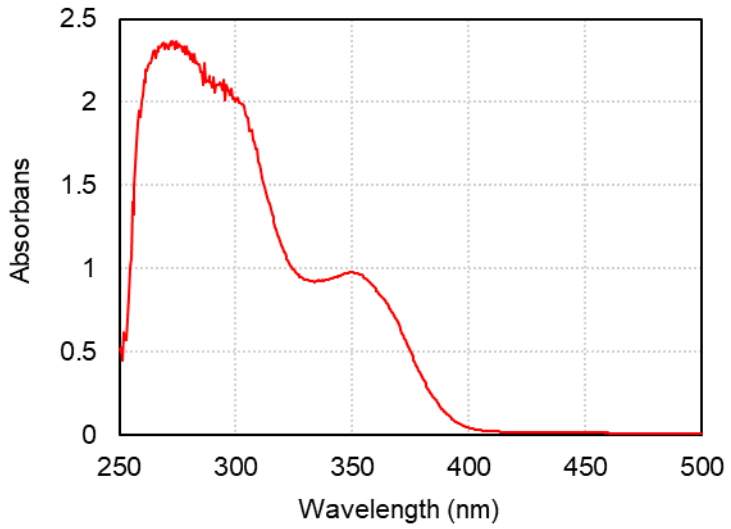

Figure S94. UV-vis absorption spectrum of PQX 60mer in MTBE containing TFAc-*L*-Pro-OMe (2.68×10^{-1} g/L, path length = 1.0 mm).

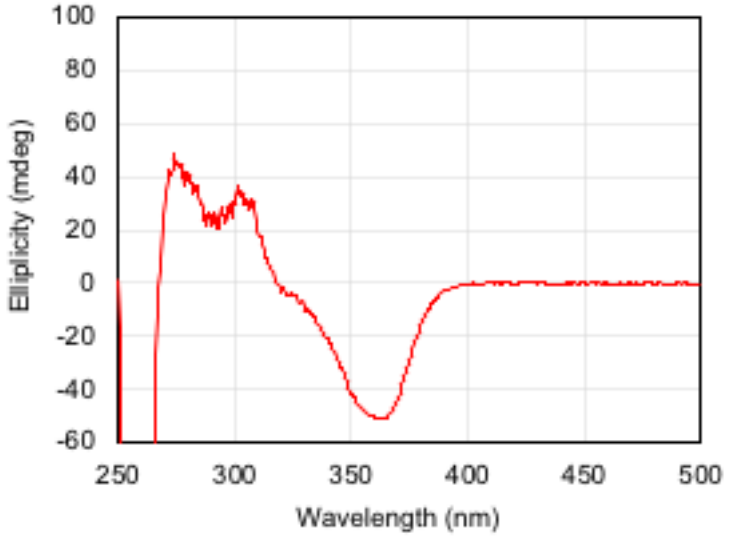

Figure S95. CD spectrum of PQX 60mer in MTBE containing TFAc-*L*-Pro-OMe (2.68×10^{-1} g/L, path length = 1.0 mm).

-for Figure 3, TFAc-*L*-Pro-OMe in MTBE (PQX 100mer)

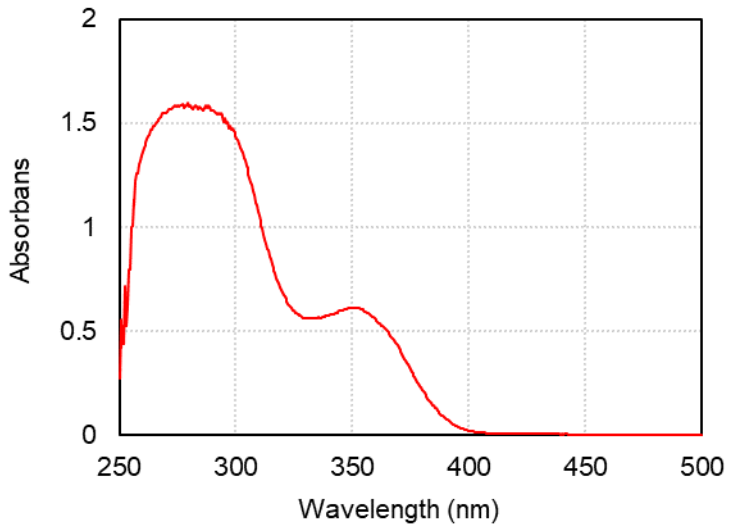

Figure S96. UV-vis absorption spectrum of PQX 100mer in MTBE containing TFAc-*L*-Pro-OMe (2.35×10^{-1} g/L, path length = 1.0 mm).

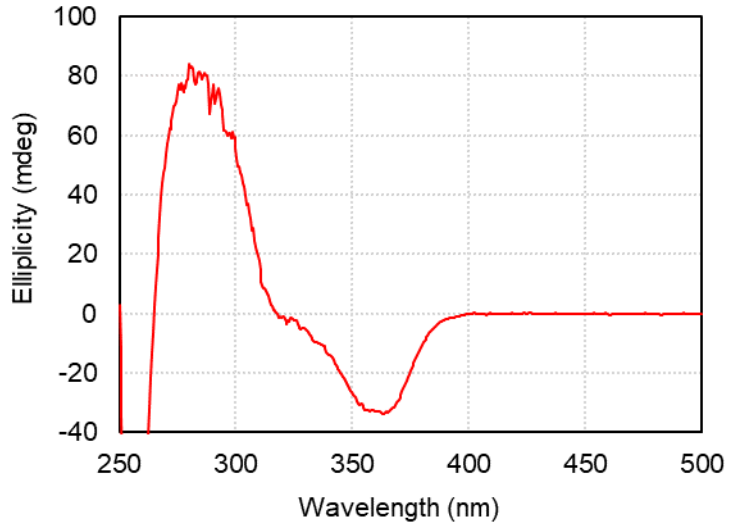

Figure S97. CD spectrum of PQX 100mer in MTBE containing TFAc-*L*-Pro-OMe (2.35×10^{-1} g/L, path length = 1.0 mm).

-for Figure 3, TFAc-*L*-Pro-OMe in MTBE (PQX 150mer)

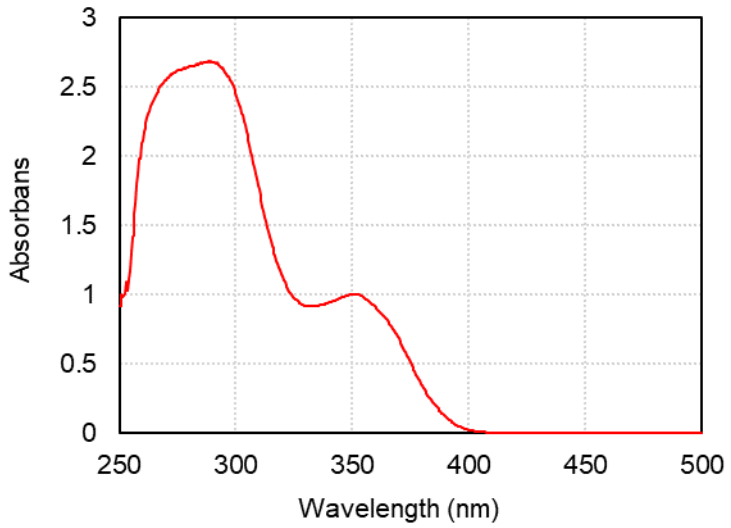

Figure S98. UV-vis absorption spectrum of PQX 150mer in MTBE containing TFAc-*L*-Pro-OMe (2.65×10^{-1} g/L, path length = 1.0 mm).

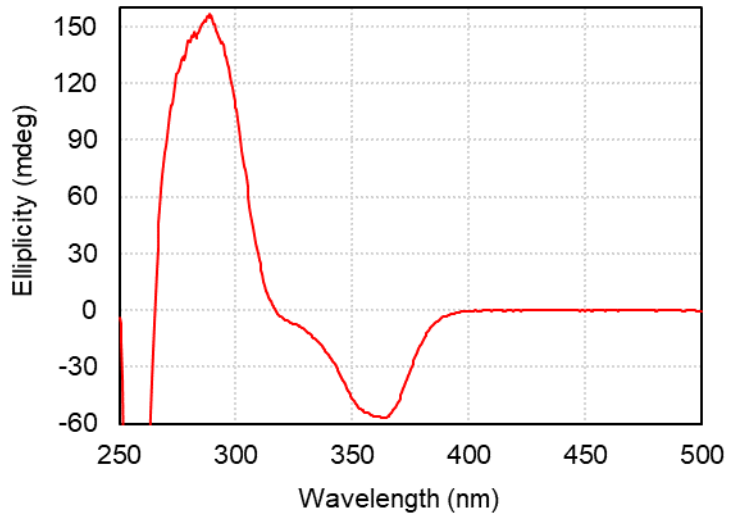

Figure S99. CD spectrum of PQX 150mer in MTBE containing TFAc-*L*-Pro-OMe (2.65×10^{-1} g/L, path length = 1.0 mm).

-for Figure 3, TFAc-*L*-Pro-OMe in MTBE (PQX 200mer)

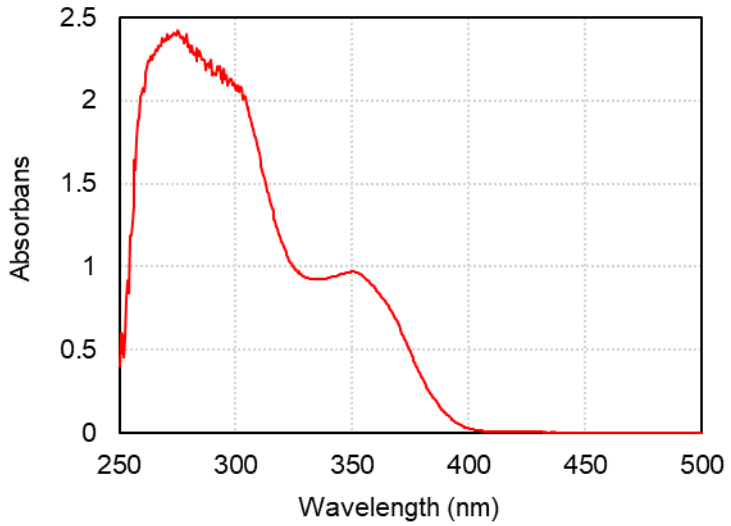

Figure S100. UV-vis absorption spectrum of PQX 200mer in MTBE containing TFAc-*L*-Pro-OMe (2.23×10^{-1} g/L, path length = 1.0 mm).

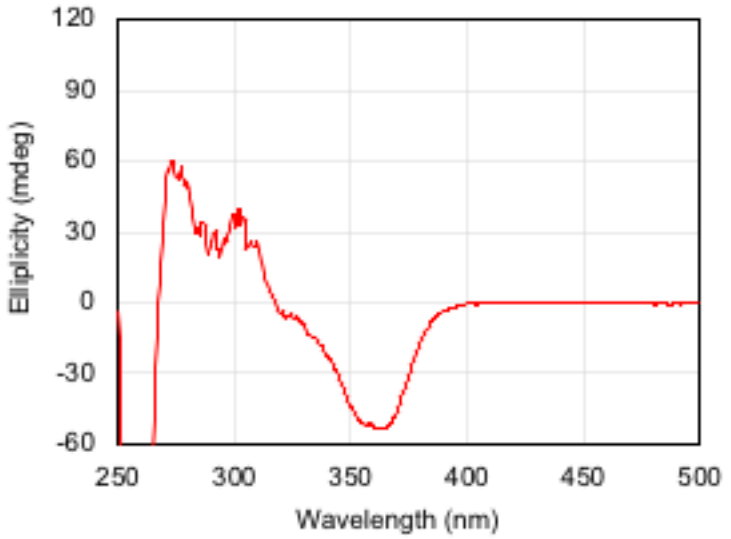

Figure S101. CD spectrum of PQX 200mer in MTBE containing TFAc-*L*-Pro-OMe (2.23×10^{-1} g/L, path length = 1.0 mm).

-for Figure 3, TFAc-*L*-Pro-OMe in MTBE (PQX 250mer)

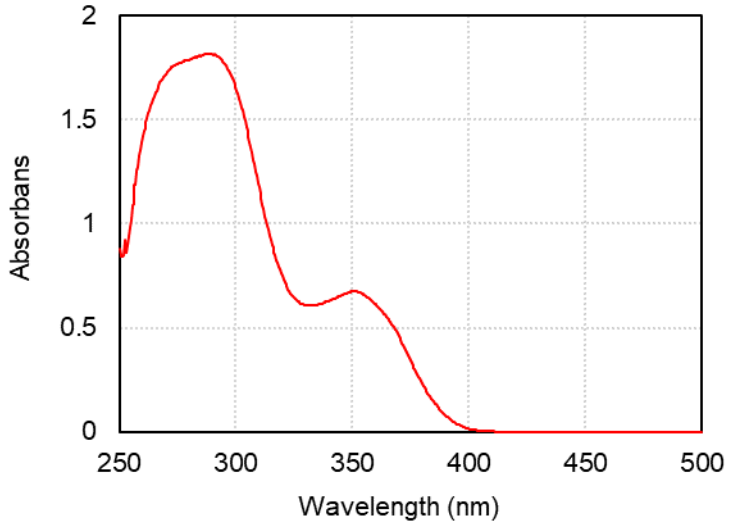

Figure S102. UV-vis absorption spectrum of PQX 250mer in MTBE containing TFAc-*L*-Pro-OMe (2.26×10^{-1} g/L, path length = 1.0 mm).

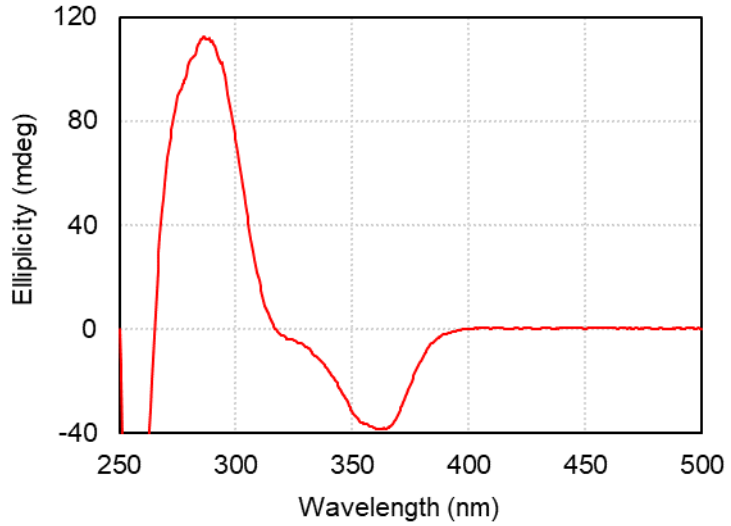

Figure S103. CD spectrum of PQX 250mer in MTBE containing TFAc-*L*-Pro-OMe (2.26×10^{-1} g/L, path length = 1.0 mm).

-for Figure 3, TFAc-*L*-Pro-OMe in MTBE (PQX 300mer)

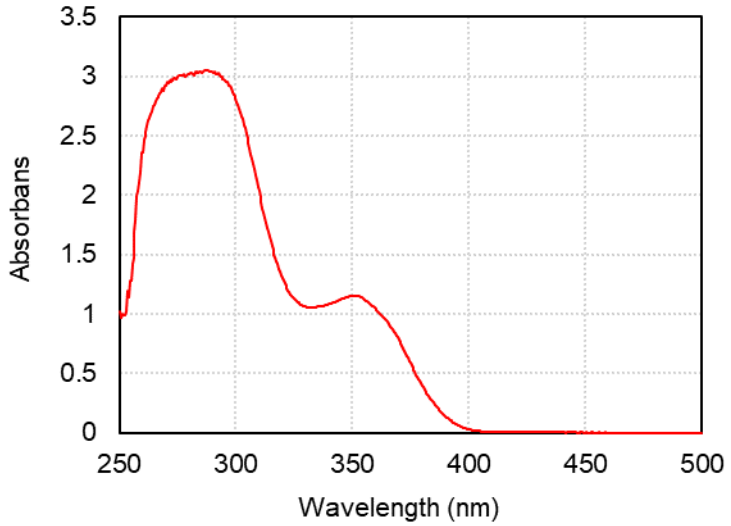

Figure S104. UV-vis absorption spectrum of PQX 300mer in MTBE containing TFAc-*L*-Pro-OMe (3.18×10^{-1} g/L, path length = 1.0 mm).

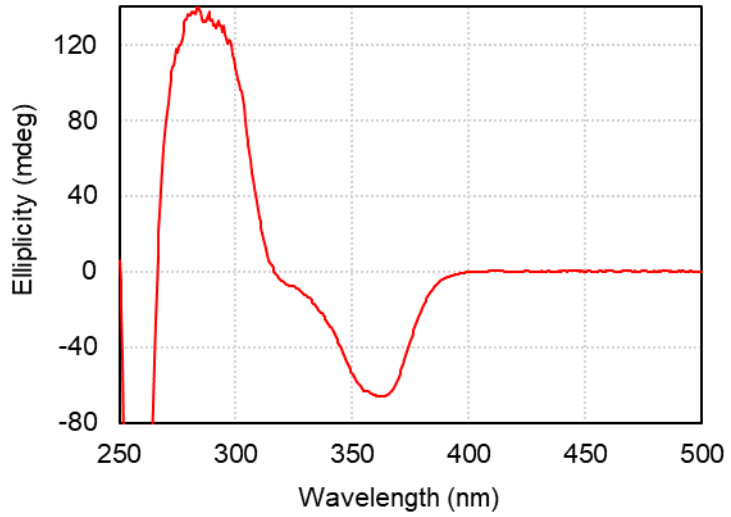

Figure S105. CD spectrum of PQX 300mer in MTBE containing TFAc-*L*-Pro-OMe (3.18×10^{-1} g/L, path length = 1.0 mm).

-for Figure 3, TFAc-*L*-Pro-OMe in MTBE (PQX 400mer)

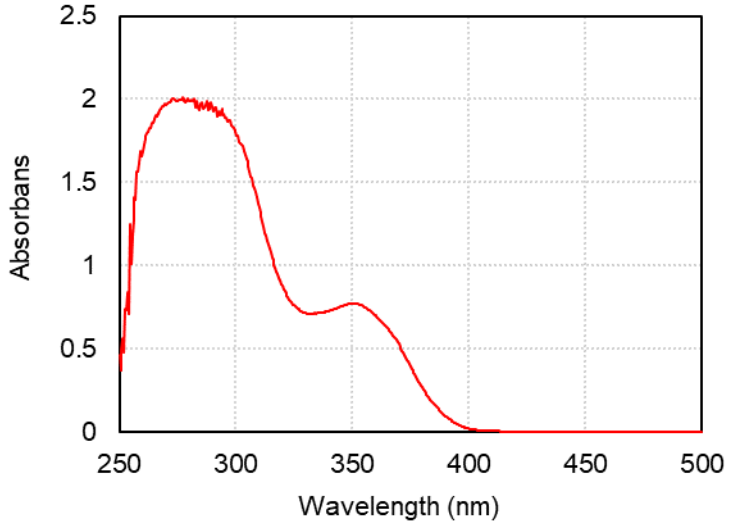

Figure S106. UV-vis absorption spectrum of PQX 400mer in MTBE containing TFAc-*L*-Pro-OMe (2.54×10^{-1} g/L, path length = 1.0 mm).

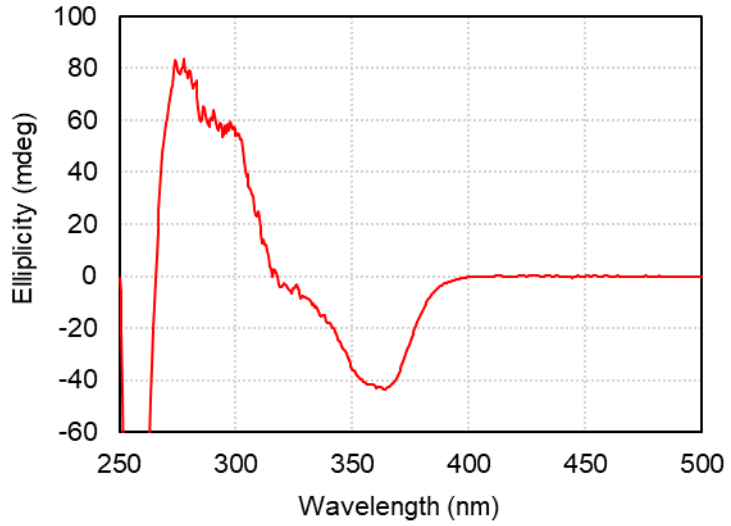

Figure S107. CD spectrum of PQX 400mer in MTBE containing TFAc-*L*-Pro-OMe (2.54×10^{-1} g/L, path length = 1.0 mm).

-for Figure 3, Ac-*L*-Pro-OMe in THF (PQX 60mer)

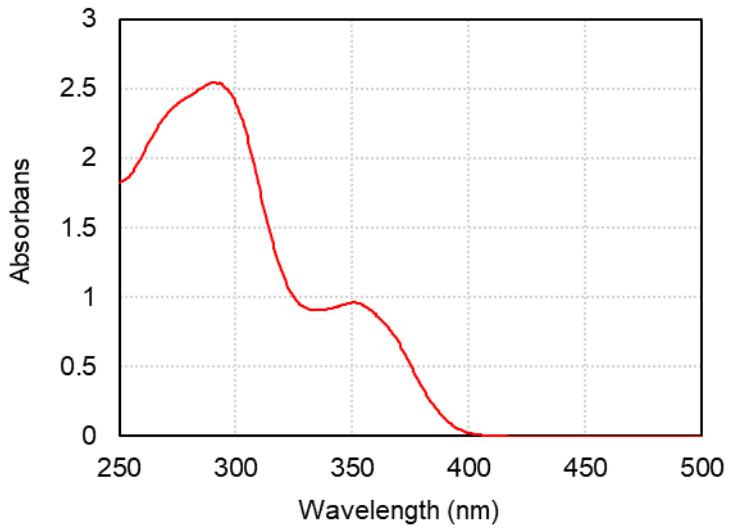

Figure S108. UV-vis absorption spectrum of PQX 60mer in THF containing Ac-*L*-Pro-OMe (2.68×10^{-1} g/L, path length = 1.0 mm).

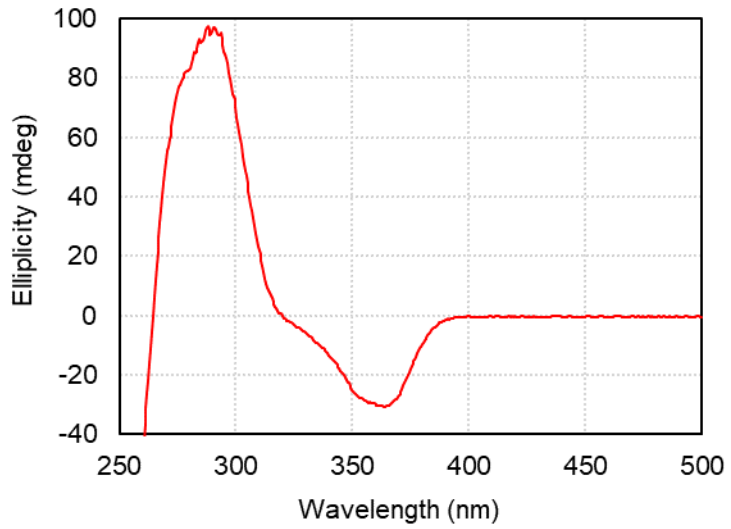

Figure S109. CD spectrum of PQX 60mer in THF containing Ac-*L*-Pro-OMe (2.68×10^{-1} g/L, path length = 1.0 mm).

-for Figure 3, Ac-*L*-Pro-OMe in THF (PQX 150mer)

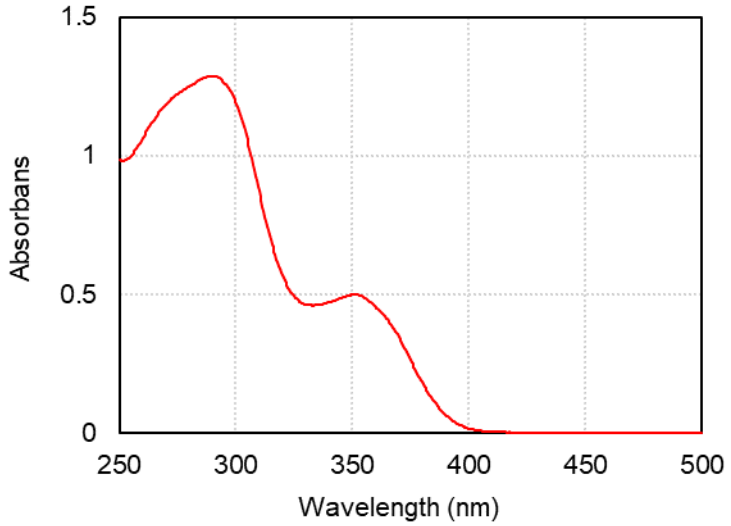

Figure S110. UV-vis absorption spectrum of PQX 150mer in THF containing Ac-*L*-Pro-OMe (2.65×10^{-1} g/L, path length = 1.0 mm).

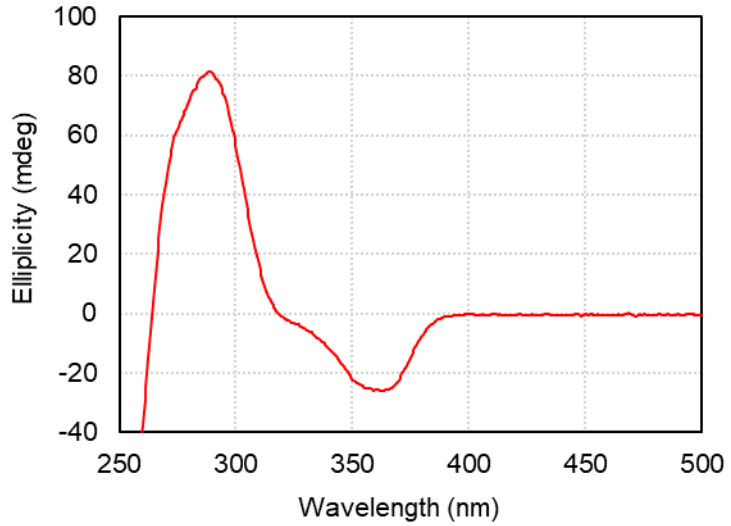

Figure S111. CD spectrum of PQX 150mer in THF containing Ac-*L*-Pro-OMe (2.65×10^{-1} g/L, path length = 1.0 mm).

-for Figure 3, Ac-*L*-Pro-OMe in THF (PQX 200mer)

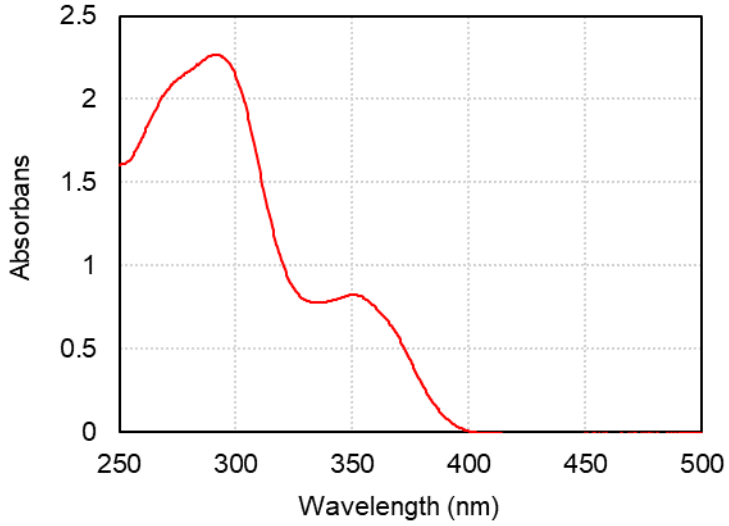

Figure S112. UV-vis absorption spectrum of PQX 200mer in THF containing Ac-*L*-Pro-OMe (2.23×10^{-1} g/L, path length = 1.0 mm).

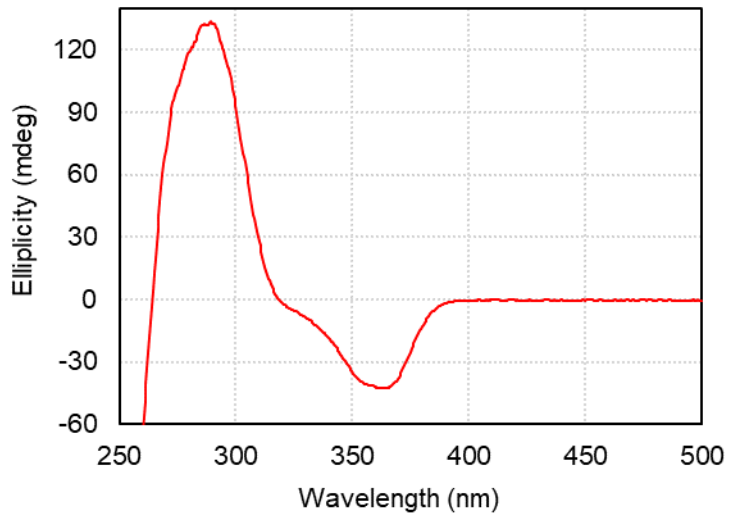

Figure S113. CD spectrum of PQX 200mer in THF containing Ac-*L*-Pro-OMe (2.23×10^{-1} g/L, path length = 1.0 mm).

-for Figure 3, Ac-*L*-Pro-OMe in THF (PQX 250mer)

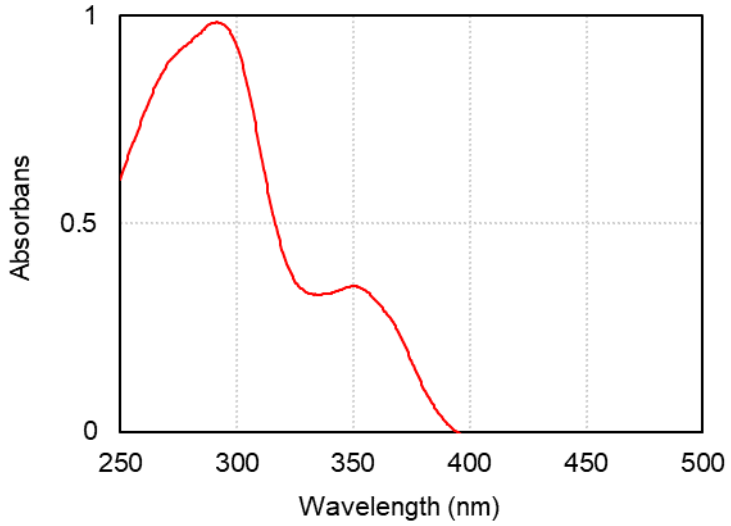

Figure S114. UV-vis absorption spectrum of PQX 250mer in THF containing Ac-*L*-Pro-OMe (2.26×10^{-1} g/L, path length = 1.0 mm).

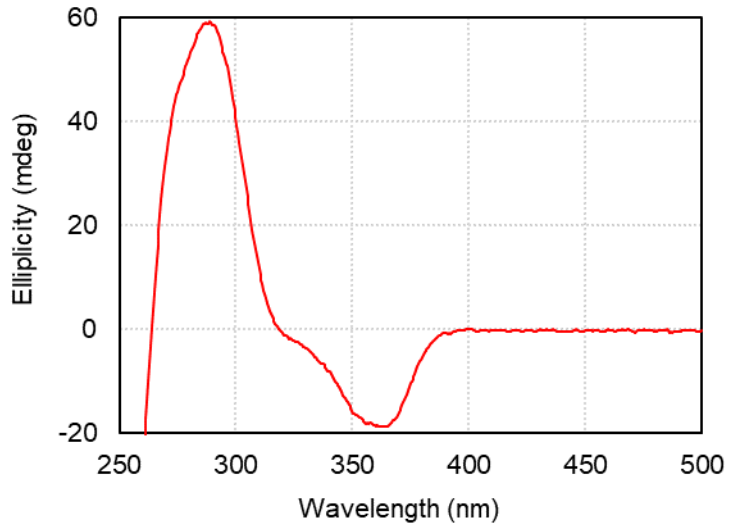

Figure S115. CD spectrum of PQX 250mer in THF containing Ac-*L*-Pro-OMe (2.26×10^{-1} g/L, path length = 1.0 mm).

-for Figure 3, Ac-*L*-Pro-OMe in THF (PQX 300mer)

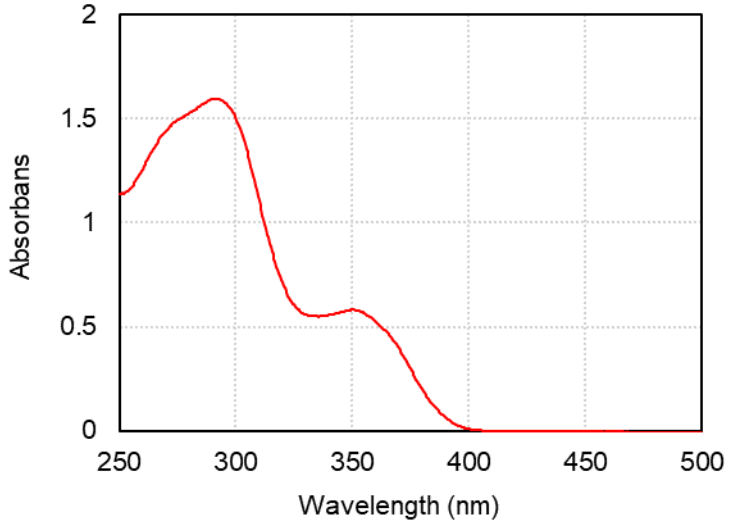

Figure S116. UV-vis absorption spectrum of PQX 300mer in THF containing Ac-*L*-Pro-OMe (3.18×10^{-1} g/L, path length = 1.0 mm).

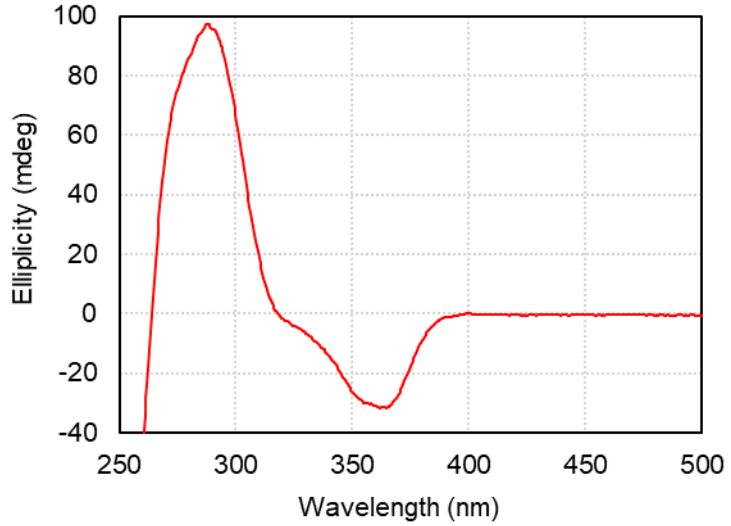

Figure S117. CD spectrum of PQX 300mer in THF containing Ac-*L*-Pro-OMe (3.18×10^{-1} g/L, path length = 1.0 mm).

-for Figure 3, Ac-*L*-Pro-OMe in THF (PQX 400mer)

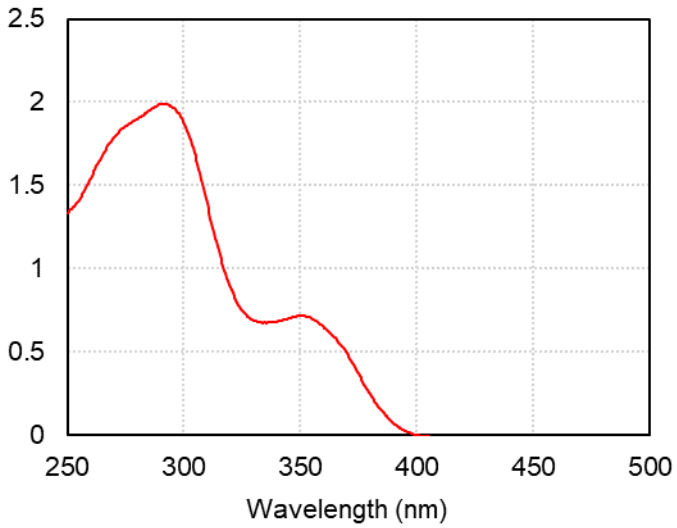

Figure S118. UV-vis absorption spectrum of PQX 400mer in THF containing Ac-*L*-Pro-OMe (2.54×10^{-1} g/L, path length = 1.0 mm).

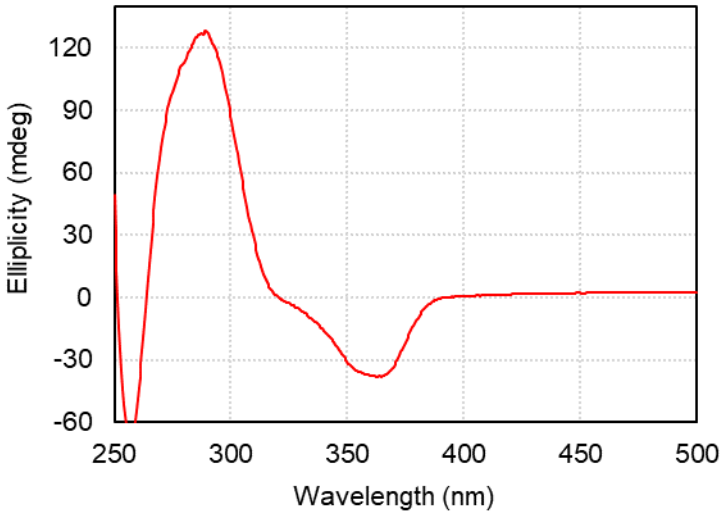

Figure S119. CD spectrum of PQX 400mer in THF containing Ac-*L*-Pro-OMe (2.54×10^{-1} g/L, path length = 1.0 mm).

-for Figure 3, Ac-*L*-Pro-OMe in MTBE (PQX 60mer)

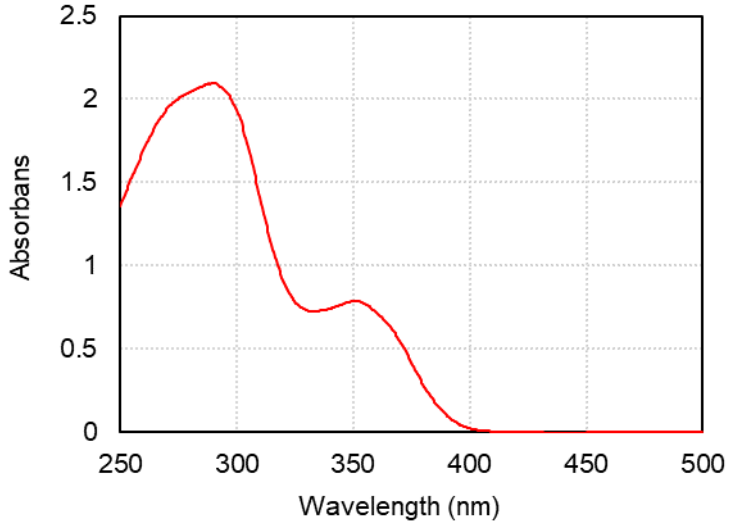

Figure S120. UV-vis absorption spectrum of PQX 60mer in MTBE containing Ac-*L*-Pro-OMe (2.68×10^{-1} g/L, path length = 1.0 mm).

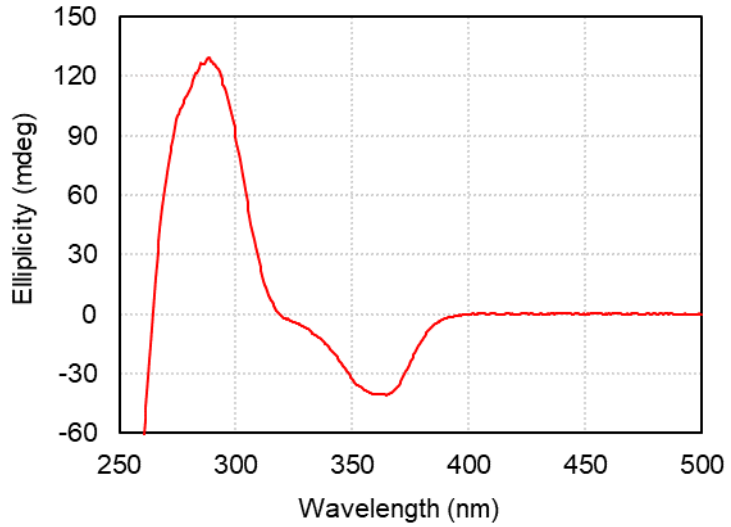

Figure S121. CD spectrum of PQX 60mer in MTBE containing Ac-*L*-Pro-OMe (2.68×10^{-1} g/L, path length = 1.0 mm).

-for Figure 3, Ac-*L*-Pro-OMe in MTBE (PQX 100mer)

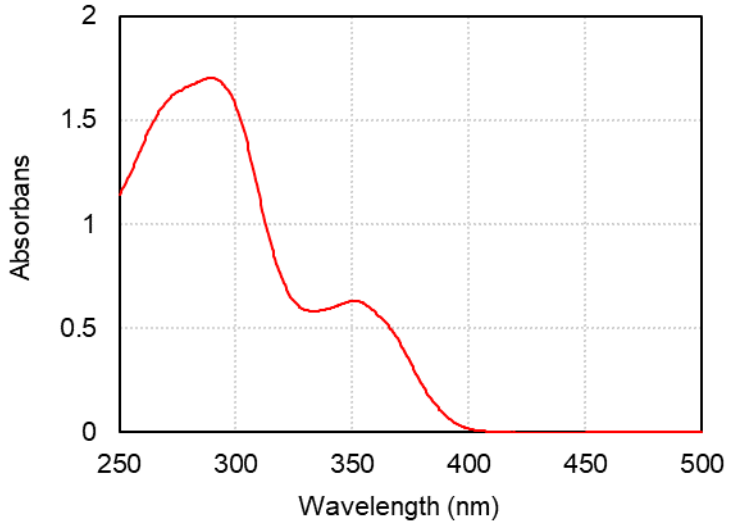

Figure S122. UV-vis absorption spectrum of PQX 100mer in MTBE containing Ac-*L*-Pro-OMe (2.35×10^{-1} g/L, path length = 1.0 mm).

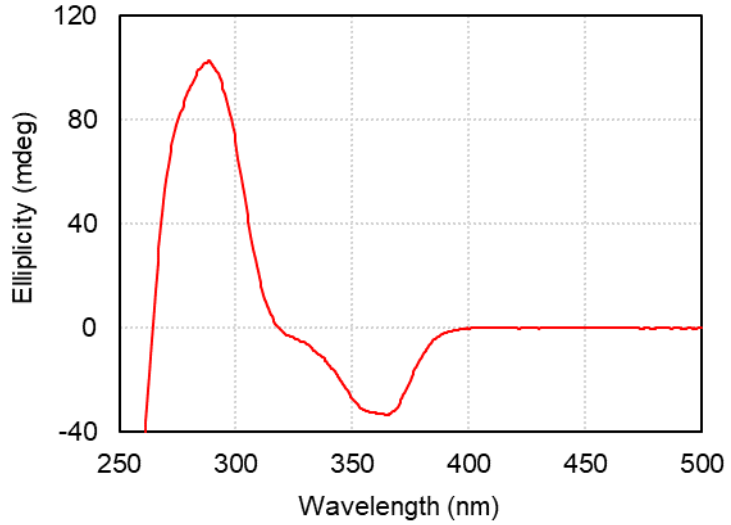

Figure S123. CD spectrum of PQX 100mer in MTBE containing Ac-*L*-Pro-OMe (2.35×10^{-1} g/L, path length = 1.0 mm).

-for Figure 3, Ac-*L*-Pro-OMe in MTBE (PQX 150mer)

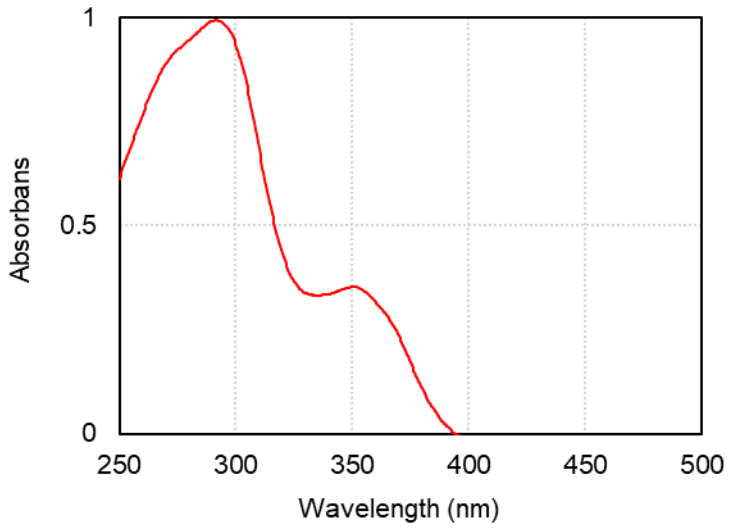

Figure S124. UV-vis absorption spectrum of PQX 150mer in MTBE containing Ac-*L*-Pro-OMe (2.65×10^{-1} g/L, path length = 1.0 mm).

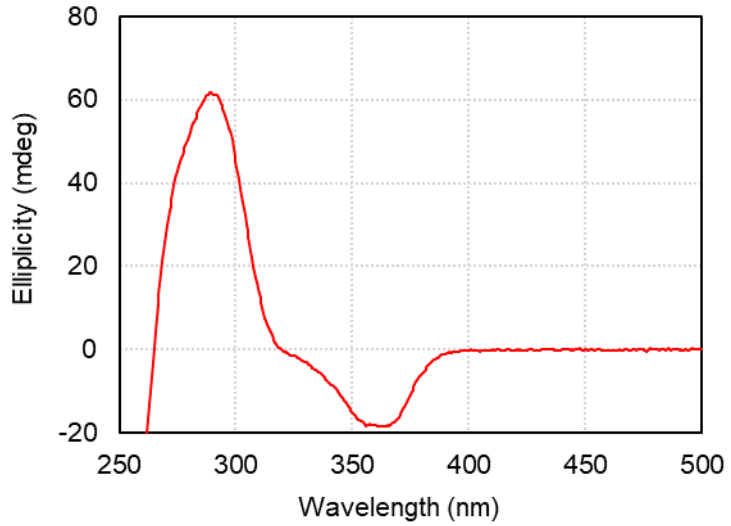

Figure S125. CD spectrum of PQX 150mer in MTBE containing Ac-*L*-Pro-OMe (2.65×10^{-1} g/L, path length = 1.0 mm).

-for Figure 3, Ac-*L*-Pro-OMe in MTBE (PQX 200mer)

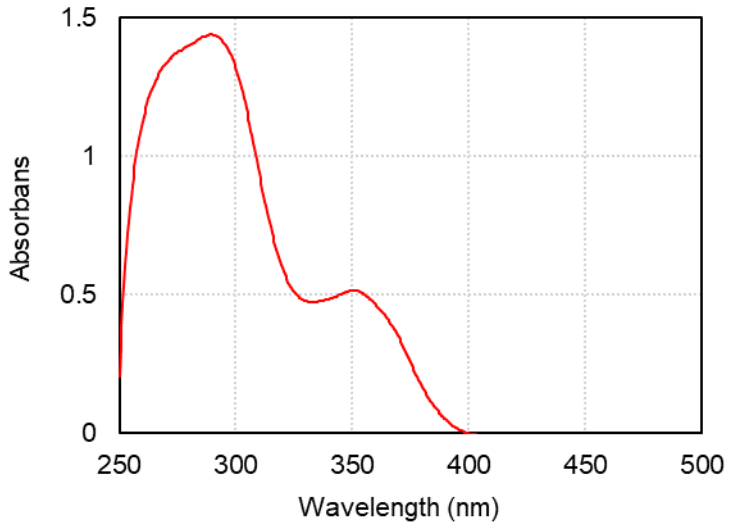

Figure S126. UV-vis absorption spectrum of PQX 200mer in MTBE containing Ac-*L*-Pro-OMe (2.23×10^{-1} g/L, path length = 1.0 mm).

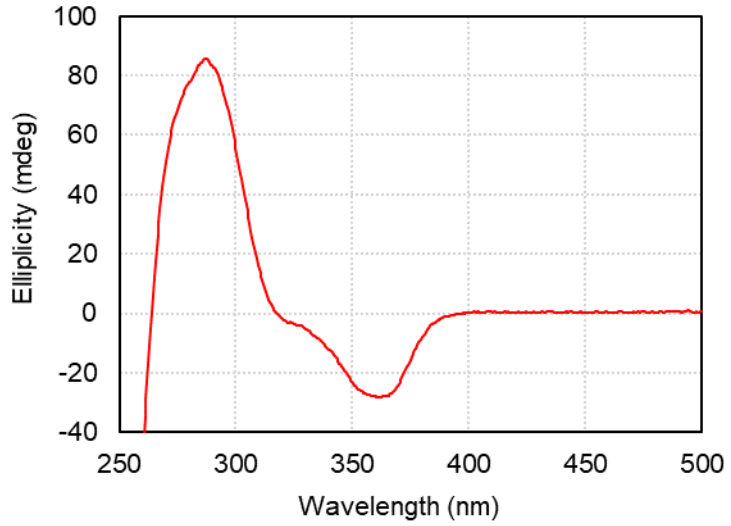

Figure S127. CD spectrum of PQX 200mer in MTBE containing Ac-*L*-Pro-OMe (2.23×10^{-1} g/L, path length = 1.0 mm).

-for Figure 3, Ac-*L*-Pro-OMe in MTBE (PQX 250mer)

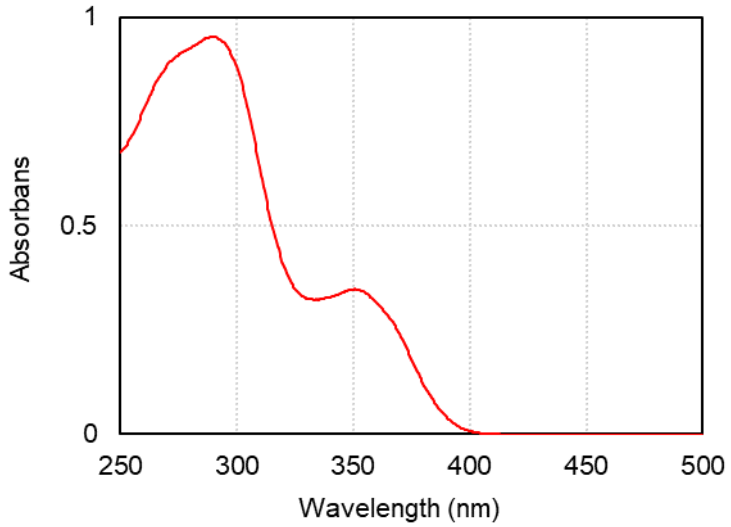

Figure S128. UV-vis absorption spectrum of PQX 250mer in MTBE containing Ac-*L*-Pro-OMe (2.26×10^{-1} g/L, path length = 1.0 mm).

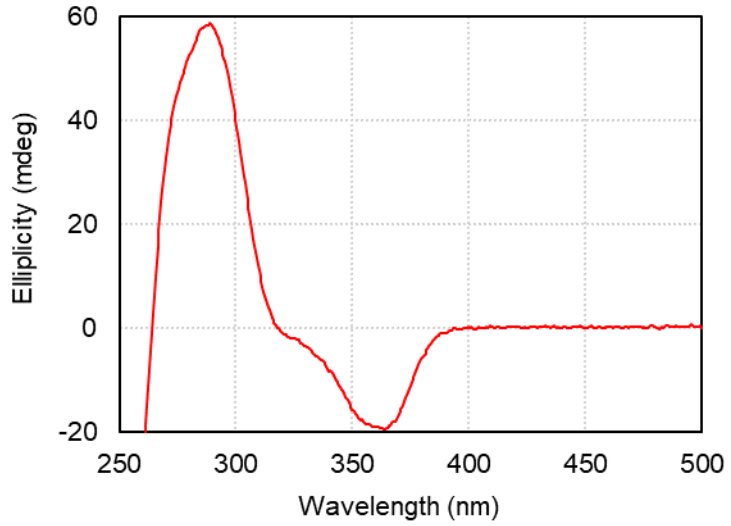

Figure S129. CD spectrum of PQX 250mer in MTBE containing Ac-*L*-Pro-OMe (2.26×10^{-1} g/L, path length = 1.0 mm).

-for Figure 3, Ac-*L*-Pro-OMe in MTBE (PQX 300mer)

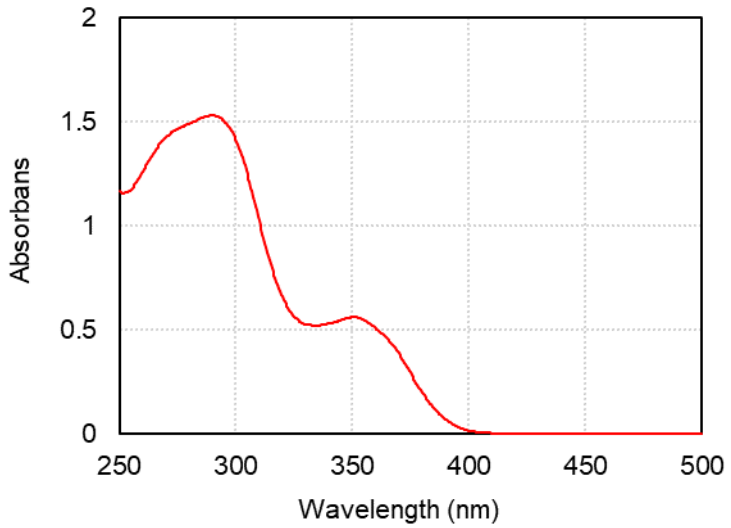

Figure S130. UV-vis absorption spectrum of PQX 300mer in MTBE containing Ac-*L*-Pro-OMe (3.18×10^{-1} g/L, path length = 1.0 mm).

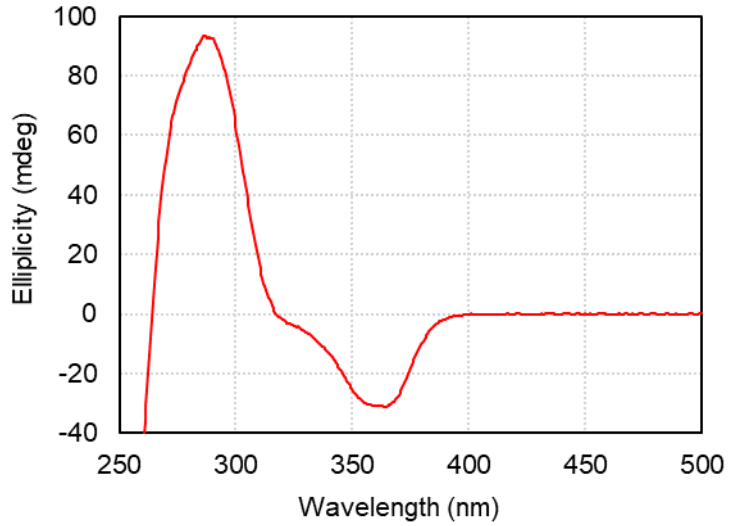

Figure S131. CD spectrum of PQX 300mer in MTBE containing Ac-*L*-Pro-OMe (3.18×10^{-1} g/L, path length = 1.0 mm).

-for Figure 3, Ac-*L*-Pro-OMe in MTBE (PQX 400mer)

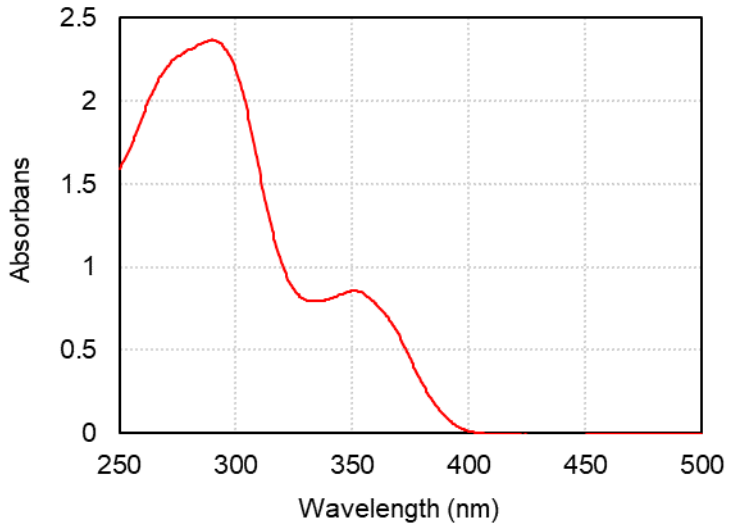

Figure S132. UV-vis absorption spectrum of PQX 400mer in MTBE containing Ac-*L*-Pro-OMe (2.54×10^{-1} g/L, path length = 1.0 mm).

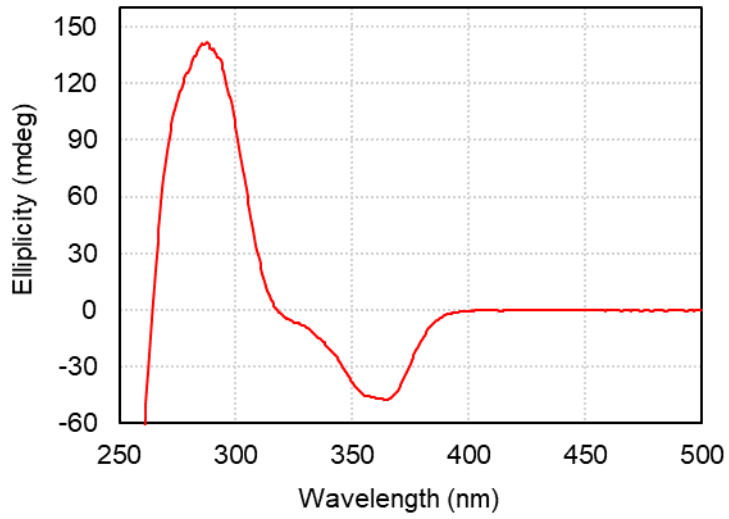

Figure S133. CD spectrum of PQX 400mer in MTBE containing Ac-*L*-Pro-OMe (2.54×10^{-1} g/L, path length = 1.0 mm).

-for Figure 4, 0.25 mol% Ac-*L*-Pro-OMe in MTBE

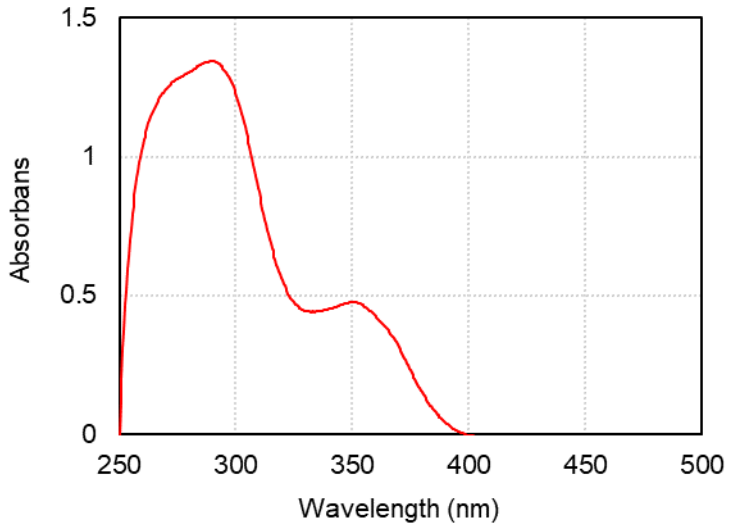

Figure S134. UV-vis absorption spectrum of PQX 1000mer in MTBE containing 0.25mol% of Ac-*L*-Pro-OMe (2.61×10^{-1} g/L, path length = 1.0 mm).

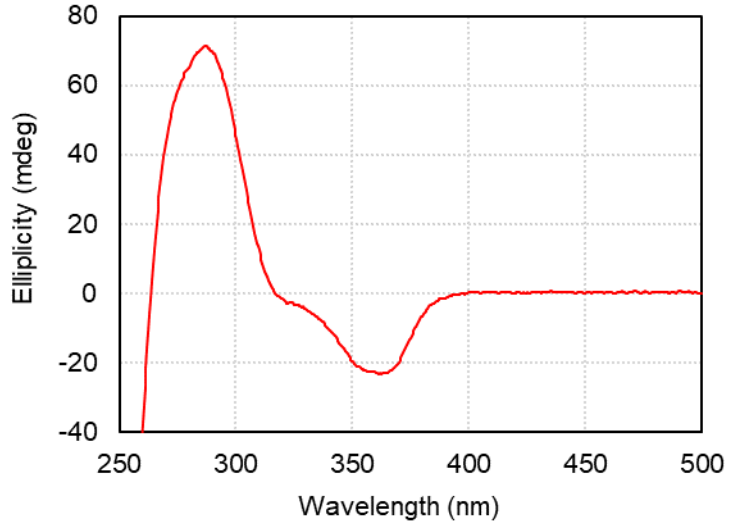

Figure S135. CD spectrum of PQX 1000mer in MTBE containing 0.25mol% of Ac-*L*-Pro-OMe (2.61×10^{-1} g/L, path length = 1.0 mm).

-for Figure 4, 0.5 mol% of Ac-*L*-Pro-OMe in MTBE

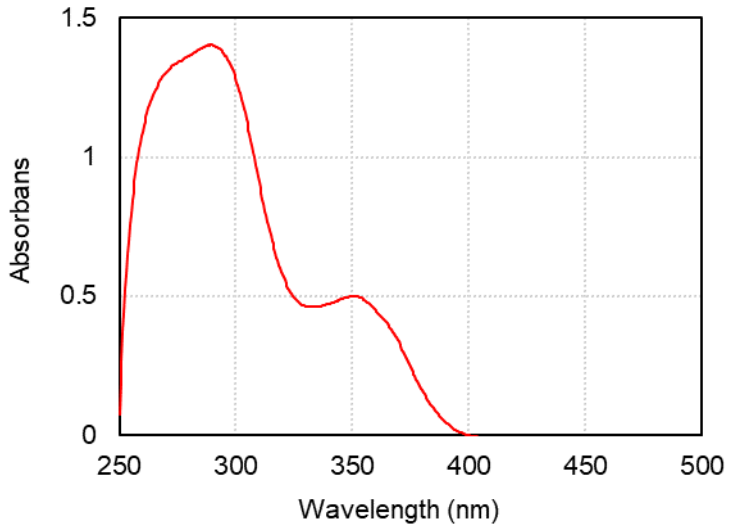

Figure S136. UV-vis absorption spectrum of PQX 1000mer in MTBE containing 0.5 mol% of Ac-*L*-Pro-OMe (2.61×10^{-1} g/L, path length = 1.0 mm).

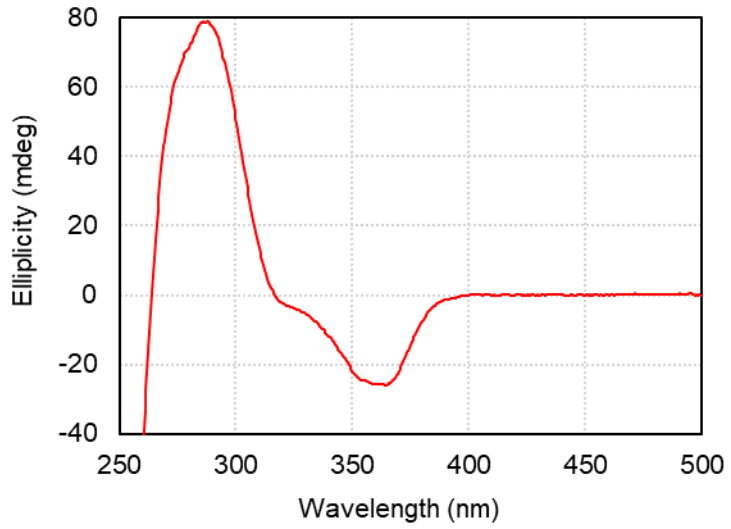

Figure S137. CD spectrum of PQX 1000mer in MTBE containing 0.5 mol% of Ac-*L*-Pro-OMe (2.61×10^{-1} g/L, path length = 1.0 mm).

-for Figure 4, 0.75 mol% of Ac-*L*-Pro-OMe in MTBE

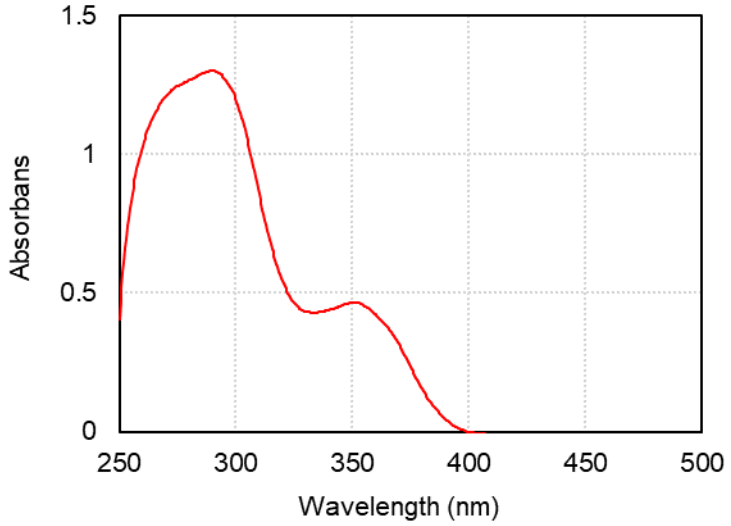

Figure S138. UV-vis absorption spectrum of PQX 1000mer in MTBE containing 0.75 mol% of Ac-*L*-Pro-OMe (2.61×10^{-1} g/L, path length = 1.0 mm).

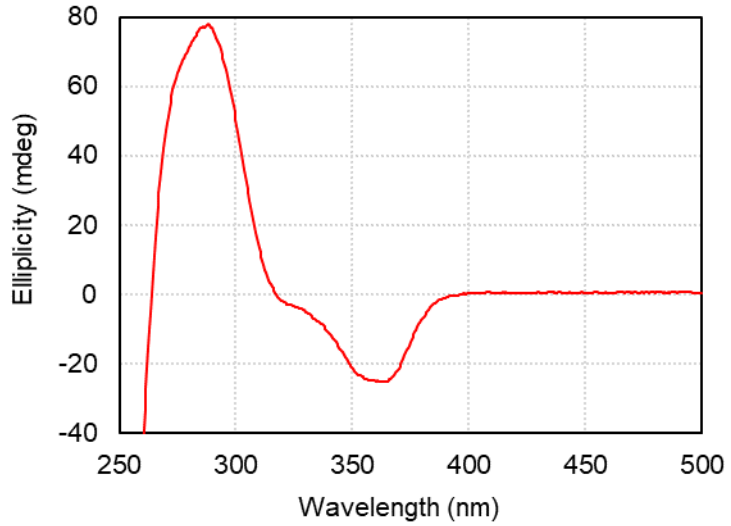

Figure S139. CD spectrum of PQX 1000mer in MTBE containing 0.75 mol% of Ac-*L*-Pro-OMe (2.61×10^{-1} g/L, path length = 1.0 mm).

-for Figure 4, 1 mol% of Ac- *L*-Pro-OMe in MTBE

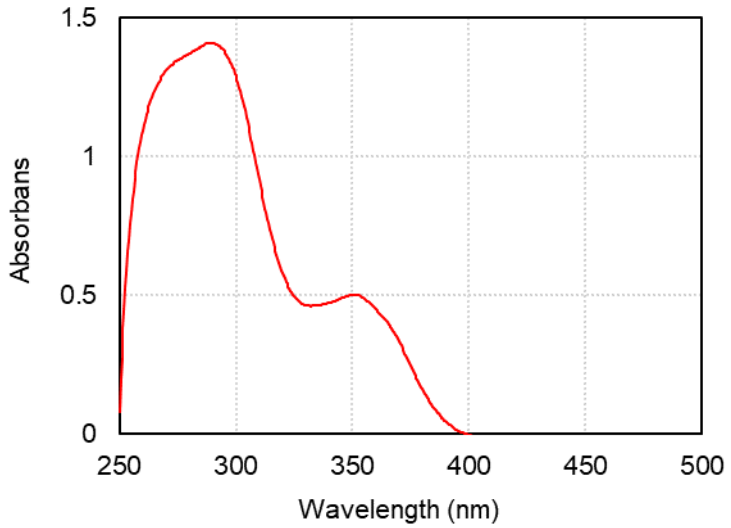

Figure S140. UV-vis absorption spectrum of PQX 1000mer in MTBE containing 1 mol% of Ac-*L*-Pro-OMe (2.61×10^{-1} g/L, path length = 1.0 mm).

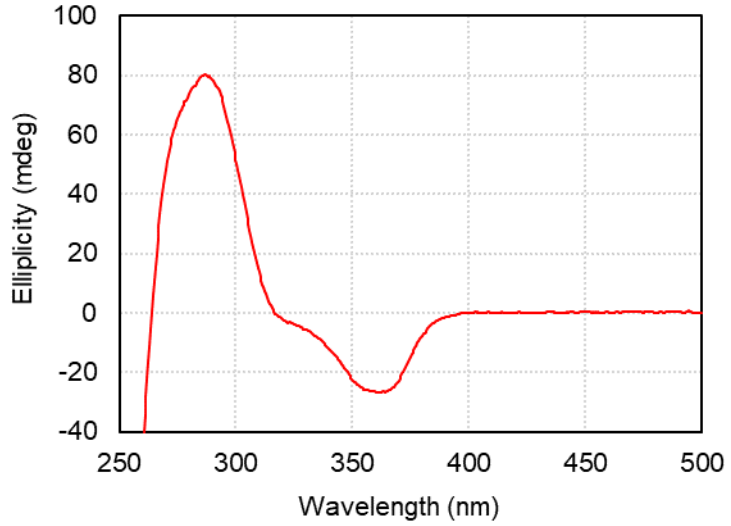

Figure S141. CD spectrum of PQX 1000mer in MTBE containing 1 mol% of Ac-*L*-Pro-OMe (2.61×10^{-1} g/L, path length = 1.0 mm).

-for Figure 4, 2 mol% of Ac- *L*-Pro-OMe in MTBE

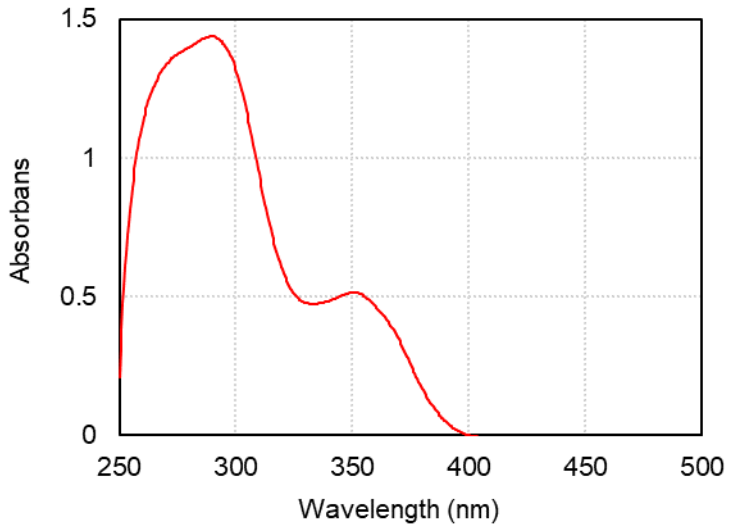

Figure S142. UV-vis absorption spectrum of PQX 1000mer in MTBE containing 2 mol% of Ac-*L*-Pro-OMe (2.61×10^{-1} g/L, path length = 1.0 mm).

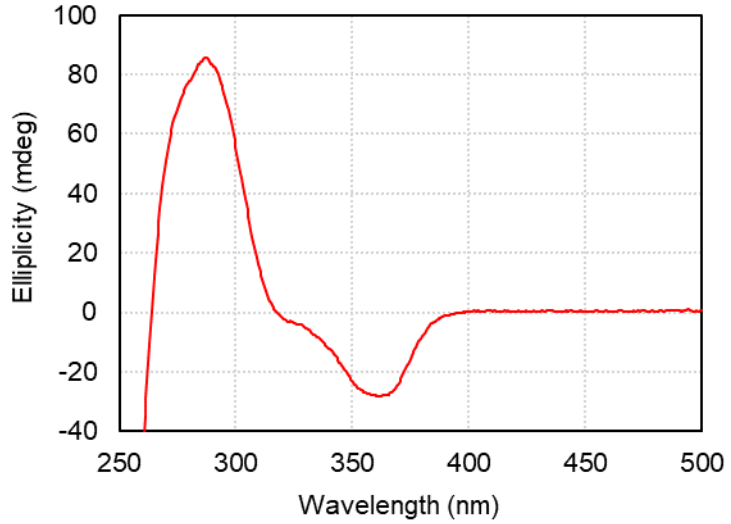

Figure S143. CD spectrum of PQX 1000mer in MTBE containing 2 mol% of Ac-*L*-Pro-OMe (2.61×10^{-1} g/L, path length = 1.0 mm).

-for Figure 4, 3 mol% of Ac- *L*-Pro-OMe in MTBE

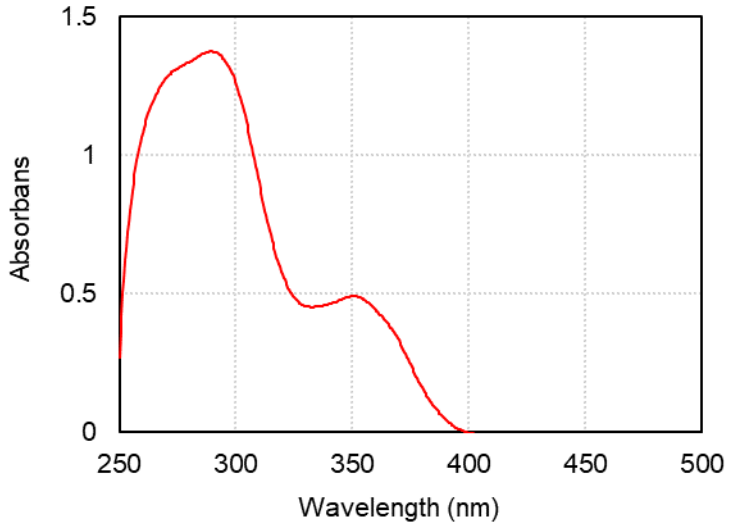

Figure S144. UV-vis absorption spectrum of PQX 1000mer in MTBE containing 3 mol% of Ac-*L*-Pro-OMe (2.61×10^{-1} g/L, path length = 1.0 mm).

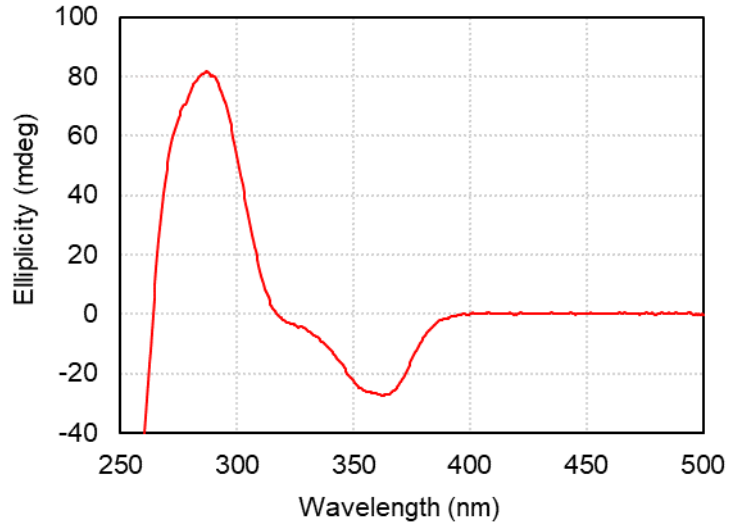

Figure S145. CD spectrum of PQX 1000mer in MTBE containing 3 mol% of Ac-*L*-Pro-OMe (2.61×10^{-1} g/L, path length = 1.0 mm).

-for Figure 4, 5 mol% of Ac-*L*-Pro-OMe in MTBE

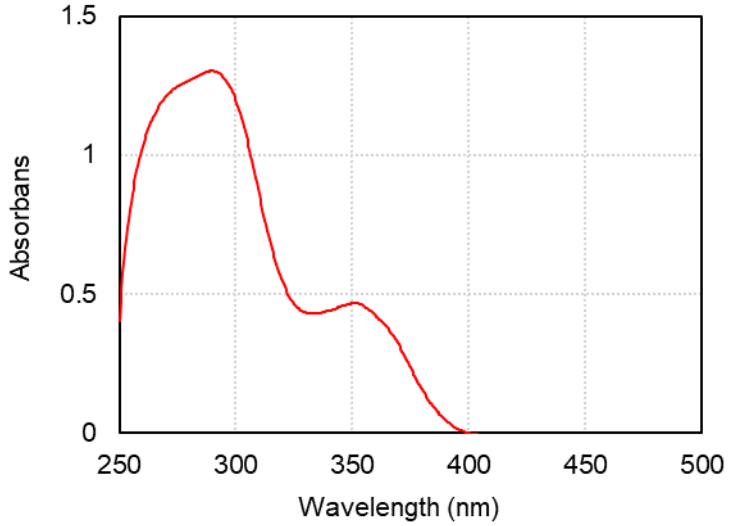

Figure S146. UV-vis absorption spectrum of PQX 1000mer in MTBE containing 5 mol% of Ac-*L*-Pro-OMe (2.61×10^{-1} g/L, path length = 1.0 mm).

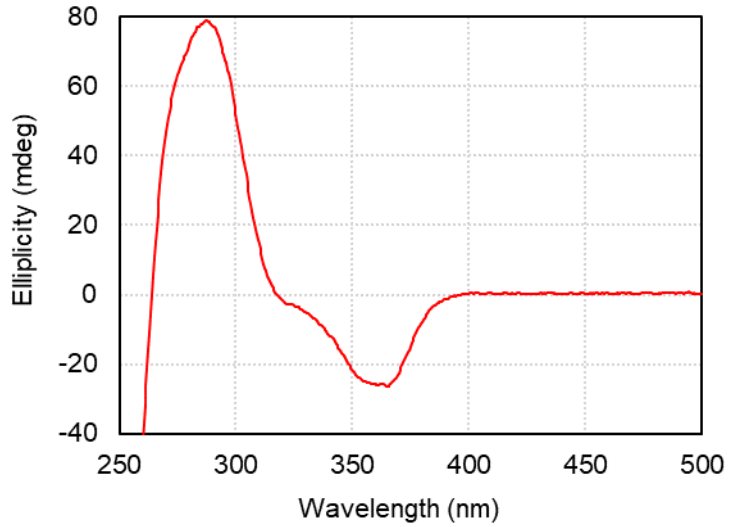

Figure S147. CD spectrum of PQX 1000mer in MTBE containing 5 mol% of Ac-*L*-Pro-OMe (2.61×10^{-1} g/L, path length = 1.0 mm).

-for Figure 4, 10 mol% of Ac-*L*-Pro-OMe in MTBE

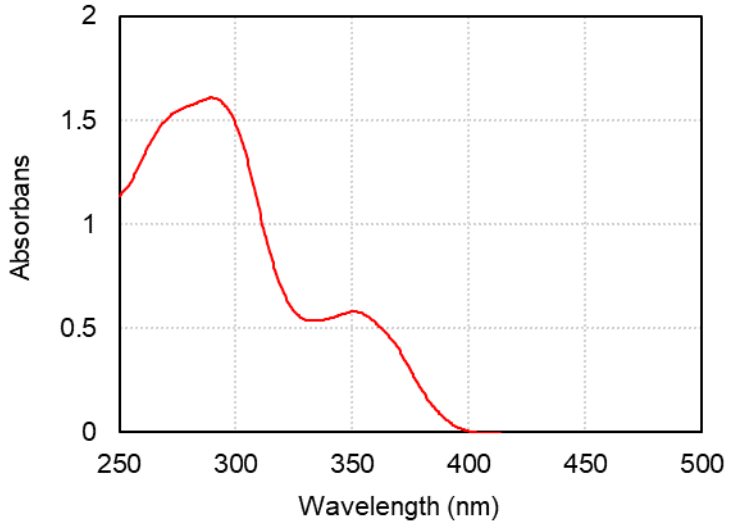

Figure S148. UV-vis absorption spectrum of PQX 1000mer in MTBE containing 10 mol% of Ac-*L*-Pro-OMe (2.61×10^{-1} g/L, path length = 1.0 mm).

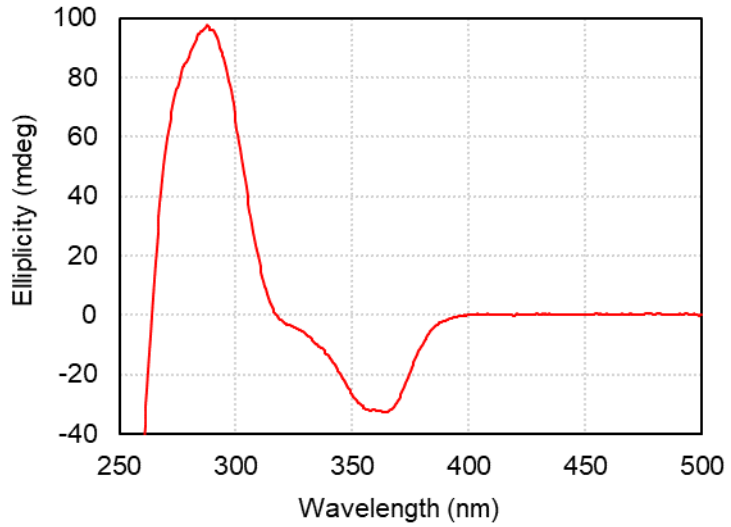

Figure S149. CD spectrum of PQX 1000mer in MTBE containing 10 mol% of Ac-*L*-Pro-OMe (2.61×10^{-1} g/L, path length = 1.0 mm).

5 NMR Spectra of PQX and PQXphos

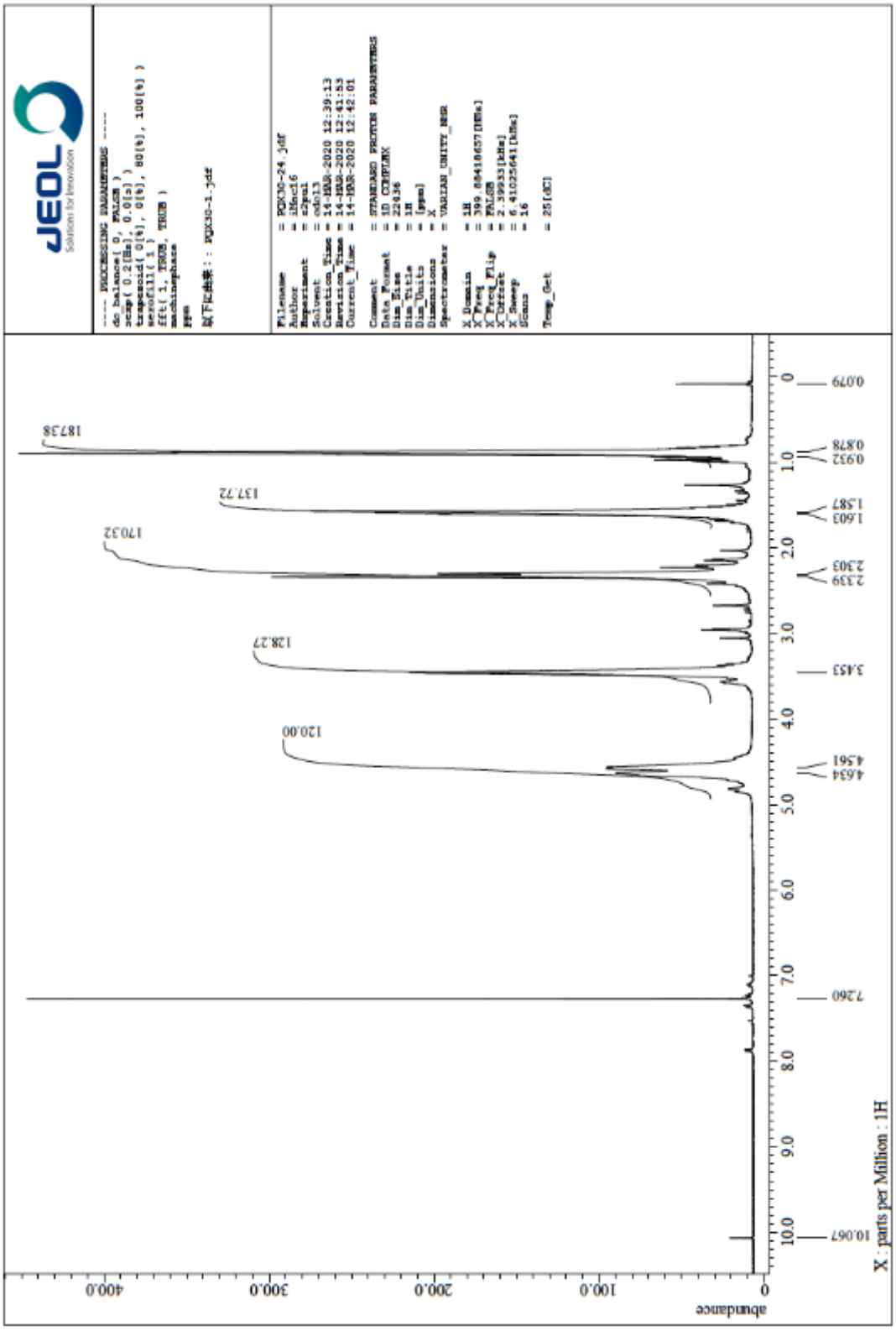

Figure S150. ^{1}H NMR spectrum of **PQX** 30mer in $CDCl_3$

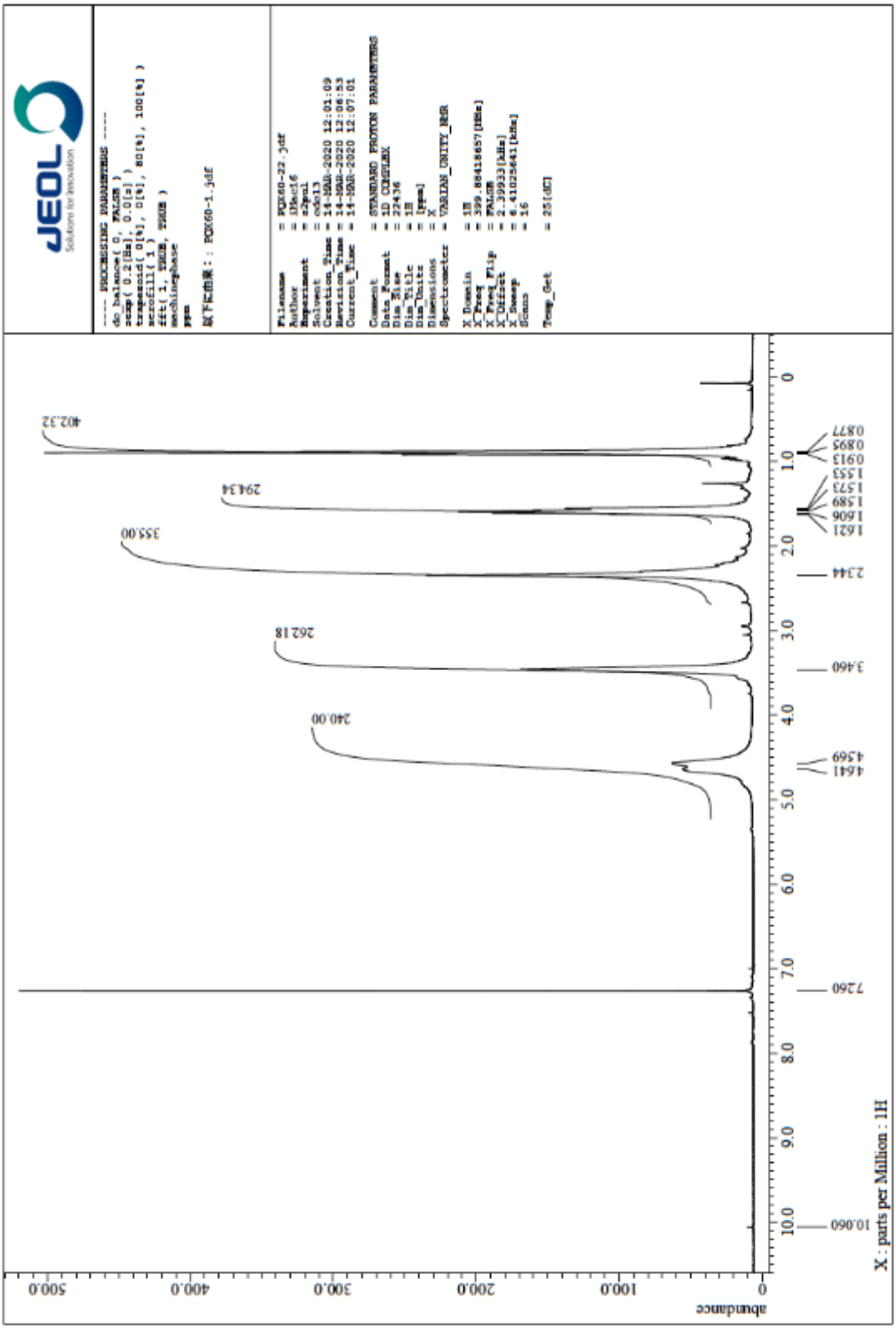

Figure S151. ^{1}H NMR spectrum of **PQX** 60mer in $CDCl_3$

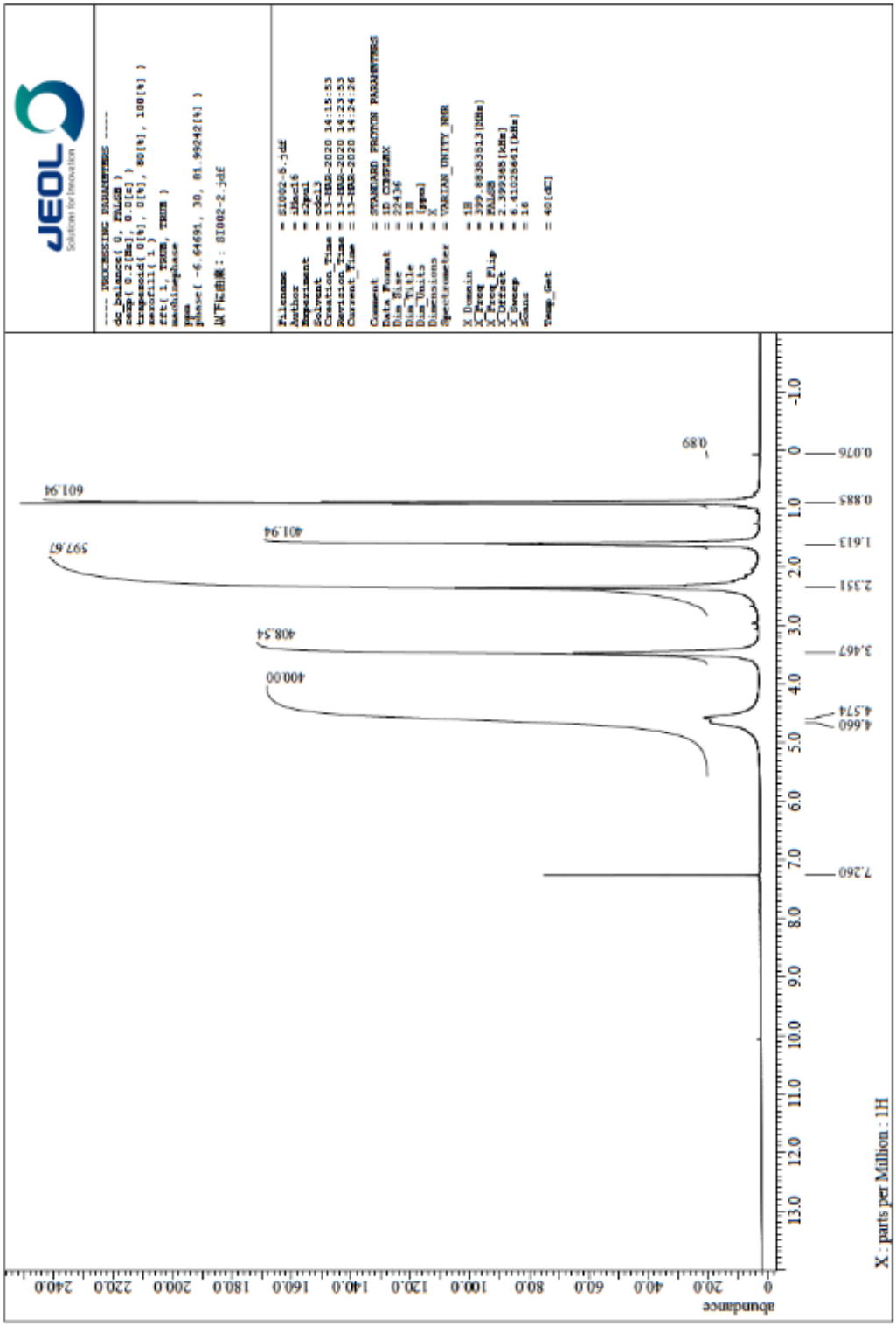

Figure S152. ^{1}H NMR spectrum of **PQX** 100mer in $CDCl_3$

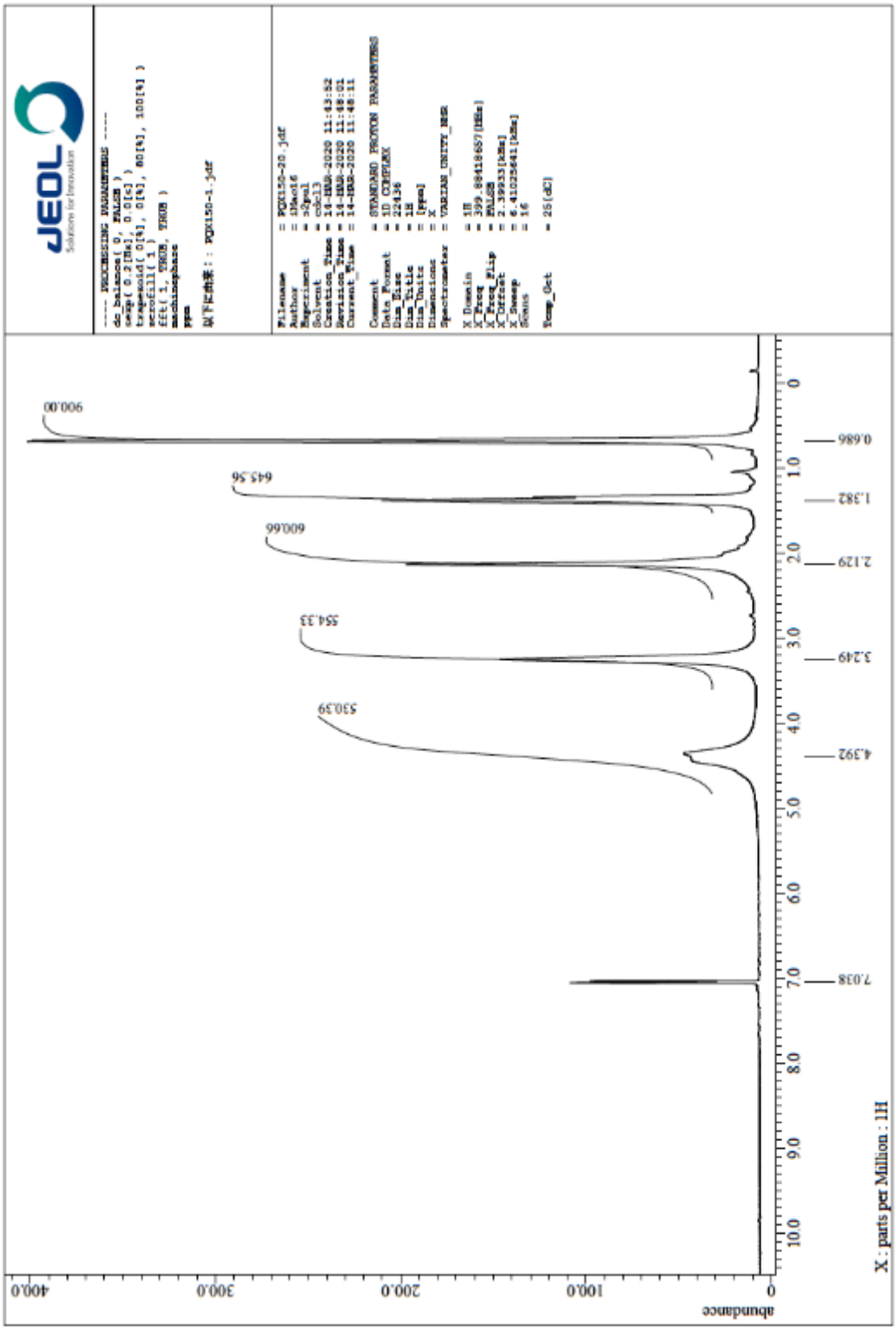

Figure S153. ^{1}H NMR spectrum of **PQX** 150mer in $CDCl_3$

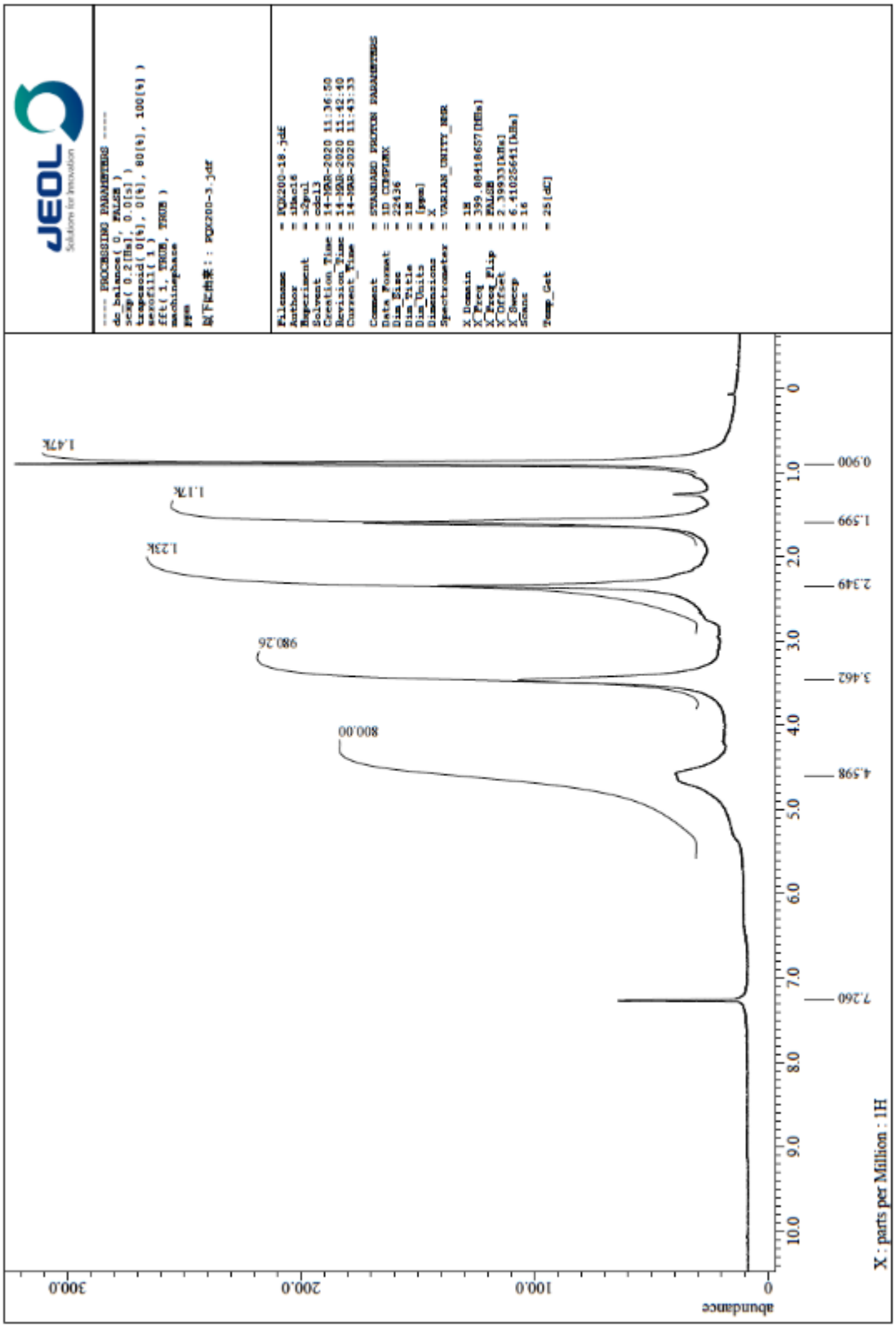

Figure S154. ^{1}H NMR spectrum of **PQX** 200mer in $CDCl_3$

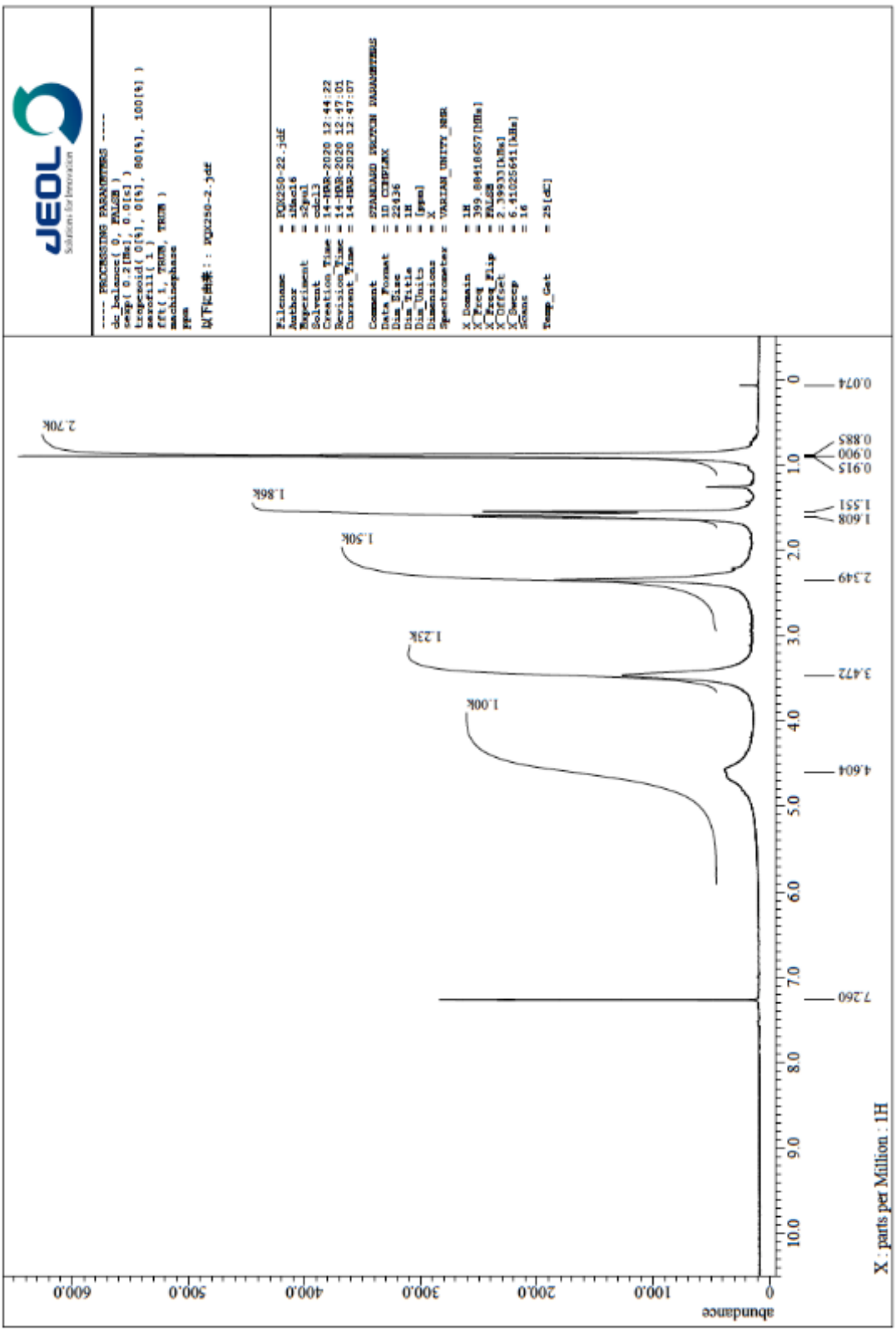

Figure S155. ^{1}H NMR spectrum of **PQX** 250mer in $CDCl_3$

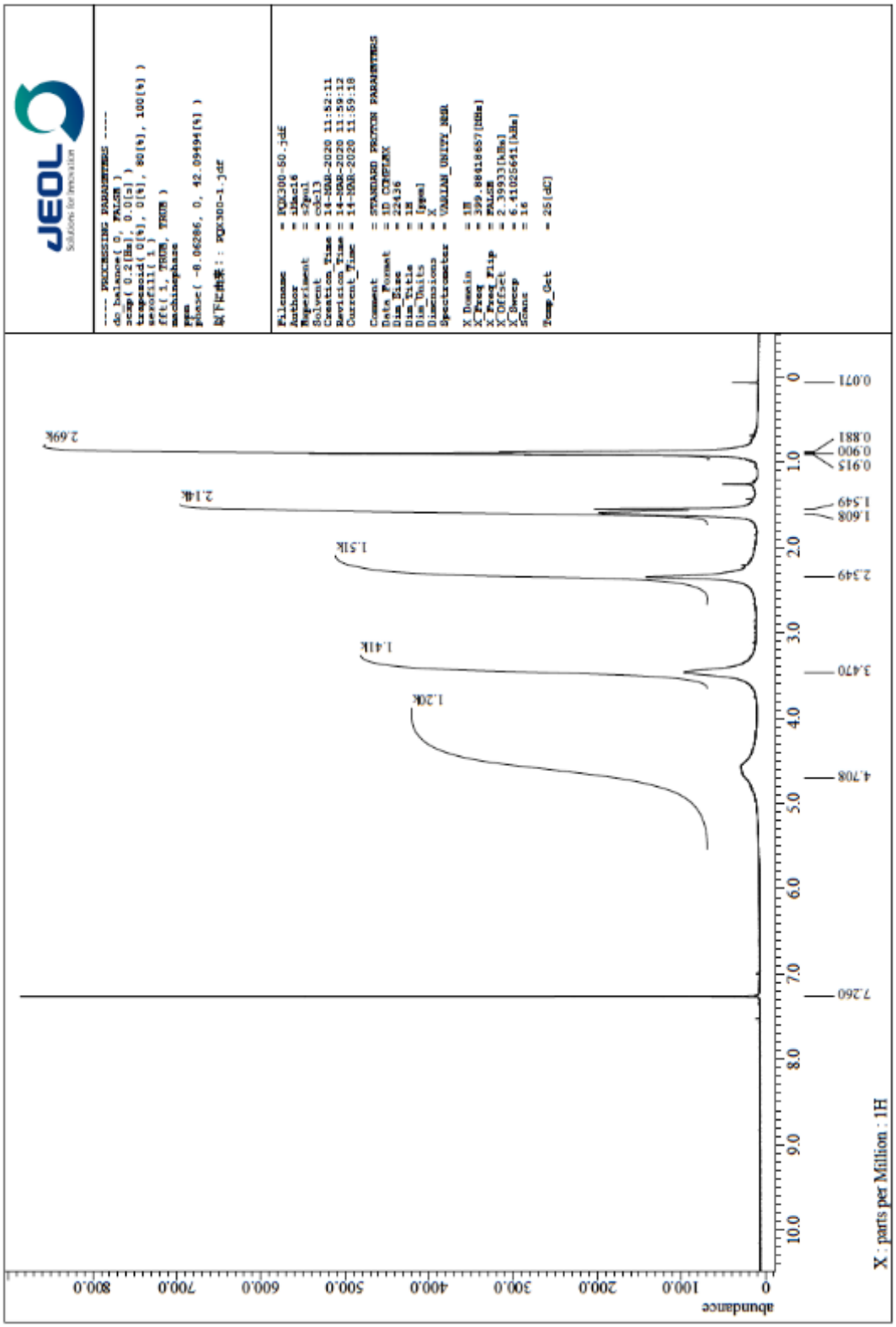

Figure S156. ^{1}H NMR spectrum of **PQX** 300mer in $CDCl_3$

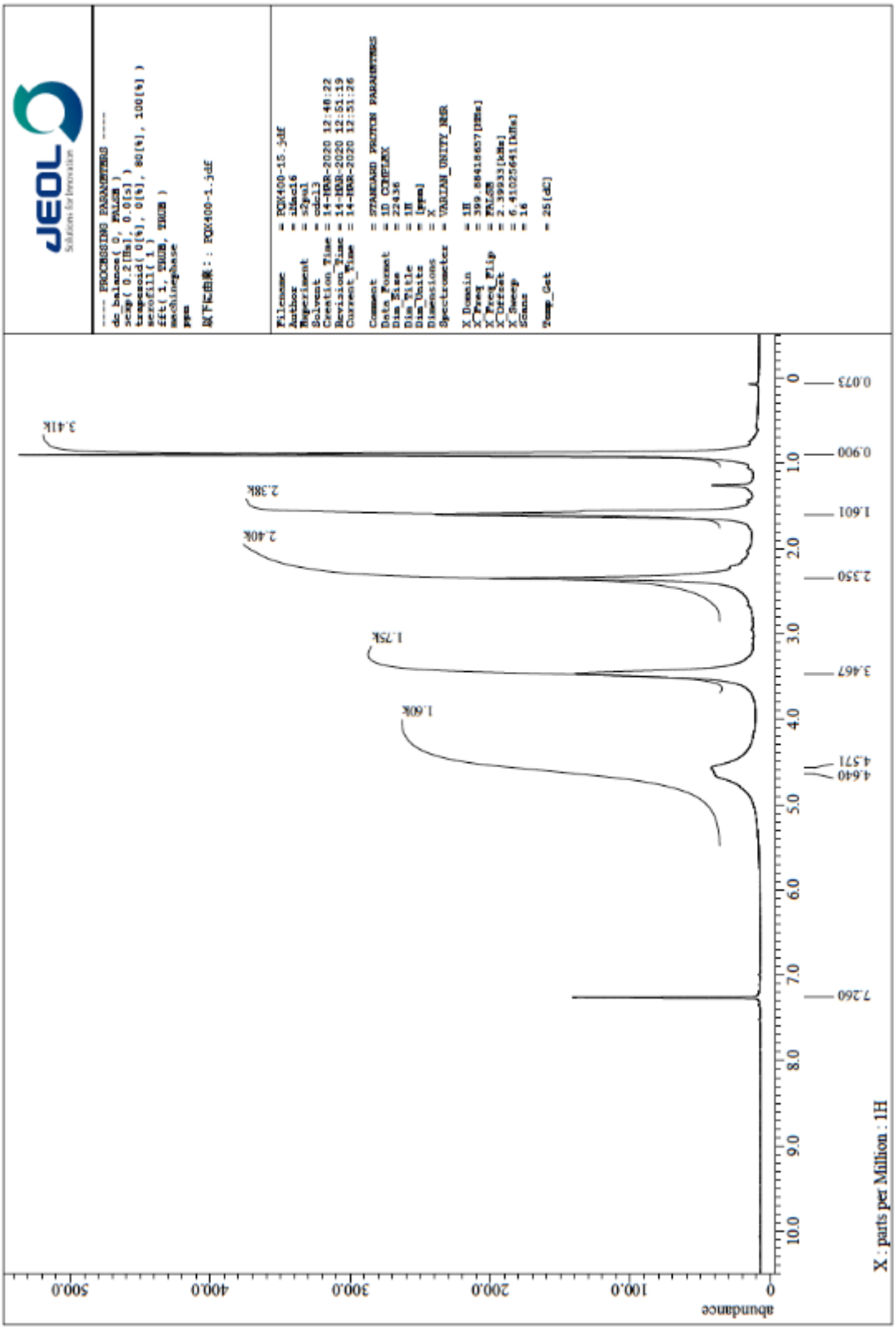

Figure S157. ^{1}H NMR spectrum of **PQX** 400mer in $CDCl_3$

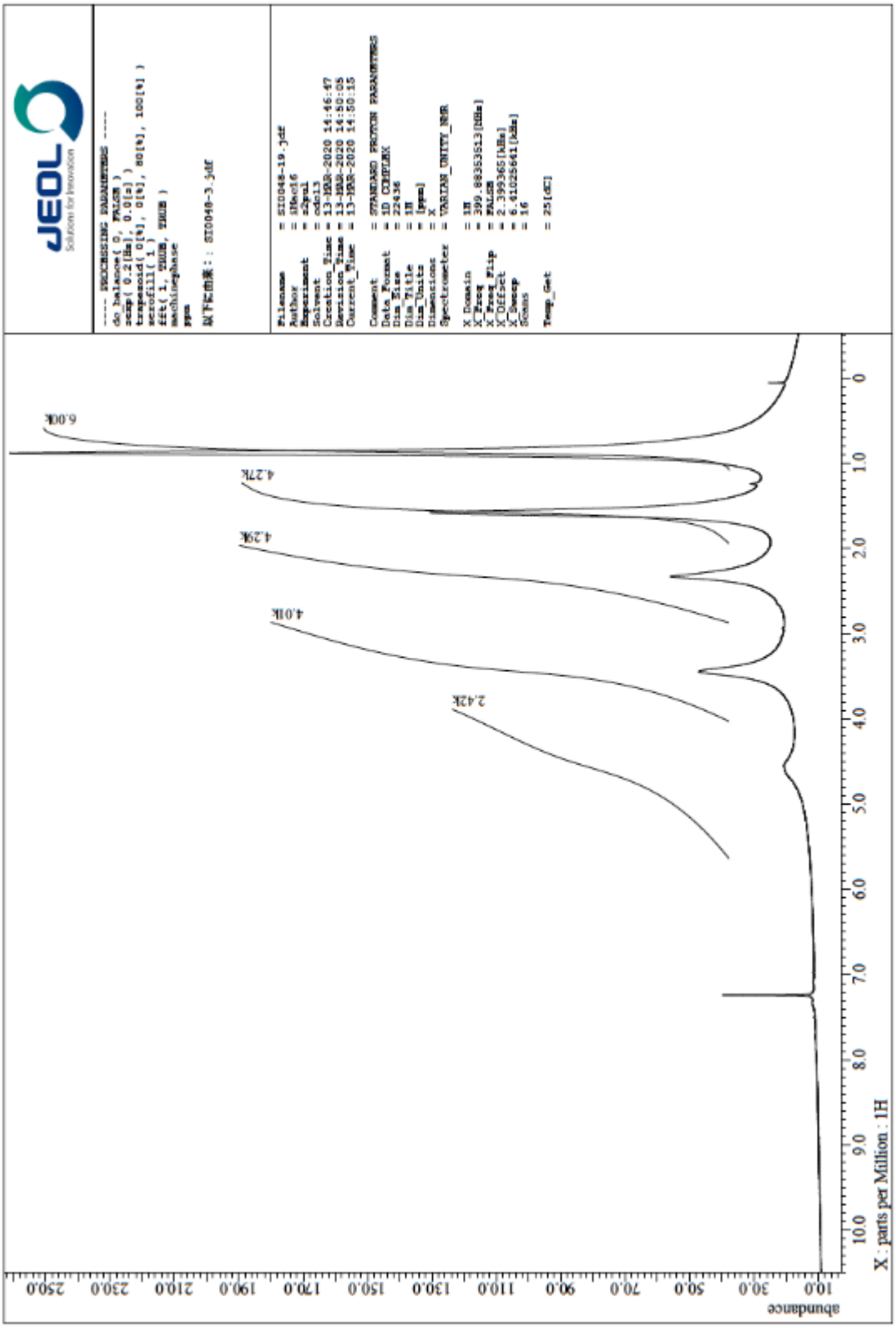

Figure S158. ^{1}H NMR spectrum of **PQXphos** in $CDCl_3$

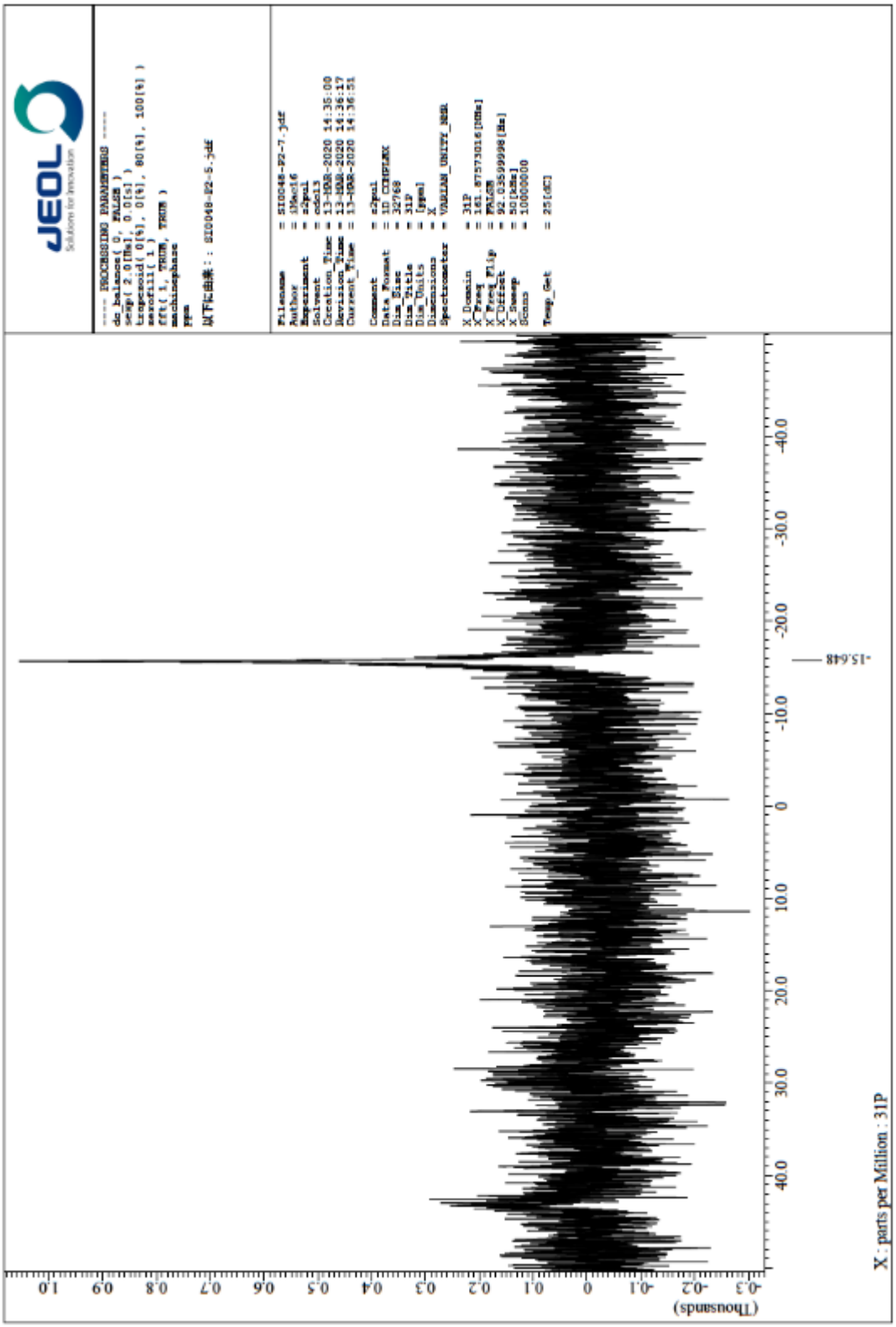

Figure S159. ^{31}P NMR spectrum of **PQXphos** in $CDCl_3$

6 Chiral HPLC traces of the Reaction Products

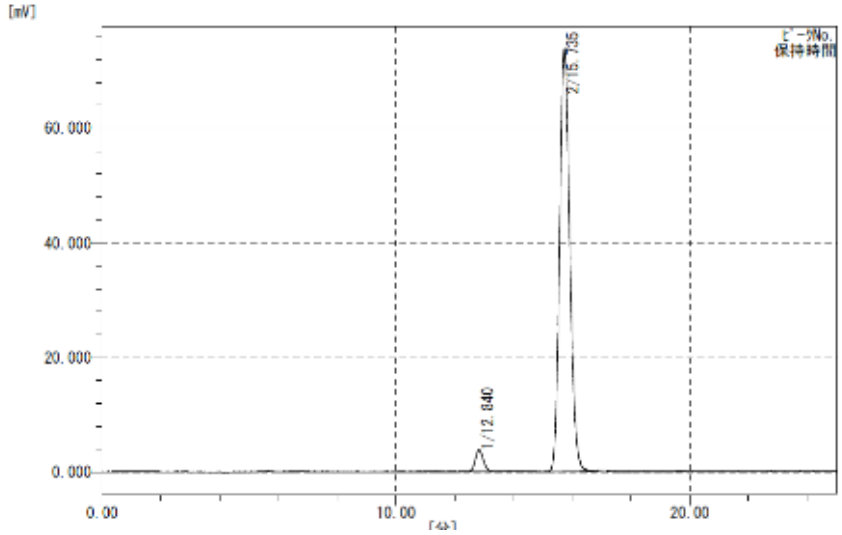

No.	Ch	時間[分]	高さ[mV]	半値幅[秒]	面積[mVx秒]	面積%	理論段数	分離能	非対称係数
1	1	12.840	3.78	17.76	70.94	3.83	10419	0.00	1.22
2	1	15.735	73.87	22.29	1782.59	96.17	9938	5.11	1.25

Figure S160. HPLC trace of the product of the asymmetric Suzuki-Miyaura cross coupling reaction (entry 4, Table 3). Enantiomeric excess was found to be 92% (*R*) (DAICEL CHIRALCELL® OZ-H, Eluent; *n*-hexane/i-PrOH (80/20), Flow rate; 0.6 mL/min).

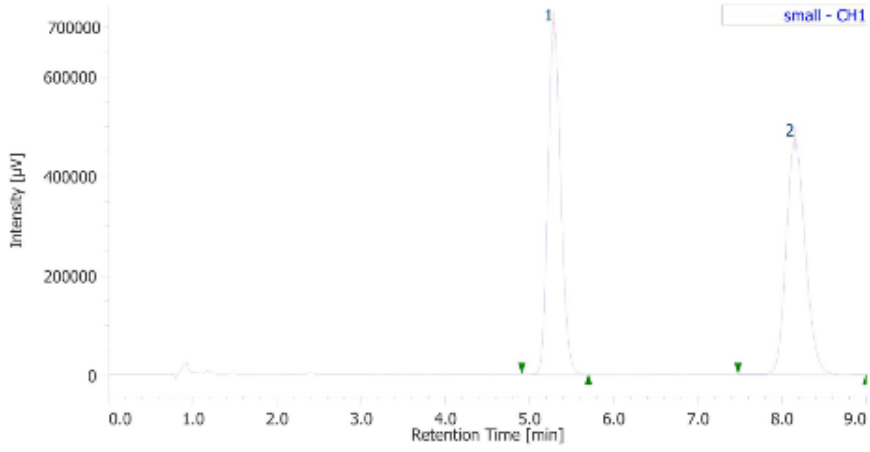

#	ピーク名	CH	tR [min]	面積 [μV·sec]	高さ [μV]	面積%	高さ%	定量値	NTP	分離度	シンメトリー係数	警告
1	Unknown	1	5.285	7436135	705941	50.224	60.011	N/A	5820	8.337	1.160	
2	Unknown	1	8.150	7369726	470408	49.776	39.989	N/A	6281	N/A	1.168	

Figure S161. HPLC trace of the product of the asymmetric Suzuki-Miyaura cross coupling reaction (entry5, Table3). Enantiomeric excess was found to be 95% (*R*) (DAICEL CHIRALCELL® AD-H, Eluent; CO_2/i-PrOH (100/25), Flow rate; 3.75 mL/min).

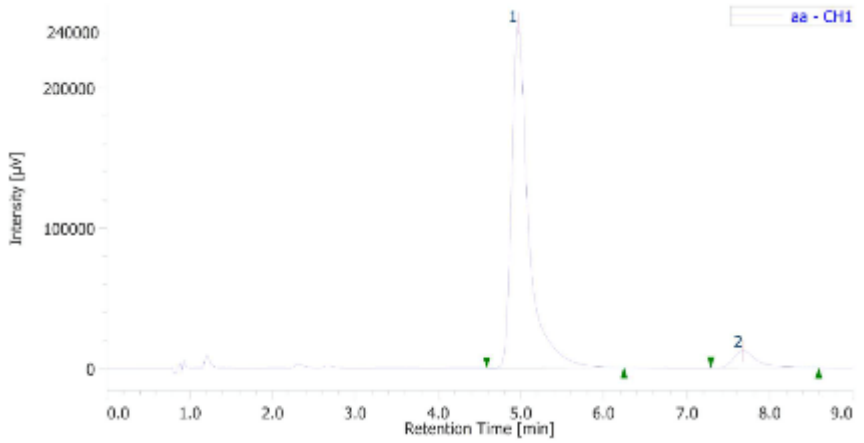

#	ピーク名	CH	tR [min]	面積 [μV*sec]	高さ [μV]	面積%	高さ%	定量値	NTP	分離度	シンメトリー係数	警告
1	Unknown	1	4.967	3511148	245596	93.638	95.298	N/A	3783	6.888	1.892	
2	Unknown	1	7.675	238541	12119	6.362	4.702	N/A	4349	N/A	1.661	

Figure S162. HPLC trace of the product of the asymmetric Suzuki-Miyaura cross coupling reaction (entry7, Table3). Enantiomeric excess was found to be 87% (*R*) (DAICEL CHIRALCELL® AD-H, Eluent; CO_2/i-PrOH (100/25), Flow rate; 3.75 mL/min).

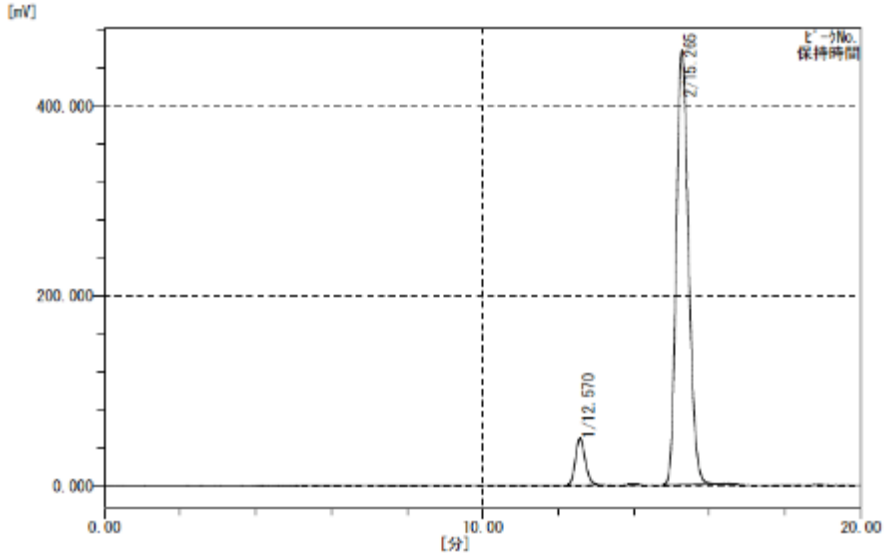

No.	Ch	時間[分]	高さ[mV]	半値幅[秒]	面積[mV×秒]	面積%	理論段数	分離能	非対称係数
1	1	12.570	49.44	16.56	885.89	7.91	11484	0.00	1.30
2	1	15.265	456.97	21.01	10320.13	92.09	10532	5.07	1.35

Figure S163. HPLC trace of the product of the asymmetric Suzuki-Miyaura cross coupling reaction (entry 8, Table 3). Enantiomeric excess was found to be 84% (*R*) (DAICEL CHIRALCELL® OZ-H, Eluent; *n*-hexane/i-PrOH (80/20), Flow rate; 0.6 mL/min).

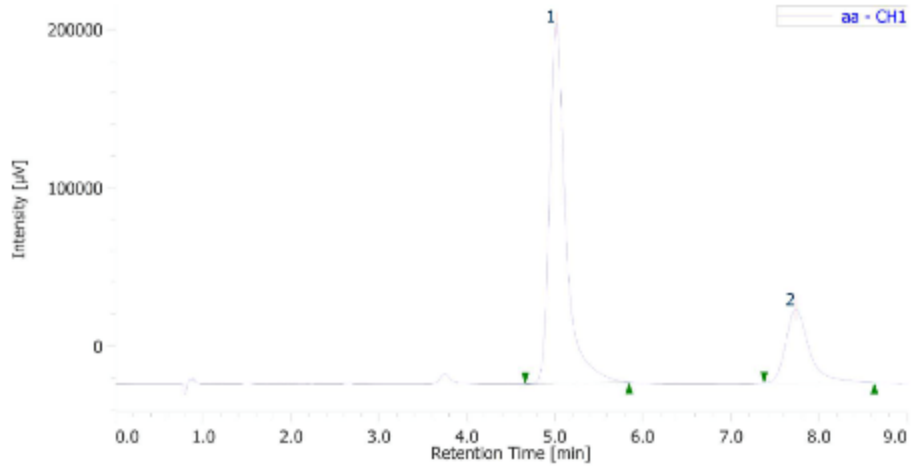

#	ピーク名	CH	tR [min]	面積 [μV·sec]	高さ [μV]	面積%	高さ%	定量値	NTP	分離度	シンメトリー係数	警告
1	Unknown	1	5.017	2962983	226925	77.226	82.968	N/A	4301	7.184	1.630	
2	Unknown	1	7.735	873791	46583	22.774	17.032	N/A	4668	N/A	1.504	

Figure S164. HPLC trace of the product of the asymmetric Suzuki-Miyaura cross coupling reaction (entry9, Table3). Enantiomeric excess was found to be 54% (*R*) (DAICEL CHIRALCELL® AD-H, Eluent; CO_2/i-PrOH (100/25), Flow rate; 3.75 mL/min).

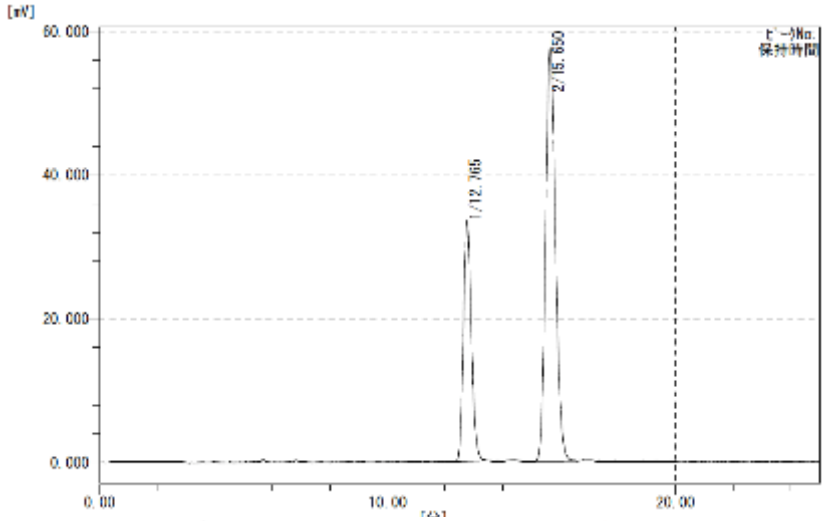

No.	Ch	時間[分]	高さ[mV]	半値幅[秒]	面積[mVx秒]	面積%	理論段数	分離能	非対称係数
1	1	12.765	33.60	17.68	643.95	31.91	10401	0.00	1.30
2	1	15.650	57.65	22.03	1374.35	68.09	10063	5.14	1.27

Figure S165. HPLC trace of the product of the asymmetric Suzuki-Miyaura cross coupling reaction (entry 10, Table 3). Enantiomeric excess was found to be 36% (*R*) (DAICEL CHIRALCELL® OZ-H, Eluent; *n*-hexane/i-PrOH (80/20), Flow rate; 0.6 mL/min).

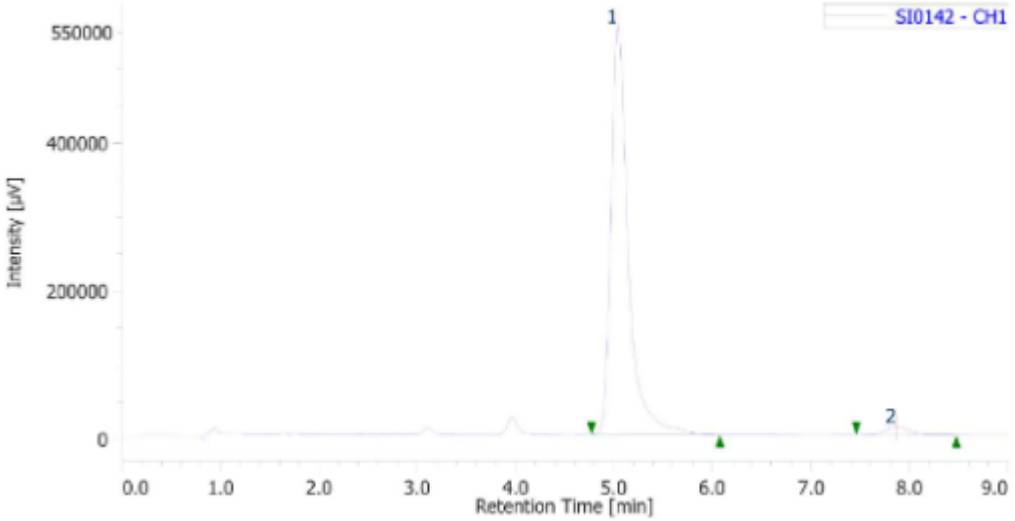

#	ピーク名	CH	tR [min]	面積 [μV·sec]	高さ [μV]	面積%	高さ%	定量値	NTP	分離度	シンメトリー係数	警告
1	Unknown	1	5.043	6776451	553699	97.290	98.077	N/A	4875	7.796	1.596	
2	Unknown	1	7.870	188782	10856	2.710	1.923	N/A	5161	N/A	1.290	

Figure S166. HPLC trace of the product of the asymmetric Suzuki-Miyaura cross coupling reaction (entry11, Table3). Enantiomeric excess was found to be 95% (*R*) (DAICEL CHIRALCELL® AD-H, Eluent; CO_2/i-PrOH (100/25), Flow rate; 3.75 mL/min).

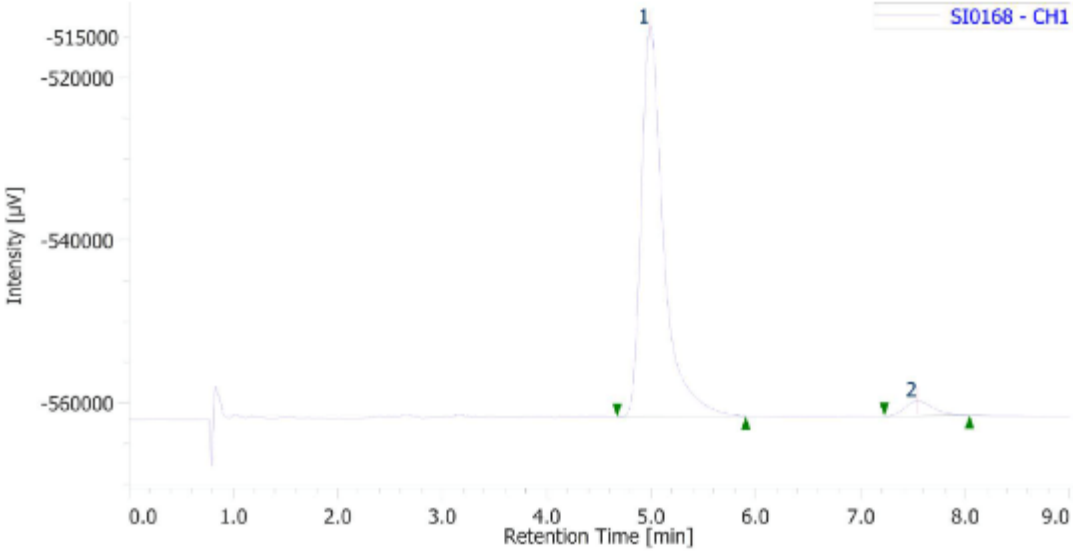

#	ピーク名	CH	tR [min]	面積 [μV·sec]	高さ [μV]	面積%	高さ%	定量値	NTP	分離度	シンメトリー係数	警告
1	Unknown	1	5.350	1258764	130395	97.678	98.368	N/A	7056	8.884	1.062	
2	Unknown	1	8.125	29929	2163	2.322	1.632	N/A	7648	N/A	1.044	

Figure S167. HPLC trace of the product of the asymmetric Suzuki-Miyaura cross coupling reaction (entry12, Table3). Enantiomeric excess was found to be 95% (*R*) (DAICEL CHIRALCELL® AD-H, Eluent; CO_2/i-PrOH (100/25), Flow rate; 3.75 mL/min).

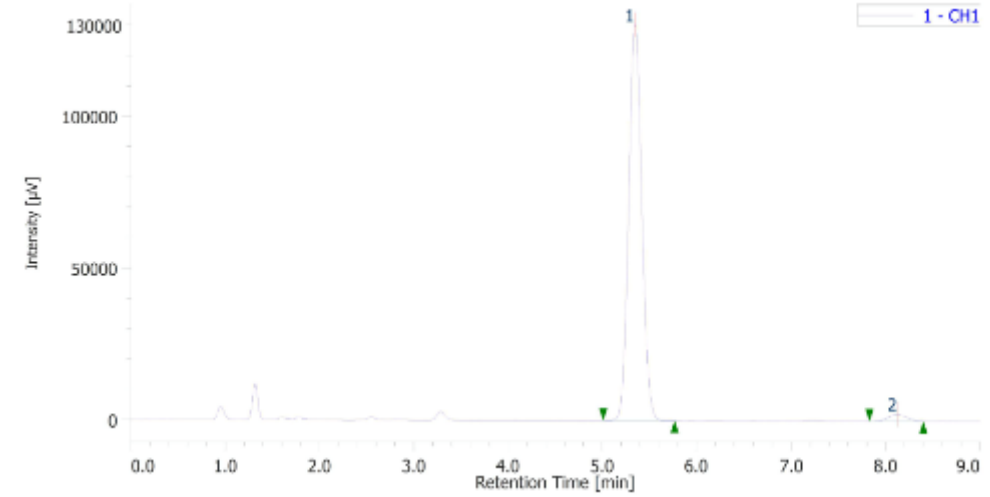

#	ピーク名	CH	tR [min]	面積 [μV·sec]	高さ [μV]	面積%	高さ%	定量値	NTP	分離度	シンメトリー係数	警告
1	Unknown	1	4.992	716128	48147	95.516	96.374	N/A	3200	6.106	1.704	
2	Unknown	1	7.545	33619	1811	4.484	3.626	N/A	3863	N/A	1.279	

Figure S168. HPLC trace of the product of the asymmetric Suzuki-Miyaura cross coupling reaction (entry13, Table3). Enantiomeric excess was found to be 91% (*R*) (DAICEL CHIRALCELL® AD-H, Eluent; CO_2/i-PrOH (100/25), Flow rate; 3.75 mL/min).

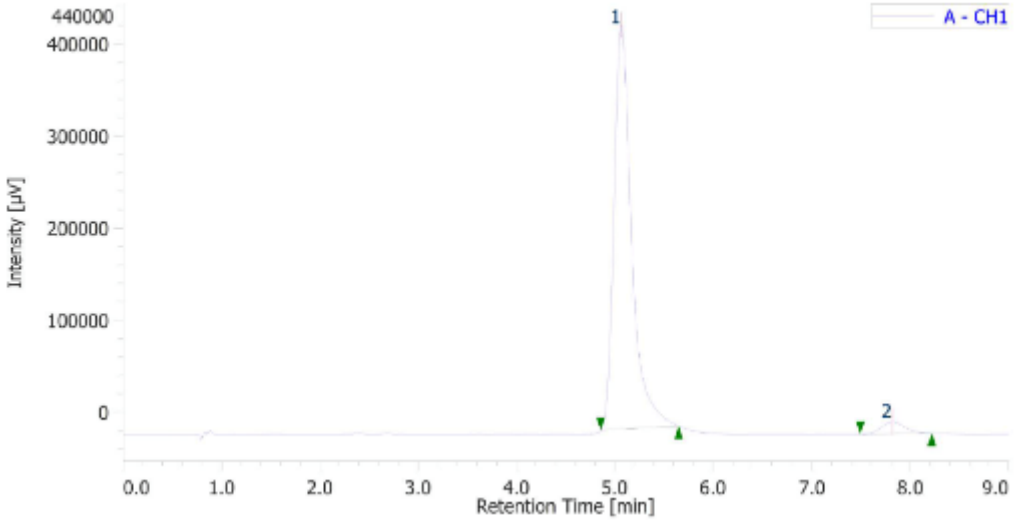

#	ピーク名	CH	tR [min]	面積 [μV·sec]	高さ [μV]	面積%	高さ%	定量値	NTP	分離度	シンメトリー係数	警告
1	Unknown	1	5.070	5481573	438711	96.285	97.186	N/A	4467	7.446	1.533	
2	Unknown	1	7.818	211511	12704	3.715	2.814	N/A	5129	N/A	1.145	

Figure S169. HPLC trace of the product of the asymmetric Suzuki-Miyaura cross coupling reaction (entry14, Table3). Enantiomeric excess was found to be 91% (*R*) (DAICEL CHIRALCELL® AD-H, Eluent; CO_2/i-PrOH (100/25), Flow rate; 3.75 mL/min).

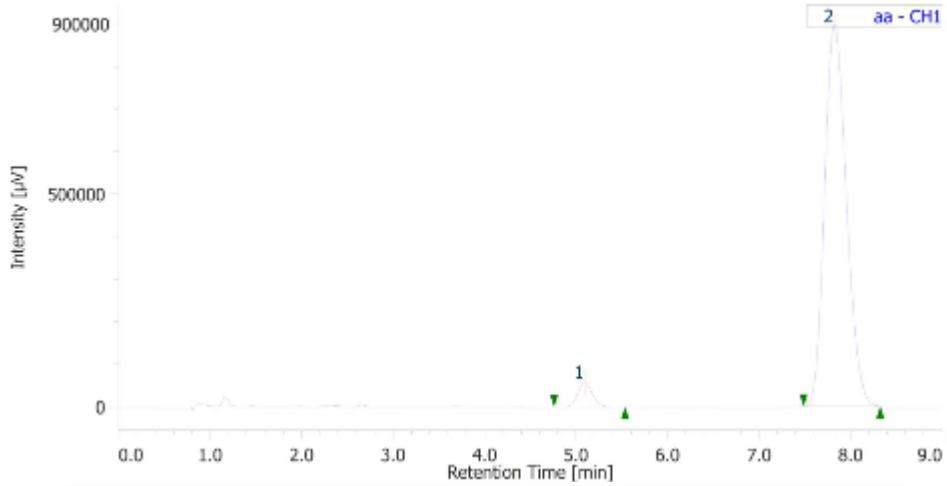

#	ピーク名	CH	tR [min]	面積 [μV sec]	高さ [μV]	面積%	高さ%	定量値	NTP	分離度	シンメトリー係数	警告
1	Unknown	1	5.092	620599	57412	4.002	6.006	N/A	5087	7.540	1.142	
2	Unknown	1	7.822	14887875	898427	95.998	93.994	N/A	5045	N/A	1.200	

Figure S170. HPLC trace of the product of the asymmetric Suzuki-Miyaura cross coupling reaction (entry16, Table3). Enantiomeric excess was found to be 92% (*S*) (DAICEL CHIRALCELL® AD-H, Eluent; CO_2/i-PrOH (100/25), Flow rate; 3.75 mL/min).